Università degli Studi di Milano
Dipartimento di Scienze Farmaceutiche
Dottorato di Ricerca in *Chimica del Farmaco – XXV Ciclo*

DESIGN, SYNTHETIC APPROACHES, BIOPHARMACOLOGICAL INVESTIGATION, AND STRUCTURE ACTIVITY RELATIONSHIPS OF NOVEL LIGANDS TARGETING NEURONAL NICOTINIC RECEPTOR SUBTYPES

Supervisor: Prof. Marco DE AMICI

Tesi di dottorato di :
Diego Yuri POME'
Matr. R08812

ANNO ACCADEMICO 2011-2012

Contents

Abbreviations

General:

3D	three-dimensional
˚C	degree Celsius
AChBP	acetylcholine binding protein
Å	Angstrom
AcOEt	ethyl acetate
Boc	*tert*-butoxycarbonyl
CAM	ceric ammonium molybdate solution
conc.	concentrated
CyHex	cyclohexane
DCM	dichloromethane
DIPEA	*N*,*N*-diisopropylamine
DMF	dimethylformamide
DMSO	dimethylsulfoxide
e.e.	enantiomeric excess
eq.	equivalents
LBD	ligand binding domain
M^+	molecular ion
MeOH	methanol
mRNA	messenger ribonucleic acid
m.p.	melting point
m/z	mass/charge
MHz	megaHertz
NaHMDS	sodium bis(trimethylsilyl)amide
PMA	phosphomolybdic acid solution
TBAC	tetrabutylammonium chloride
TBAF	tetrabutylammonium fluoride
TEA	triethylamine
TFA	trifluoroacetic acid

THF	tetrahydrofuran
TLC	thin layer chromatography
TBSCl	*tert*-butyl-dimethylsilyl chloride

Spectroscopic:

J	NMR coupling constant
δ	chemical shift (ppm)
ppm	parts per million
s	singlet
bs	broad singlet
d	doublet
dd	doublet of doublets
t	triplet
m	multiplet
sex	sextplet
Hz	Hertz
i	*iso*
o	*ortho*
m	*meta*
p	*para*

1. Introduction

1.1. The cholinergic neurotransmission

The neurotransmitter acetylcholine (ACh) exerts its regulatory effects on the central nervous system (CNS) and peripheral nervous system (PNS) through two distinct families of receptors: the muscarinic and nicotinic ACh receptors.

Nicotine, a natural alkaloid synthesized by several plants from the *Solenaceae* family (principally *Nicotiana tabacum*), has been assumed for centuries by the natives in South and North America and, later on, by the Europeans, as a major component of tobacco plants manufactured in the cigarettes making process. In 1857, the French physiologist Claude Bernard identified the chemical nature of transmission at the neuromuscular junction by exposing muscles to the plant toxin nicotine. Subsequently, it was shown that ACh is released in the neuromuscular junction cleft and that it diffuses into a very small extracellular space, where it acts on postsynaptic receptors and thereby mediates neurotransmission. These effects were inhibited by an induced paralysis through the action of the natural nicotinic blocking agent curare, while the muscle could still be directly stimulated by an electrical current.

Studies on plant extracts, such as nicotine, curare and the natural alkaloid muscarine, the latter isolated from the mushroom *Amanita muscaria*, have facilitated the distinction between nicotinic and muscarinic cholinergic neurotransmission, as a function of differential sensitivity either to nicotine or muscarine. The dual action of ACh through individual cholinergic pathways was further supported by the discovery of distinct endogenous target proteins: the muscarinic receptors (M_1 – M_5), which are metabotropic or G-protein coupled receptors, and the nicotinic receptors, that belong to the family of ionotropic or ligand-gated channels.

1.2. Neuronal nicotinic acetylcholine receptors

Neuronal nicotinic acetylcholine receptors (nAChRs) are pentameric ligand-gated ion channels widely distributed in both the nervous system and non-neuronal tissues. In the CNS they are principally found at presynaptic or preterminal sites where are associated with the modulation of neurotransmitters release. On the other hand, nAChRs located on cell bodies or dendrites are known to mediate postsynaptic effects if stimulated to a threshold level.[1]

The nAChRs mediate fast synaptic transmission in ganglionic neurons, whereas in the mammalian CNS they exert mainly a modulatory influence, being involved in a wide range of physiological and pathophysiological processes related to cognitive functions, learning and memory, arousal, reward, motor control, and analgesia.[2] In addition to rapid changes in membrane potential, activation of these ligand-gated ion channels can generate longer-lasting effects in the receptive neurons, which contribute to the elaboration of complex intracellular signals that mediate medium- to long-term events.[3] It is primarily because of their modulatory input to neurotransmitter systems other than ACh that neuronal nAChRs have been proposed as potential therapeutic targets for the treatment of pain, nicotine and other drugs addiction, epilepsy, and a wide range of neurodegenerative and psychiatric disorders such as Alzheimer's disease, Parkinson's disease, Tourette's syndrome, schizophrenia, anxiety, and depression.

The nAChRs are formed by five subunits arranged around a central pore that is permeable to cations. To date, 12 mammalian neuronal nicotinic subunits ($\alpha2$ – $\alpha10$ and $\beta2$ – $\beta4$) have been identified and cloned, resulting in a huge diversity of possible combinations (Figure 1), though only a small subset of stoichiometries gives rise to functionally and physiologically relevant channels.[2] These subunits can form homomeric pentamers (consisting of only one type of subunit, as in the case of $\alpha7$ nAChRs) or heteromeric pentamers (consisting of combinations of various α and β subunits).[4]

Conversely, the muscle nAChRs, localized within the neuromuscular plate, are shaped by the arrangement of five different subunits: α1, β1, γ, δ and ε. Each nAChR subunit is encoded by a single gene, generating a cluster of 16 genes widely distributed in the 23 human chromosomes.[5,6] It is assumed that these genes have progressively diverged from a common ancestor by gene duplications and mutations, leading to the gene structures observed at present in humans. In this respect, it is worth mentioning that closely related nAChRs have been conserved throughout evolution in the simplest forms of life, such as molluscs, worms, echinoderms.[7] Moreover, several lines of evidence suggest that the ionotropic ion channels found in bacteria, which share a high degree of structural homology with the human nAChRs, can be used as prototypes in the elucidation of the 3D structure of the nAChRs.[8,9]

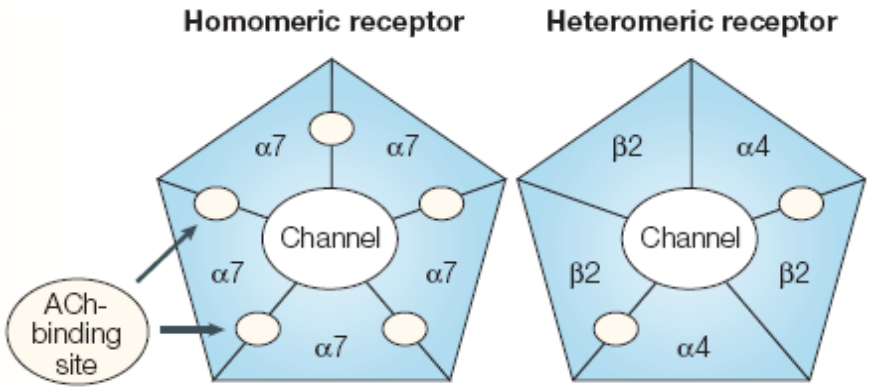

Figure 1. Examples of homomeric and heteromeric nACh receptors.

Each subunit of the neuronal nAChRs consists of a number of distinct functional domains (Figure 2):[10]

- a long *N*-terminal extracellular domain (consisting of about 210 amino acids), which is involved in binding to endogenous neurotransmitter ACh or exogenous ligands and holds a conserved disulfide bridge between two cysteine residues separated by 15 amino acids (known as the *Cys*-loop).
- four highly hydrophobic α-helical transmembrane domains, about 20 residues long, called M1, M2, M3 and M4.[11] The M2

segments shape the lumen of the pore in the ion channel and determine ion's conductance and selectivity.

- a long cytoplasmic loop between M3 and M4 containing several phosphorylation sites, which are important in the functional modulation, and other shorter loops connecting the domains.
- a short extracellular *C*-terminal domain.

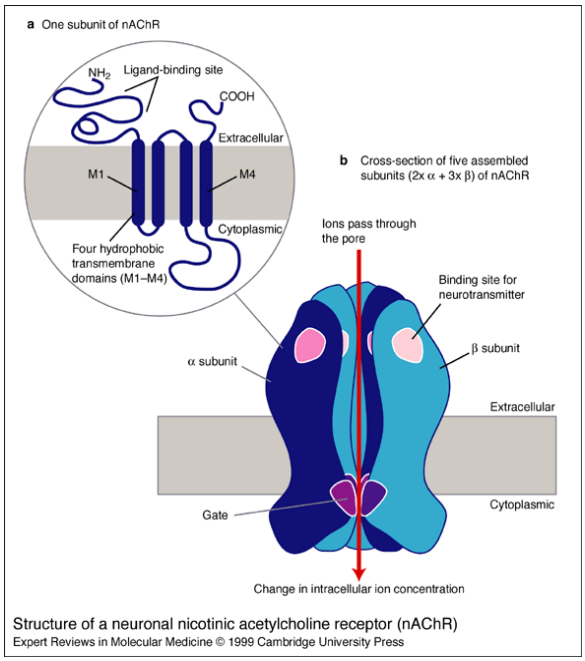

Figure 2. Structure of a neuronal nicotinic acetylcholine receptor. (a) Functional domain of the receptor through the membrane: the amino terminal hydrophilic portion, four transmembrane domains and the small hydrophilic *C*-terminal domain. (b) Schematic representation of the receptor, the location of the two acetylcholine (ACh) binding sites between an α and β-subunit (or α–α subunit) and the central ion conducting channel.

The orthosteric binding sites (i.e., the binding sites for ACh) are located at the interface between two adjacent subunits, that are an α and a β subunit in the case of heteropentameric receptors, or two α subunits in the case of homopentamers. The α subunit constitutes the principal component of the binding site (the major subunit), whereas the adjacent subunit provides the complementary site (the minor subunit). The major subunit shapes an aromatic region of the orthosteric binding site known as the *aromatic box*, and is characterized by a disulfide bridge between two adjacent cysteine residues

known as the *C*-loop. α-Homopentamers can host and bind five molecules of ACh or exogenous orthosteric ligands, while α/β heteromeric receptors are bound by a variable number of ligands depending on the ratio of α and β subunits. Like all cell-surface ligand-gated ion channels, nAChRs modulate the flow of ions across the cell membrane and are under the control of an extracellular signalling molecule. A net influx of cations (usually Na^+, Ca^{2+} and K^+ cross nicotinic channels) through the associated channel pore depolarizes the cell membrane and increases neuronal excitability, thereby causing an excitatory postsynaptic potential (EPSP).

1.3. Functional states of nAChRs

ACh, the natural endogenous ligand for nAChRs, is released from presynaptic cholinergic axon terminals and binds to the extracellular ligand binding domain (LBD) of the receptor that, in turn, influences the rate constants between three distinct functional states of the receptor itself (Figure 3): the resting (R), the open or active (A) and the desensitized (D and I) state.[2,12,13]

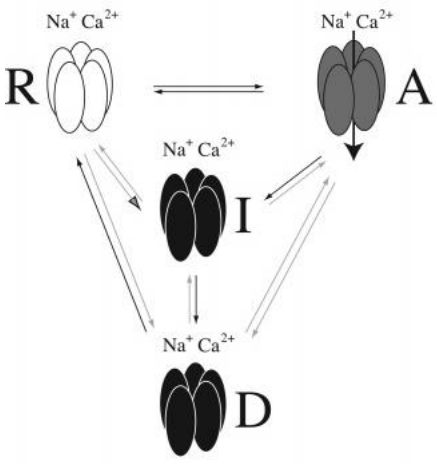

Figure 3. Functional states of nAChRs according to the Monod-Wyman-Changeux (MWC) model. Allosteric transitions between the resting (R, white complex), active (A, dark-gray complex), and fast-onset (I) and slow-onset (D) desensitized states (black complexes) of the nAChR.[2]

The equilibrium between two states is determined by the differences in the free energy of the states and the rate for the transition from one state to another is controlled by the energy barrier between the two states. The activation process is rapid and transient (microsecond-to-millisecond range), while the desensitization is slower (millisecond-to-second range). The rate constants between the functional states are highly dependent on the specific combination of subunits and the chemical nature of the ligand that is bound at the LBD. Therefore, different rates of the activation and desensitization processes were observed among different nAChR subtypes and this could account for the pharmacological diversity within this receptor family. The transition rates can also be affected by endogenous or exogenous allosteric modulators (i.e., compounds binding to protein recognition sites different from the orthosteric site) of the channel function *via* an effect on the equilibrium between the resting and the active receptor states or on the desensitization kinetics.

Binding of an agonist to the orthosteric sites of the nAChR stabilizes the active state of the channel, while a competitive antagonist favours the resting states. Agonists are characterized by higher affinity for the active than for the resting state whereas antagonists have higher affinity for resting/inactive receptor states. In addition, nAChRs show spontaneous constitutive activity in the absence of agonist, however binding of an agonist to the orthosteric sites dramatically increases the probability of channel opening.

The synchronized release of neurotransmitter at a synapse leads to a sharp rise in ligand concentration at the postsynaptic membrane such that many receptors become occupied and then open within a few milliseconds. Neurotransmitter levels fall quickly due to active reuptake into presynaptic sites or metabolic breakdown and diffusion away from the synapse. The low affinity of fast ligand-gated channels for the endogenous agonist allows for very fast dissociation from the binding site and thus a rapid termination of postsynaptic signalling. These specific biophysical properties of nAChRs are critical for fast synaptic transmission at excitatory autonomic ganglia and at the neuromuscular junction. However, in the mammalian brain, nAChRs are

primarily located on presynaptic, perisynaptic and extrasynaptic sites, and neuronal nAChRs thus exert a preferred functional role in modulating the release of various neurotransmitters (e.g., glutamate, GABA, dopamine, norepinephrine) *via* presynaptic sites of action (Figure 4).

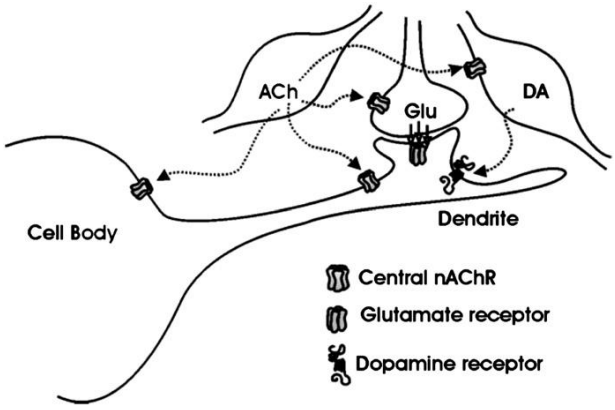

Figure 4. Neurotransmission mediated by nAChRs in the mammalian brain. Nicotinic receptors reside primarily outside of the synaptic cleft and influence cell excitability on postsynaptic cells and neurotransmitter release at presynaptic sites. In contrast, nicotinic receptors at the neuromuscular junction and the autonomic ganglia mediate fast synaptic transmission.

1.4. Receptor activation, deactivation and desensitization

An agonist is defined as a small molecule that binds to a receptor and activates it. As previously described, when the natural neurotransmitter ACh binds to the extracellular domain of nAChRs, the resulting change of conformation opens the channel triggering ion gating and propagation of electrical signals.[14]

Partial agonists, discovered in the 1950s, are defined as agonists that could produce only a sub-maximal response (less than a full agonist) even in case of saturation of the binding sites.[15] The model proposed for ion channel receptors consisted in an equilibrium between a shut and an open conformation, with the binding of the agonist being able to shift such an equilibrium towards the open state, due to the higher affinity of the agonist for the open than the shut state. Recent reports[14,16] on the nature of partial

agonism in the nicotinic receptor superfamily have proposed the existence, in the presence of the ligand, of an intermediate pre-open state called *flip*-state and have hypothesized that the partial agonism is not a property associated to the open-shut transition, but arising in the earlier conformation change from the resting state to this flipped state (Figure 5).

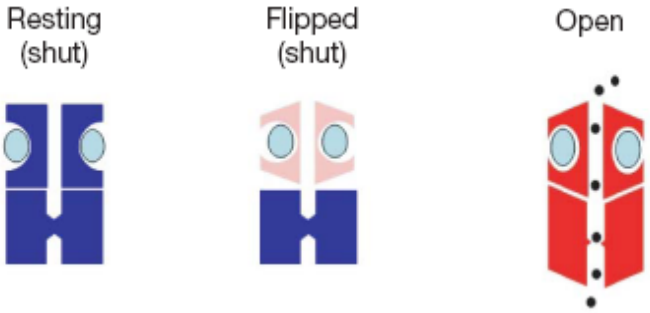

Figure 5. The three states of the fully saturated receptor.[11]

Crystals of the ACh binding proteins (AChBPs) LBD from *Lymnea stagnalis* and *Aplysia californica* have enabled atomic resolution of the structure of the *N*-terminal domain and its association with agonists and antagonists.[17-20] Crystal structures comparing apo conformations to ligand-bound conformations reveal large movements of the *C*-loop of the principal component, which adapts its configuration to the structural characteristics of the ligand entering the binding pocket, swinging as much as 11 Å between the two most extreme positions. The available data suggest that the *C*-loop, which harbours two adjacent cysteins, has a certain degree of mobility and that agonists are compounds that stabilize it in a contracted form in close apposition with the adjacent subunit, whereas antagonists stabilize it in an extended form.[21,22] The changes in the conformation of the *C*-loop might control the opening/closure of the channel. After all, it has been also proposed that the channel conductivity is modulated by the reciprocal interaction of three specific amino acids, and therefore ligands can act perturbing their contacts leading to the activation the channel.[23]

From the agonist-bound open conformation, nAChR channels will transit to a non-conducting state, either by dissociation of the agonist from the receptor,

known as deactivation, or by an agonist-bound conformational change to a high affinity, non-conducting state, called desensitization. Deactivation is the transition from the open state to the resting state associated with dissociation of the agonist from the LBD. The rate of deactivation plays a critical role in determining the fraction of channels in the open state, which is the faster the rate of deactivation is, the greater will be the drive from the open state back to the resting state. Deactivation is particularly important in controlling steady-state macroscopic currents in response to sustained exposure to low agonist concentrations. Some positive allosteric modulators have been demonstrated to enhance steady-state current by slowing deactivation rate. Receptor desensitization is a conformational transition to a relatively stable and non-conducting agonist-bound state that has high ligand affinity. This inactivating effect emerges mostly at high agonist concentration or at prolonged agonist exposure. Parameters that characterize receptor desensitization include the rate of desensitization, the degree of inhibition caused by sustained agonist exposure and the rate of recovery from desensitization upon removal of the agonist. It is worth mentioning that α and β subunits contribute differentially to the desensitization properties of heteromeric receptors.[24] Moreover, the desensitization of a receptor can further be influenced by kinases and phosphatases activity, suggesting the possibility of dynamic modulation of receptor functions.[24]

1.5. Receptor upregulation

It is generally accepted that sustained exposure of ligands to various cell surface receptors causes, at first, receptor activation and downstream cellular responses, followed by consequent receptor internalization and therefore *downregulation* of the receptor at the cell surface. Surprisingly, several data have reported an increase in surface nAChRs levels following repeated exposure to nicotine in both laboratory animals and *in vitro* studies.[25,26] This *upregulation* process, which causes also an increase in functional response

as measured by agonist-evoked whole cell current of Ca^{2+} influx, appears to be intrinsic to the receptor and can be explained by some post-translational conformational involvements, since nAChR subunit mRNA levels are not changed. Upregulation has been reported for different receptor subtypes including $\alpha4\beta2$, $\alpha7$, or $\alpha3$- and $\alpha6$-containing receptors, but the time course, the amplitude of the changes, as well as the sensitivity to nicotine vary depending on the subunit combinations.[27] Interestingly, incorporation of the accessory subunit $\alpha5$ into $\alpha4\beta2$ receptors prevents nicotine-induced upregulation *in vivo*.[28] This process has been identified as fully reversible upon removal the nAChR ligand, which can be either nicotine or other non-natural nAChR agonists. As a matter of fact, $\alpha4\beta2$ or $\alpha7$ agonists/partial agonists upregulate nAChRs *in vitro* or *in vivo*, typically about 1.5 to 5 fold, suggesting that some of these compounds are more potent at upregulating that at activating nAChRs. Nicotinic antagonists, albeit with lower potency, can also upregulate nAChRs, whereas they may be 2-3 orders of magnitude less potent at upregulating than at antagonizing ACh-induced receptor activation. Several mechanisms have been proposed to underlie functional receptor upregulation, such as:

- decreased receptor turnover.
- increased conformational transition of cell surface receptors from low to high sensitivity state.
- increased synthesis of new proteins.
- increased receptor assembly with increased receptor trafficking to the cell surface.
- nicotine or other nAChRs ligands acting as a chemical *chaperone*.
- changes in the subunit stoichiometry of receptors.

1.6. The generation of Ca^{2+} signals

Intracellular Ca^{2+} signals play an important role in the survival of developing neurons, the modulation of their activity and their demise.[3,29] It is thought that nAChRs are involved in the increase of intracellular Ca^{2+}. This process occurs both by direct permeation of the nAChR channel and by recruiting Ca^{2+} from several sources, including voltage-operated Ca^{2+} channels (VOCCs), which might be activated as a consequence of membrane depolarization following nAChRs activation. This amplification of the intracellular Ca^{2+} responses by activating VOCCs seems to be controlled by nAChR subtypes that do not contain α7-subunits. In turn, α7 nAChRs are highly permeable to Ca^{2+} and appear to be coupled functionally to direct activation of ryanodine (RY) receptor-dependent internal stores and the inositol (1,4,5)-triphosphate (IP3) second-messenger system, generating Ca^{2+}-induced Ca^{2+} release inside the cytoplasm (Figure 6).[3]

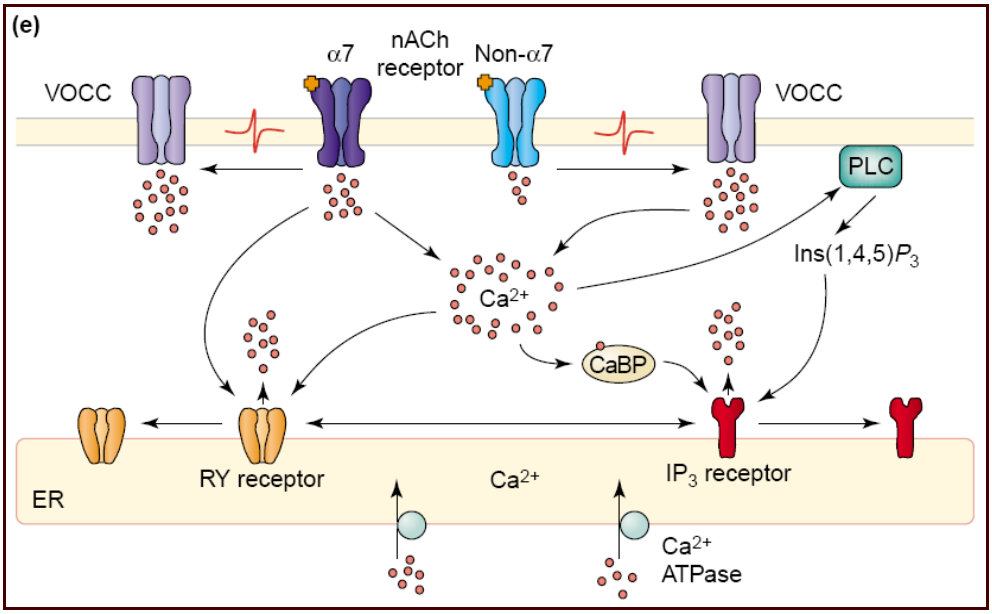

Figure 6. Generation of nAChR-dependent Ca^{2+} signals.

1.7. nAChR genes and subtypes

As mentioned previously, nAChR pentamers are formed by the association of different subunits that confer distinct structural and functional properties to the resultant nAChR subtypes, in terms of agonist affinity potential, kinetics of activation, closure, desensitization, resensitization and internalization.[4] Homopentamers are the simplest form of nAChRs as exemplified by $\alpha 7$ receptors. These receptor complexes are widely distributed in both the CNS and PNS and have been proposed to contribute to multiple physiological functions.[5] Heteropentameric nicotinic channels are composed of two or more subunit types and display a broad spectrum of physiological and pharmacological properties and functions. When considering heteromeric receptors, it is essential to examine the ratio of α to β subunits, which has been shown to influence receptor function. Of the many different subtype combinations, the most abundant are $\alpha 4\beta 2$, $\alpha 7$ and $\alpha 3\beta 4$. The $\alpha 3\beta 4$ subtype is found mainly in the PNS, whereas approximately 90% of nAChRs in the CNS are believed to be the $\alpha 4\beta 2$ subtype and the majority of the rest to be the $\alpha 7$ subtype.[2,30,31]

Genes encoding for the $\alpha 1$-$\alpha 10$ subunits are termed CHRNA (1-10) and genes encoding for the $\beta 1 - \beta 4$ subunits are referred to as CHRNB (1-4). The additional muscle subunits γ, δ and ε are encoded by CHRNG, CHRND and CHRNE genes. The chromosomal localization of the different genes encoding for the muscle and the neuronal nAChR subunits are presented in Figure 7.

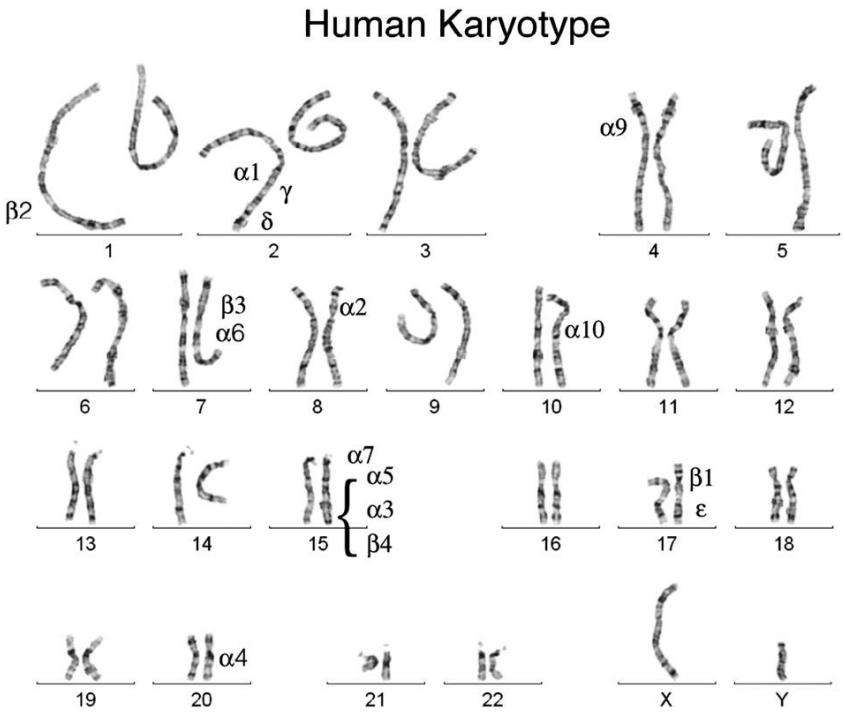

Figure 7. Typical human karyotype with the representation of the location of the genes encoding for the nAChR subunits.

The CHRNA2 gene

The CHRNA2 gene encodes for the α2 subunit and it is highly expressed in the frontal cortex. Receptors containing the α2 subunit seem to be involved in the regulation of cognitive functions and a point mutation in the CHRNA2 gene is associated with a form of nocturnal epilepsy.[32,33] However, the knowledge about the distribution and function of the α2 subunit is still limited.

The CHRNA3, CHRNB4 and CHRNA5 gene cluster

Chromosome 15 in humans groups together the CHRNA3, CHRNB4 and CHRNA5 genes, which show a close expression interaction, even between their regulatory elements, as supported by the association of certain phenotypes, such as nicotine-dependence, with this gene cluster.[34] The α3β4* channel (the asterisk indicates that other subunits may be present in the pentameric receptor architecture) is essentially expressed in ganglia, but recent studies demonstrate high levels of this receptor in other tissues and in the CNS, mainly in the interpeduncular nucleus (IPN), the medial habenula

(MHb) and the fasciculus retroflexus, a bundle of axons connecting the two structures.[35]

The exact nature of the receptor stoichiometry is still somewhat elusive. It has been proposed that at least two distinct α3β4* subtypes co-exist with different ratios of the α3 and the β4 subunits, since two forms of the α-conotoxin AuIB inhibit native ganglionic α3β4* nAChRs in a different manner, revealing a high and a low affinity site for these toxins.[36] The α3β4* complex nature is made even more complicated by the accessory α5 subunit, which is encoded by the third gene of the chromosome 15 cluster and co-precipitates with α3 and β4 subunits in a single pentamer.[37] The presence of the α5 subunit in the receptor complex changes the functional properties of the channel, particularly for the α3β4* receptors expressed in ganglia, as shown by significant discrepancies with recombinant expressed α3β4 nAChRs. While these results indicate a limited influence of the α5 protein within the CNS, more recent studies have elucidated how α5 knock–out mice display lower nicotine-evoked dopamine release and nicotine intake. The effect was completely eliminated by the re-expression of the α5 subunit in the MHb, suggesting that the α5 containing receptors are active within the IPN-MHb α3β4* system as well.[38]

Compelling evidences support the connection of the IPN-MHb pathway and nicotine-reinforcement, dependence and withdrawal by influencing the mesolimbic dopamine system.[39] The habenular blockade of α3β4* nAChRs modulates the mesolimbic dopamine response to acute nicotine, whereas an inhibitory action at the IPN level causes an increase of nicotine self-administration in animal models. This could be explained by the anatomical linkage of the MHb and the lateral habenula (LHb), a distinct compartment connected to the mesolimbic structure which controls the negative reward process. Nicotine acts in the MHb to inhibit the lateral habenular glutamatergic neurons, and the blockade of α3β4* nAChRs in the MHb removes this inhibition. However, the potential positive effects of α3β4* antagonism on chronic nicotine exposure are still uncertain.

The CHRNA4 and CHRNB2 genes

The CHRNA4 gene on chromosome 20 and the CHRNB2 on chromosome 4 encode for the α4 and β2 subunits, whose assembly leads to the major central heteromeric α4β2 nAChR. This channel protein is characterized by a high affinity for nicotine and a wide distribution in the CNS, making the α4β2 receptor the most implicated in neurotransmission processes and neurotransmitters release control among all the other nicotinic subtypes; therefore its involvement in physiological functions and pathological conditions is extensive.

It is generally accepted that the α4β2 receptor is an assembly of two α4 and three β2 subunits. However, several data have suggested the presence of two distinct α4β2 pentamers that exhibit different ACh concentration-activation curves. A high and a low sensitivity α4β2 nAChR correspond to different α4/β2 ratios present in the receptor complex, with diverse functional properties (e.g. agonist sensitivity and ion permeability) as well.[40]

The CHRNA6 gene

Located on chromosome 8, the CHRNA6 gene encodes for the α6 subunit, predominantly expressed in the ventral tegmental area (VTA) and the mesolimbic system. Its specific localization in the CNS has proposed the involvement of the α6 subunit in the striatal dopamine release and its behavioural consequences, giving much attention to this receptor subtype for the modulation of nicotine-elicited locomotion and acute or chronic nicotine self-administration. Indeed, the reduction of α6 containing cholinergic neurons has been correlated with progression of the Parkinson's disease.[41] Moreover, removal of the α6 subunit in α6 knock-out mice significantly alters their behaviour in comparison with wild type mice. The α6 protein is able to form functional heteromeric complexes such as the α6β2* receptors, which display high affinity to epibatidine, a ligand specific for heteromeric nAChRs, and overall pharmacological properties different from those of α4β2 channels,

such as enhanced ACh sensitivity, slower desensitization and markedly distinct desensitization rate and potency with nicotine.[42]

The CHRNA7 gene

The CHRNA7 gene is thought to be the closest ancestor to that evolved millions of years ago and seems to have preserved specific functionalities, as its encoded protein, the α7 subunit, is able to form functional homomeric receptors widely distributed in the CNS, PNS and other extra-neuronal tissues and cells (e.g., lungs, macrophages), with high calcium permeability, fast desensitization and specific sensitivity to certain toxins (e.g. bungarotoxin). Intensively used as a tool to examine nAChRs structure-function relationships, the α7 channel is with no doubt involved in several pathological conditions, from central cognitive disorders, such as schizophrenia and Alzheimer's disease, to peripheral processes, like inflammation and mutagenesis.

CHRNA7 is located on chromosome 15 and has a unique structural organization with a different number of introns and splicing sites than other nicotinic genes. Moreover, exons 6-10 of CHRNA7 are duplicated nearby in a gene copy termed CHRFAM7A. This duplicated gene is expressed in certain cells and the corresponding protein product is thought to somehow interact with the α7 receptor. The activity of CHRFAM7A might *downregulate* the functionality of the α7 pentamer, which could serve as an additional mechanism to fine-tune functional expression of nAChRs.[43] Recently it has been reported that the α7 subunit may potentially co-assemble with other nAChR monomers. Particularly, receptors co-expressing α7 and β2 are inhibited by amyloid β (Aβ), thus correlating this novel and interesting nAChR complex with the cognitive impairments observed in Alzheimer's patients.[44]

The CHRNA8, CHRNA9 and CHRNA10 genes

Few studies have focused their attention towards the α8 subunit, encoded by the CHRNA8 gene. This protein is quite similar to the α7 subunit, but the corresponding homomeric channel is poorly distributed and therefore less studied.

Conversely, the homopentamer α9, built up of five CHRNA9 gene proteins, is still sparsely found in the CNS, but with a distinctive expression in the outer hair cells of the inner ear, giving the α9 nAChRs a potentially meaningful pharmacology. Furthermore, new studies have pointed out the presence of this protein complex in other tissues other than the inner ear, i.e. it could play a role also in the pain perception pathway.[45]

The CHRNA10 gene encodes for the α10 subunit, which has displayed the attitude to co-assemble with the α9 protein. High level of α9α10 nAChRs have been found in the sensory neurons of the sacculus in the vestibular organ.

The CHRNB3 gene

The CHRNB3 gene is probably the less studied nicotinic gene. Encoding for a subunit lacking the two adjacent cysteines which form the *C*-loop, and therefore for a β subunit, this gene might be related to some pathological conditions, since variants and mutations of CHRNB3 have been associated with certain smoking behaviours, as well as alcohol consumption and bipolar disorders. The β3 protein may behave as an accessory and modulatory subunit, since it is expressed in a few peculiar nicotinic channels, such as the α6β4β3α5 subtype.

1.8 Therapeutic potential of nicotinic drugs

The correlation of neuronal nAChRs with neurotransmission and physiological processes raised a lot of interest in the nicotinic system as potential target for a number of psychiatric, neurological and peripheral disorders. However, only one nAChR ligand has been approved and introduced into the market in the last 50 years: the α4β2 partial agonist varenicline for smoking cessation. The main reasons for the lack of effective nicotinic therapies reside mainly in the unsatisfactory clinical efficacy and in a relatively high incidence of adverse events. In the case of nicotinic drugs, the most common side effects appear to be gastrointestinal and CNS

consequences, while the less common cardiovascular events have to be monitored given the nicotine effects on both heart rate and blood pressure.

It is well accepted that the lack of efficacy showed by nicotinic drugs could be explained as a result of several factors:

- the nicotinic target may not be directly involved in the pathology of the disease.
- at clinical doses the compound may not achieve efficacious unbound concentrations at the target receptor.
- the compound may have insufficient potency and/or selectivity for the target subtype.

Pharmacological, biological and genetic evaluations are required to better understand the physiopathology of a certain disease or disorder, and drug delivery systems represent the technological response to specifically increase the drug levels at the target compartment. On the other side, medicinal chemistry, through both structure-activity relationships (SAR) and molecular modelling studies, is the science called to improve the interaction between drugs and the biological counterparts at a molecular level. That means to increase potency (in terms of either binding affinity or functional activity) and selectivity (i.e., the ratio of affinities at the target to other proteins/target subtypes) of a candidate drug. For example, a compound with moderate potency and suboptimal pharmacokinetics will require high doses for a therapeutic effect, but its selectivity may be insufficient to prevent a high incidence of side effects. Thus, although a high binding selectivity for a nAChR target vs. other nicotinic subtypes is typically reached at a nM/μM ratio level, when considering functional activation/inactivation potencies, which usually require concentrations (EC_{50} or IC_{50}) in a relatively narrow μM range, a compound can display high binding selectivity and be functionally non-selective at all. As previously described, aiming at nAChR subtypes selectivity can reduce the overall count of side effects and also lead to the modulation of the specific nicotinic ion channel involved in the signal pathway that exacerbates the targeted pathological condition or symptoms.

Alzheimer's Disease

Alzheimer's Disease (AD) is a neurological degenerative disorder in which the cholinergic pathways are severely affected and it is characterized by a progressive deterioration of higher cognitive functions. AD is the most common form of dementia and an involvement of nAChRs in AD is supported by the consistent reduction of these receptors observed in post-mortem brain tissues from patients, significantly associated with cognitive impairments.

Extracellular neuritic senile plaques and intracellular neurofibriallary lesions are considered typical marks of the disease; moreover, it has been shown that, in patients with AD, choline acetyltransferase activity is decreased.

Recent efforts have focused on the high affinity interactions between nAChRs, mainly $\alpha7$ and $\alpha4\beta2$ subtypes, and Aβ, a constitutive peptide which under normal physiological conditions has several roles in enzymes activation and hormone levels regulation, and it is, on the other hand, the main component of neuritic amyloid plaques found in brains of patients with AD. The specific interaction between $\alpha7$ nAChR and Aβ is very effective under normal physiological conditions (binding affinity in the low pM range) and it may play an important role in the regulation of synaptic plasticity and, consequently, neuronal degeneration.[46] From a functional standpoint, binding of Aβ to both $\alpha7$ and $\alpha4\beta2$ nAChRs has been reported either to inhibit or to activate the receptors.

AD patients treated with both $\alpha7$ or $\alpha4\beta2$ nicotinic partial/full agonists have shown interesting improvements in concentration and some verbal and non-verbal skills, suggesting that AD could benefit from the development of more selective nicotinic drugs, notably targeting the $\alpha7$ channel. Besides, enhancing the cholinergic transmission via ACh-esterase inhibitors is still the best protocol today for the treatment of AD patients.

Parkinson's Disease

Parkinson's Disease (PD) is a progressive neurodegenerative disorder involving the dopaminergic neurons of the *substantia nigra*. Similarly to AD, a marked reduction in nAChRs activity, resulting in impaired cognitive functions,

has been observed. The disease is characterized by muscle rigidity, tremor, a slowing of physical movements and, in extreme cases, a loss of physical movements. Secondary symptoms may include cognitive dysfunctions and subtle language problems. PD is both chronic and progressive and it has been shown by epidemiological studies that a negative correlation exists between smoking and the incidence of PD, suggesting that nicotine in tobacco contributes to the biological protection against neurodegeneration of dopaminergic neurons. The two nAChR populations largely responsible for the nicotine-evoked dopamine release in striatum are the $\alpha4\beta2$ and $\alpha6\beta2$* subtypes, the latter displaying a higher connection to nigrostriatal damage induced in animal models. Thus, targeting specific nAChR populations represents a promising strategy for long-term neuroprotection against further striatal damage and for a symptomatic relief by enhancing dopamine outflow.

The use of full/partial $\alpha6\beta2$* or $\alpha4\beta2$ agonists should evoke dopamine release by activating nicotinic ion channels that are still present in patients affected by PD. Nevertheless, a second possible mechanism, which seems to be less dependant on the presence of functional $\alpha6\beta2$* and $\alpha4\beta2$ nAChRs, is the selective pharmacological chaperoning of nAChR number and stoichiometry, by which nicotine or other nAChR ligands could restore to some extent the receptor deficit in the *substantia nigra*. In this case, both nAChR agonists and antagonists could have a therapeutic effect by acting as chaperones and increasing the number of functional $\alpha6\beta2$* or $\alpha4\beta2$ receptors.[47]

Tourette's Syndrome

Tourette's Syndrome (TS) is an inherited hyperkinetic neuropsychiatric movement disorder related to excess dopamine transmission in the striatum, with symptoms of persistent, sudden, rapid and brief, stereotyped motor movements or verbal tics. Onset of symptoms typically occurs in childhood and the exact mechanism of the pathology is not fully understood but it is believed that nAChRs are involved. In fact it has been shown that transdermal

nicotine can reduce some of the symptoms, probably desensitizing the nicotinic receptors that control dopamine release ($\alpha4\beta2$ and $\alpha6\beta2$* subtypes).

Schizophrenia

Schizophrenia is a psychiatric diagnosis that describes a mental disorder characterized by abnormalities in the perception or expression of reality. It most commonly manifests as auditory hallucinations, paranoid or bizarre delusions or disorganized speech and thinking in the context of significant social or occupational dysfunction. The constellation of symptoms can be subdivided into positive (e.g., hallucinations and delusions), negative (e.g., flat affect and social withdrawal) symptoms and impaired cognition. Typically, the antipsychotic drugs used in the schizophrenia treatment are efficacious at the positive and to some degree negative symptoms, while there's a great need for the treatment of the cognitive impairments associated with this disorder, which could represent the core of the disease.

Various studies have demonstrated that the use of tobacco transiently restores the schizophrenic patient's cognitive and sensory deficits.[48] The number of $\alpha7$ nAChRs is reduced in post-mortem schizophrenic patients and the association of $\alpha7$ receptor subunit gene with an auditory deficit was found,[49] suggesting the development of novel $\alpha7$ selective agonists for the treatment of this pathology.[48,50] There are less biological data linking the $\alpha4\beta2$ nAChR to schizophrenia, but substantial preclinical evidence has shown that agents that selectively interact with $\alpha4\beta2$ nAChRs could enhance cognitive performance in schizophrenic patients.

Pain

The effects of nicotinic ligands in antinociception and analgesia are well established[51,52] and the activation of nAChRs produces antinociception in a variety of acute or chronic animal pain models.[53] Control of pain is one of the most promising therapeutic applications of nicotinic drugs and the $\alpha4\beta2$ nicotinic subtype receptor has been identified as being involved in the antinociceptive activity, but other subtypes could also contribute.[52,54] Gao

and co-workers have individuated the superficial dorsal horn of the spinal cord as the site where several nAChR subunits (mainly α3, α4, α5, α7, β2 and β4) increase inhibitory GABAergic and glycinergic transmissions, which have a prominent role in pain suppression.[55] The authors have found that an agonist-induced activation of α4β2 nAChRs is necessary, but not sufficient, for analgesic activity. Indeed, activation of α3 might play an additional role, while the α7 proteins seem to be less relevant. Several α7 agonists tested in animal models producing analgesic effects have failed to potentiate inhibitory synaptic transmission in the spinal cord at selected doses. As a matter of fact, the analgesia observed for these compounds required high doses, resulting in a narrow therapeutic range.

Smoking cessation

Tobacco smoking is one of the leading causes of preventable mortality in industrialized countries and nicotine-dependence is probably mediated through the activation of multiple nAChRs, in particular the α4β2 subtype.[56] Partial agonists of α4β2 nAChRs could enhance the activity of these receptors sufficiently to blunt craving and withdrawal without associated abuse potential;[57] these considerations led to the development of the partial agonist varenicline[56] (by Pfizer) as a novel protocol to treat smoking cessation. It is uncertain whether higher agonist activity would improve clinical efficacy or negatively impact the side effect profile, in particular abuse liability. However, it seems that minimal agonist activity is necessary, since α4β2 antagonists are not very effective in smoking cessation treatments.

More recently, two novel nAChR subtypes emerged as potential targets for the treatment of nicotine addiction. The α6β2* nAChRs are activated by nicotine at the concentrations in the smokers' brain, with slower desensitization rate, leading to substantial striatal dopamine release.[42] Many α4β2 nicotinic drugs for smoking cessation, varenicline as well, display also an α6α4β2 partial agonist profile. At last, as described previously, the MHb α3β4* nAChRs inhibit the LHb glutamatergic system, which interacts with the neurons of the VTA, implicated in the reward circuit by mediating dopamine

release at the mesolimbic level.[39] So, α3β4* blocking agents might be considered as innovative and alternative molecules for the treatment of nicotine abuse and dependence.

Alcohol use disorder and other drugs dependence

The high comorbidity of nicotine and alcohol dependence can be in part explained by common underlying cholinergic mechanisms. Ethanol, but also several other drugs of abuse (e.g., cocaine, opioids, stimulants like amphetamine), can influence many receptor systems and activate the brain's reward system through nAChRs. As mentioned above, the α3β4* receptors localized in the MHb and IPN modulate the sense of reward by suppressing the LHb-mesolimbic pathway. Thus, numerous α3β4* partial agonists, as well as α4β2 selective compounds like varenicline, have been monitored for the treatment of alcohol use disorder.

On the other hand, updated experiments describe the ineffectiveness of habenular α3β4* receptor blockade on accumbal dopamine release enhancement stimulated by acute injection of addictive drugs.[39] As a matter of fact, the α3β4* negative allosteric modulator 18-methoxycoronaridine (18-MC) more potently restrains craving and withdrawal induced by nicotine than the same effects induced by other drugs of abuse. This difference may occur because an acute nicotine injection directly stimulates nicotinic receptors in both the MHb-IPN and the mesolimbic dopamine pathway. The linkage of nicotinic receptors and accumbal dopamine release enhancement induced by other drugs, such as opioids or stimulants, may only occur as a result of modulation of the mesolimbic pathway by the MHb-IPN system and after chronic or sensitizing regimen of drug administration. This is evidenced by the decrease of chronic self-administration of methaamphetamine and morphine in animal models treated with α3β4* blocking agents such as 18-MC or α-conotoxin AuIB.

Depression

The Janovski's cholinergic-adrenergic hypothesis of depression postulates that hyperactivity of the cholinergic system contributes to depression, a state of low mood and aversion to activity that can have a negative effect on a person's thoughts, behaviour, feelings, world view and physical well-being. Since ACh esterase inhibitors can elicit or exacerbate depression symptoms, it is thought that nAChR antagonists or partial agonists may have positive effects, as shown by the natural nicotinic antagonist mecamylamine. The reduction of activity of $\alpha4\beta2$, $\alpha7$ or $\alpha3\beta4$* nAChRs seems to be the key to decrease the cholinergic transmission and to relief depression mood.

1.9. Pharmacophore models

A pharmocophore is generally considered to be an ensemble of the *minimal* structural features common to active molecules that are recognised by an individual receptor.[56] Early nicotinic $\alpha4\beta2$ pharmacophore models were based on distances between common elements in the classical agonists, typically (i) a basic nitrogen (N^+) (which is protonated under physiological conditions) and (ii) a hydrogen bond acceptor (HBA) and/or a π-electron rich moiety (π) with a relative separation of cationic and HBA/π groups ranging from 4.4 to 6 Å (Figure 8).

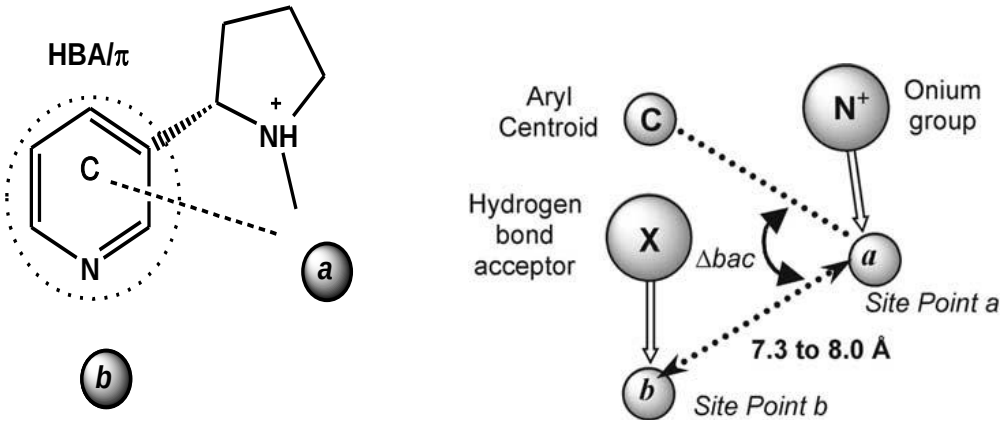

Figure 8. Pharmacophore elements and (*S*)-nicotine.

Recent studies[57-59] have indicated a more complex mode of action, and variations between the proposed pharmacophore models could derive from the individuation of additional elements: a ring centroid (*C*) or an atom in the ligand defining the direction of the ligand-receptor hydrogen bond, a planar area on the receptor recognizing the π-electron rich moiety of the ligand, one or two points (*a* and *b*) on the receptor, with which N^+ and HBA interact, and the angle between two distance vectors chosen out of those joining the various pharmacophore elements. Experimental applications of this new pharmacophore model put in evidence that the N^+-HBA and the N^+-*b* distances are not related to the binding affinity, which has been found to be more correlated with certain molecular space limits: the distances from points *a*, *b* and *c* and the $\Delta bâc$ angle. High nAChRs binding affinity has been correlated with specific values of *a*-*b* (7.3-8.0 Å) and *a*-*c* (6.5-7.4 Å) distances as well as values of the $\Delta bâc$ (30.4-35.8°) angle.

This simplistic, but detailed, model containing the required pharmacophoric elements able to drive affinity at the nAChRs does not depict the diversity that must exist among the nAChR subtypes to account for ligands selectivity. In addition, it is conceivable that subtly different pharmacophores exist not only for different nAChR subtypes but also for different states of a particular subtype, with different molecular features preferentially favouring the stabilization of one state over the others.[57]

The 3D crystal structures of several AChBPs co-crystallized with nicotinic agonists, partial agonists or antagonists have led to human nicotinic receptor homology models engineering. Triangulating binding affinity data and docking analysis data from human nAChR models, a true target-based drug design approach became possible to obtain novel selective nicotinic ligands and raise the overall potential of the nicotinic drugs arsenal.

1.10. Octahydropyrrolo[3,4,*c*]pyrrole derivatives

A recent paper by William Bunnelle and co-workers, from the Abbott company, has underlined the importance of subtype selectivity, performing an exhaustive SAR study of a family of octahydropyrrolo[3,4,*c*]pyrrole derivatives, a group of compounds characterized by a diazabicyclic moiety in which one nitrogen is linked to a heteroaromatic ring (Figure 9a).[60] The investigated basic scaffold contains two stereogenic centers, but only two possible stereoisomers: in Figure 9a the active configuration of the series is shown. The introduction of a basic bicyclic core into the skeleton of nicotinic drugs represents a strategy that has been frequently followed to build more rigid ligands that might facilitate nAChRs selective recognition. In this case, a second nitrogen atom is present into the basic core to prevent any additional chiral carbons and therefore any further stereochemical issues. The lead compound Bun6 **1** (Figure 9b), presenting a secondary amine and bearing a 3-pyridyl ring, is a full agonist at both $\alpha4\beta2$ and $\alpha7$ nAChRs, with some preference for the heteromeric subtype.

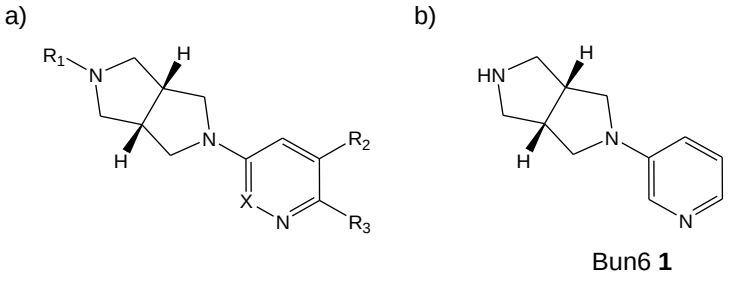

Figure 9. Structures of model compounds.

The selectivity profile of analogues of Bun6 **1** was described to be strictly dependent on the substitution pattern on the heteroaromatic nucleus (R_2 and R_3 groups). Particularly, the complementary recognition by $\alpha4\beta2$ receptors allows only small substituents in *para* position, like halogens, while in contrast more hindered R_2 groups, either aromatic or linear/ramified aliphatic chains, promote an increased binding affinity. Compounds bearing an ethoxy or *n*-propoxy substituent in *meta* position (Bun13 **2** and Bun14 **3**, Figure 10) lead

to a massive α4β2 vs. α7 selectivity ratio (41000 and >240000, respectively). The ligand Bun14 **3** exhibits high potency towards the α4β2 receptor subtype (EC_{50} = 0.37 μM) with a full agonist functional profile (118 ± 10% ACh maximum response).

On the contrary, high α7 affinity and selectivity profiles are compatible with the presence of bulkier R_3 aromatic or heteroaromatic rings, while even small *meta* functionalizations lead to a loss of α7 affinity. Compound Bun46 **4** (Figure 10), with an indolyl substituent on a pyridazine nucleus, shows an α7 vs. α4β2 selectivity ratio higher than 400000 and an almost full agonist profile at the α7 receptor (87 ± 11% ACh maximum response) coupled with high potency (EC_{50} = 0.32 μM). The α7-selective octahydropyrrolo[3,4,*c*]pyrrole termed A-582841 **5** (Figure 10), presenting a phenyl ring in position 6 of the pyridazine nucleus, was studied in phase I clinical trials as a novel enhancer of cognitive properties. This α7 ligand, which shows an α7 binding value in the low nanomolar range (K_i = 17 nM) and a better pharmacokinetic profile than **4**, has unfortunately failed phase I tests due to some adverse reactions (mainly tremors and weight loss) in an early 10-days repeated dose study.[61]

The α4β2 nAChR binding is also influenced by the nature of the aromatic ring (see group X in Figure 9): a pyridine connected to the basic core in position 3 is essential for the interaction with the heteromeric receptor complex. The α7 receptor subtype seems to be, instead, more flexible, as it tolerates various aromatic rings, i.e. pyridine, pyridazine and biphenyl.

Further interesting observations have been made upon the degree of substitution of the basic nitrogen (R_1 group). Among the α4β2-preferring ligands, secondary amines possess the correct electronic properties for a complementary and selective binding to the orthosteric site, whereas an increased substitution, moving from tertiary amines to quaternary salts, produces a significant loss of affinity. Considering the α7-selective ligands, in this case the methylation of secondary amines has a positive effect on both affinity and selectivity and, in addition, some quaternary salts do not display any drop of affinity.

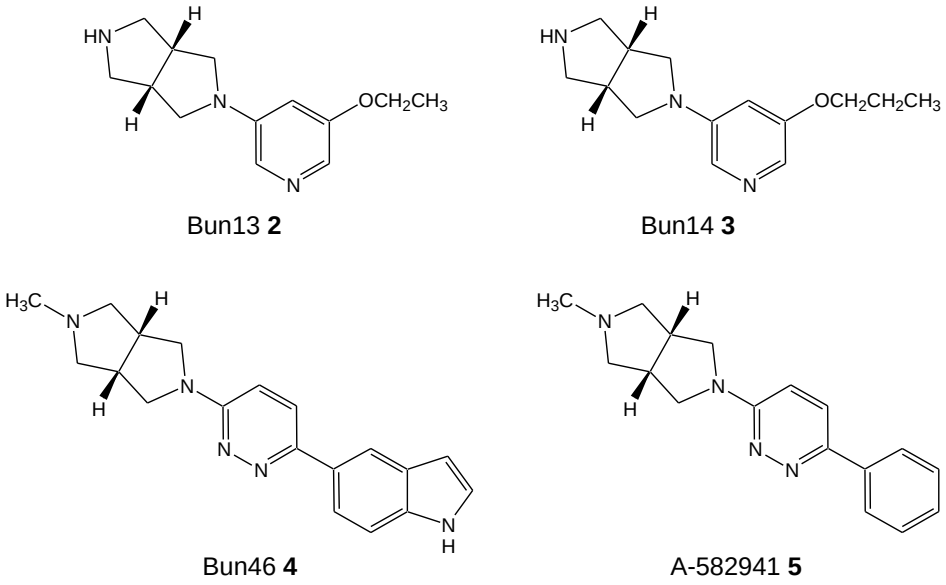

Figure 10. Structures of model compounds.

1.11. Quinuclidine-containing nicotinic ligands

The quinuclidine (1-azabicyclo[2.2.2]octane) ring system is a first choice scaffold for several α7 nAChR selective ligands. Incorporation of the basic nitrogen into this bicyclic structure has been proposed to constrain the orientation of the protonated nitrogen in a manner that facilitates both α7 nAChR binding and receptor activation. The search for novel α7 selective agonists based on the quinuclidine molecular skeleton has been and is still today an attractive goal due to the synthetic accessibility of such ligands.

In 2000, G. Mullen and coworkers[62] from Astra-Zeneca discovered AR-R17779 **6** (Figure 11), a conformationally restricted analogue of the cholinergic agonist carbachol. Compound **6** was the first reported full agonist at the rat α7 nAChR subtype, showing a meaningful α7 vs. the α4β2 selectivity of the affinity profile.

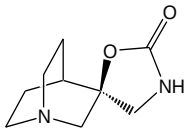

AR-R-17779 **6**

Figure 11. Structure of model compound AR-R17779.

This spirooxazolidinone derivative **6** is a potent full agonist (efficacy = 96%) for the α7 nicotinic receptor, twice as potent as (–)-nicotine, which however is a partial α7 nicotinic receptor agonist (efficacy = 59%). Whereas nicotine is poorly selective for the α4β2 nicotinic receptor, AR-R17779 **6** is selective for the α7 receptor (approximately 35000-fold more selective than (–)-nicotine). Despite a less than desirable pharmacokinetic profile, compound **6** served as an invaluable tool for *in vivo* assessment of α7 nAChR function, validating a link between its activation and a variety of biological effects.[62] A clear stereochemical preference has been observed for the (*S*)-(–) versus the (*R*)-(+) enantiomer of **6**. In addition to the poor affinity for the α7 receptor, (+)-**6** also possesses weak intrinsic activity. These results suggest that the location of the carbonyl functionality in AR-R17779 **6** is crucial to mimic ACh for molecular recognition by the α7 receptor. AR-R17779 **6** has displayed varying degrees of effects in cognition models but the shortcomings of this derivative *in vivo* have been attributed, as underlined above, to its poor pharmacokinetic characteristics.[62]

The Abbott laboratories have intensively focused their effort on quinuclidine nicotinic ligands as well. In the recent years they reported ABT-107 **7** as a novel α7 selective full agonist for the treatment of Alzheimer's disease and other cognitive disorders (Figure 12).[63] ABT-107 **7** has two distinct molecular features that are able to drive selectivity towards the α7 channel: a quinuclidine core and a pyridazine nucleus bearing an indolyl ring in *para* position. Prepared as pure *exo* epimer, this compound reveals a quite similar molecular skeleton to that of **4** (a pyridazine bearing an indolyl ring), with oxygen that in this case links the basic core to the heteroaromatic moiety. Since the linking atom has been shifted by one position compared to **4** (the oxygen atom is not part of the bicyclic structure), the protonated nitrogen has

been moved too to fulfil the pharmacophoric distances. ABT-107 **7** shows high potency in activating the α7 nAChR (EC_{50} = 50-90 nM) and in evoking human α7 receptor current (about 80% of the normalized value to ACh). In spite of its quite promising potential, ABT-107 **7** failed phase I clinical trials due to severe adverse reactions (headache, sleepiness, tremors).[64]

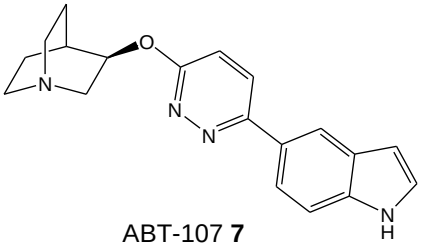

ABT-107 **7**

Figure 12. Structure of model compound ABT-107.

In 2009, after a joint venture between Targacept and Astra-Zeneca, T. A. Hauser and coworkers described TC-5619 **8** (Figure 13a) as an innovative and potent quinuclidine α7 selective anti-schizophrenia agent.[65] In the molecular structure of TC-5619 **8**, the quinuclidine core has been coupled with an aromatic amide function, which can be correlated to some extent to the ester group of ACh. A similar bioisosteric substitution was present in the structure of AR-R17779 **6**, but in the case of **8** the H-bonding chain is not constrained in a spirocyclic system, resulting in some degree of freedom. In addition, TC-5619 **8** presents an additional 3-pyridinyl-methyl substituent in position 2 of the basic scaffold. The parent series of TC-5619 **8** can be identified in a group of quinuclidine aromatic amides patented by the Bayer AG company (Figure 13b).[66] These nicotinic ligands were initially described as α7-preferring molecules, even though their affinity and pharmacological properties at other receptor systems were not discussed. The incorporation of the aromatic side pendant accomplished by the Targacept researchers apparently improved both the α7 affinity and selectivity profiles of TC-5619, which was found efficacious in the treatment of cognitive impairments in schizophrenic mouse models. Among several aromatic side chains, the 3-pyridinyl-methyl substituent evidenced better binding values and improved

functional properties. Furthermore, the authors have evaluated the required stereochemistry, indentifying the *cis* configuration as the most favourable for binding at the α7 channel.[67] TC-5619 **8** has been characterized as a potent full agonist at the α7 nAChRs (K_i = 1 nM, EC_{50} = 33 nM, 100% ACh current response), with a good selectivity towards the heteromeric α4β2 subtype (K_i = 2.3 μM). In animal models of schizophrenia, this nicotinic ligand exhibited promising control of both positive and negative symptoms. However, when tested in humans, TC-5619 **8** failed phase II clinical trials due to inadequate pharmacokinetic results.

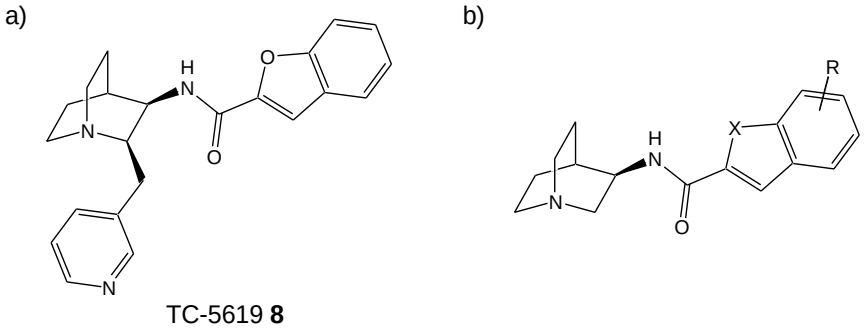

TC-5619 **8**

Figure 13. Structure of model compound TC-5619 and its parent series.

1.12. AChBP and model natural compounds

AChBPs are ligand-gated ion channels isolated from the glial cells of several molluscs and used as tools to characterize and study nAChRs and to develop novel nicotinic drug candidates. The 3D structures of different AChBPs co-crystallized with both natural and synthetic nicotinic ligands have been resolved, permitting the comprehension of the overall molecular interactions between the channel and its respective nicotinic modulators. Moreover, homology models of human nAChR subtypes have been engineered.

Analysis within the LBD of the AChBPs isolated from *Lymnea stagnalis* (*L*-AChBP) and *Aplysia californica* (*A*-AChBP) co-crystallized with the three natural nicotinic model ligands (*S*)-(–)-nicotine **9**[68], epibatidine **10**[69] and

anabaseine **11**[70] (Figure 14) allowed identification of the key residues responsible for the receptor recognition. Among them, a group of aromatic or hydrophobic residues from the major subunit (using the *L*-AChBP numeration: Tyr89, Trp143, Trp145, Tyr185, Tyr192 and Cys187-188 linked together as the *C*-loop) is highly conserved both in diverse AChBPs and in mammalian nAChR subtypes. In contrast, residues from the minor subunit (Trp53, Gln55, Leu102, Arg104, Met114 and Val116 in *L*-AChBP) are less conserved and are generally characterized by a more pronounced hydrophilic nature.

The whole LDB can be described as a hydrophobic cavity with an aromatic portion on the major subunit (known as the *aromatic box*), which allocates the rigid and hydrophobic cyclic scaffold of the natural model compounds. The cation-π interaction, one of the strongest interactions known in chemistry, between the protonated nitrogen of the ligands and the centre of the Trp145 aromatic side chain is the driving force that directs the binding of a nicotinic ligand. The positive charge of the ligands is further stabilized by additional interactions with some carbonyl groups located in the backbone structure of the *aromatic box*. The pyridine nitrogen of the three alkaloids, recalling the ester function of ACh, is bound to the LBD through an H-bond involving certain residues, which can be either on the minor subunit (Leu102 and Met114 in *L*-AChBP) or on the major one (Trp147 and Ile118 in *A*-AChBP).

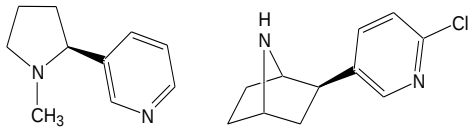

(*S*)-Nicotine **9**

Epibatidine **10**

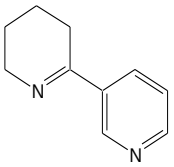

Anabaseine **11**

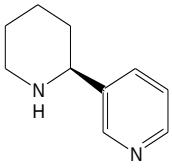

Anabasine **12**

Figure 14. Structure of natural model compounds.

Further comments should be done for anabaseine **11**. Isolated from the skin of the sea worm *Paranemertes peregrina*, this molecule is chemically correlated to anabasine **12** (Figure 14), a minor component of *Nicotiana tabacum* and a higher ring-size homologue of (–)-nicotine **9**. Adding an unsaturation to the piperidine ring of **11** abolishes the stereogenic centre of **12** and changes the nature of the basic nitrogen from a secondary amine to a cyclic imine. The imine ring of anabaseine **11** undergoes an imine-enamine tautomerism: an equilibrium between the non-protonated imine ring, the cationic closed immonium core and the charged open ammonium-ketone is possible under physiological pH conditions. Several studies established that the charged immonium ring is the active species of anabaseine **11**.[71] In addition, the unsaturation of the cyclic imine core is partly delocalized by the pyridine electron orbitals, hence allowing a modest coplanarity between the two ring systems. Conversely, (–)-nicotine **9** and epibatidine **10** show a perpendicular orientation of the basic scaffold with respect to the pyridine ring.

Recently, it has been proposed that water molecules might have a relevant role in the ligand-receptor interaction. The 3D structures of two AChBPs co-crystallized with (–)-nicotine **9**[68] and anabaseine **11**[70] put in evidence the presence of a water molecule in the LBD that is able to positively contribute to the stabilization of the receptor-ligand complex (Figure 15). Indeed, a water bridge connects the pyridine nitrogen to some protein residues (Leu102 and Met114 in *L*-AChBP and Ile106 and Ile118 in *A*-AChBP). However, it is unclear whether the water molecule contributes by directly creating a H-bond with the ligand or by enhancing the electronic and hydrophilic properties of the LBD. The water molecule might have a primary action by bridging some key residues from the LBD to the ligand, but it might also play a role in predisposing an accessible environment within the LBD. As reported, the nicotinic orthosteric cavity is predominantly hydrophobic in nature, which should prevent the interaction with charged compounds. The LBD solvation mediated by water molecules might contribute to creating a less hydrophobic environment which facilitates the hosting of the ligand.

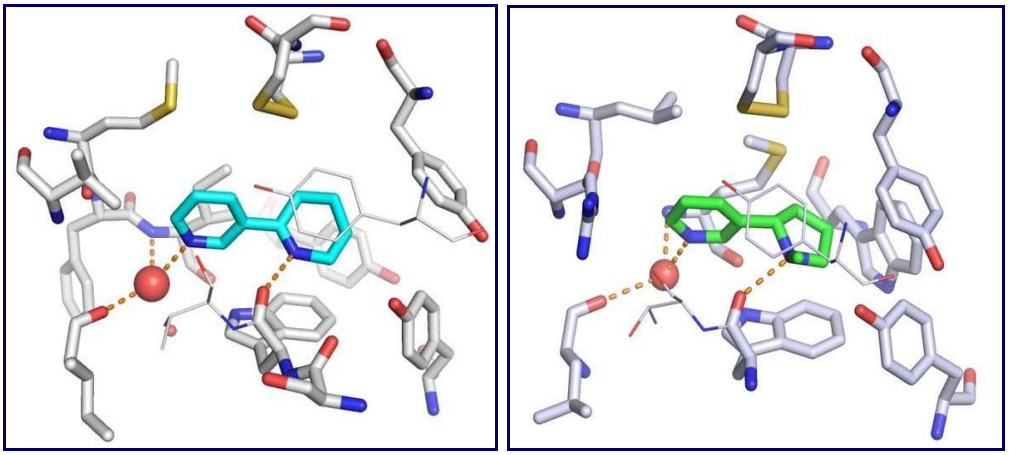

Figure 15. LBD of *L*-AChBP co-crystallized with anabaseine **11** (left) and *A*-AChBP co-crystallized with (*S*)-nicotine **9** (right). The water molecules are depicted as red spheres.

Our research team elaborated and validated the models for the human α4β2, α3β4 and α7 nAChRs,[72,73] and preliminary molecular docking and dynamics were performed to evaluate also the putative role of water molecules in the binding mode of the reference alkaloid epibatidine **10** into the active site of the α4β2 homology model. Epibatidine **10** was docked within the α4β2 LBD and a water molecule bridging the backbones of β2-Leu119 and β2-Asn107 to the pyridine nitrogen of the ligand was included, thus reproducing the spatial arrangement found in the crystal structure of (–)-nicotine **9** within *L*-AChBP.[68] As highlighted in Figure 16, after 10 ns of molecular dynamics simulations, the water molecule was still bound to the carbonyl groups of β2-Leu119 and β2-Asn107, whereas the distance between the pyridine nitrogen of epibatidine **10** and the oxygen atom belonging to the water molecule was slightly higher than that typical of an optimal hydrogen bond.

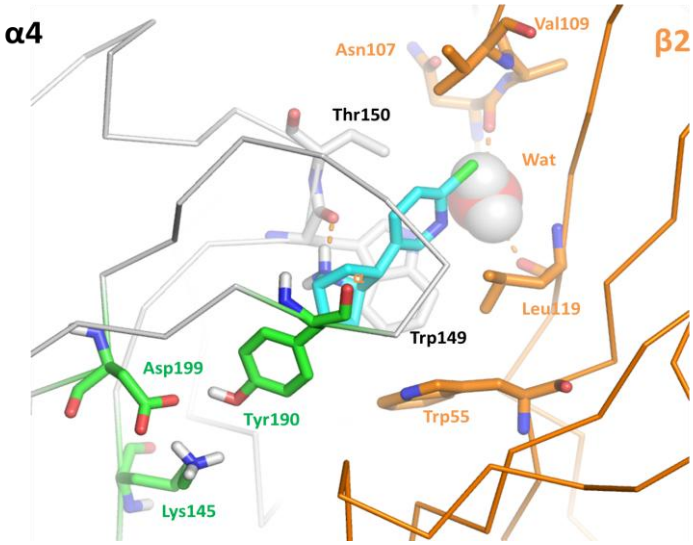

Figure 16. Epibatidine **10** (cyan) docked within the α4β2 LBD.

The same analysis was applied to the complex deschloroepibatidine/α4β2. Deschloroepibatidine **13** (Figure 17) is an analogue of epibatidine, in which the chlorine atom is missing, which shares the same affinity of the parent derivative at the α4β2 receptors. Once again, molecular dynamics simulations indicated that the water molecule was firmly bridged to the pyridine nitrogen of the ligand and to the backbone chains of β2-Leu119 and β2-Asn107. As illustrated in Figure 17, the average distances between the atoms belonging to the water molecule and the β2-backbone carbonyl groups and the pyridine nitrogen are less than 3 Å. At variance with what observed with epibatidine, the absence of the halogen atom in the structure of deschloroepibatidine **13** could promote a better interaction of the ligand with the solvated receptor binding site.

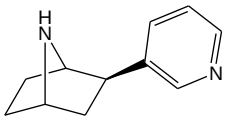

Deschloroepibatidine **13**

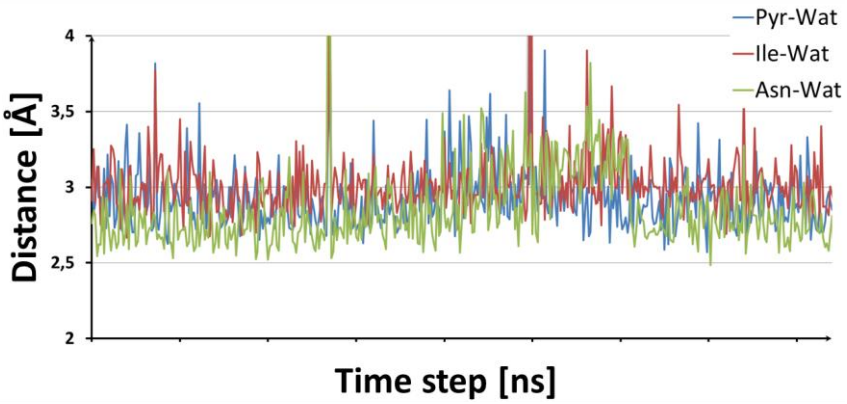

Figure 17. Structure of model compound deschloroepibatidine **13** and the distance fluctuations between the water oxygen atom and the backbone of Leu119, Asn107 and the pyridine nitrogen of the ligand during the molecular dynamics simulation performed on the **13**/α4β2 complex.

The role of solvent molecules in the nAChRs/ligand interaction has been debated in the literature: several experimental results, and even our data, suggest that water molecules, lying into the active cavity of nAChRs as well as in AChBPs, contribute to decrease the overall hydrophobicity of the binding site, giving rise to an optimal environment to accept the lone pair belonging to the pyridine nitrogen of naturally occurring nicotinic derivatives. Moreover, Hansen and coworkers have already stated that, even though the crystal structure of *A*-AChBP co-crystallized with epibatidine **10** doesn't enclose any solvent residues, the pyridine nitrogen of the nicotinic ligand may be bridged to the backbone of *A*-AChBP-Ile108 by a water molecule.[69]

2. Aims and Objectives

The aim of the current research project was to design, synthesize and pharmacologically evaluate novel ligands targeting neuronal nicotinic acetylcholine receptor subtypes. To identify novel agonists/partial agonists/antagonists towards the $\alpha4\beta2$, $\alpha7$ and $\alpha3\beta4$ subtypes, this experimental research focused on three different classes of nicotinic compounds. Firstly, the substitution strategy applied by Bunnelle *et al.* was taken as model protocol to design novel 2,5-diazabicycle[2.2.2]octane derivatives. Secondly, a group of molecular hybrids was synthesized in the search for novel selective $\alpha7$ agonists/partial agonists containing the quinuclidine core (the basic structure present in the model compounds AR-R17779 **6** and ABT-107 **7**) and the 3-pyridinyl-methyl substituent in position 2 (the side pendant found in the model compound TC-5619 **8**). Finally, the structures of the model alkaloids (–)-nicotine **9** and anabaseine **11** and the synthetic nicotinic ligand deschloroepibatidine **13** were modified to generate a set of unprecedented analogues to investigate the putative role of the water molecule in the ligand-receptor interaction.

2.1. 2,5-Diazabicycle[2.2.2]octane derivatives

In the search for novel selective nicotinic ligands, the 2,5-diazabicycle[2.2.2]octane derivatives **14**-**23** (Figure 18) were designed and synthesized, applying the previously discussed substitution approach of Bunnelle and coworkers.[60] Compound Bun6 **1** was built choosing an octahydropyrrolo[3,4,*c*]pyrrole system as the basic core, which has two stereogenic centres and two stereoisomers. On the contrary, the 2,5-diazabicycle[2.2.2]octane nucleus is a symmetric and more rigid scaffold, in which the degree of freedom of the protonatable system is reduced.

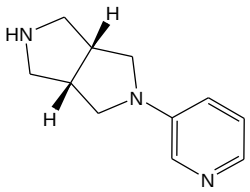

Bun6 **1**

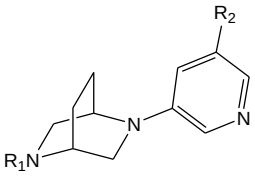

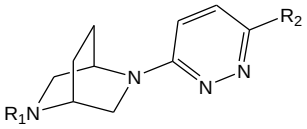

14 $R_1 = H$ $R_2 = H$

15 $R_1 = (CH_3)_2$ $R_2 = H$

16 $R_1 = H$ $R_2 = OCH_2CH_3$

17 $R_1 = H$ $R_2 = OCH_2CH_2CH_3$

18 $R_1 = H$ $R_2 = Cl$

19 $R_1 = H$ $R_2 = Ph$

20 $R_1 = CH_3$ $R_2 = Ph$

21 $R_1 = (CH_3)_2$ $R_2 = Ph$

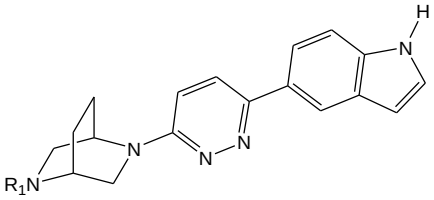

22 $R_1 = H$

23 $R_1 = CH_3$

Figure 18. Structures of target compounds based on the diazabicycle-octane core.

Bunnelle and his research team, describing a large number of nicotinic ligands endowed with different molecular skeletons, reported the $\alpha4\beta2$ binding data of the target compound **14**, characterized by a low K_i value in the sub-nanomolar range, thus displaying a 10-fold higher affinity than the model compound Bun6 **1**.[74] By the way, the $\alpha7$ binding affinity of **14** was not reported. The basic bicycle found into the molecular structure of **14** exhibits some new interesting chemical features, compared to the model scaffold:

- a reduced degree of freedom and therefore a more constrained orientation of the protonated nitrogen within the LBD of nAChRs.
- the absence of stereoisomers and thus, in theory, an easier synthetic approach.
- a quinuclidine-like structure, which is more generally accepted by nAChRs (particular the $\alpha7$ subtype).

Preliminary molecular docking analysis, performed within the α4β2 human homology model elaborated by our research group, had already put in evidence that a similar binding mode and a significant overlapping exist between Bun6 **1** and its 2,5-diazabicycle[2.2.2]octane analogue **14** (Figure 19).[75]

On the other hand, by means of our α7 human homology model, we tested *in silico* the reference ligand Bun46 **4** and its virtual 2,5-diazabicycle[2.2.2]octane analogue **23** within the human α7 LBD.[75] Again, a similar binding interaction between the two ligands was observed (Figure 20).

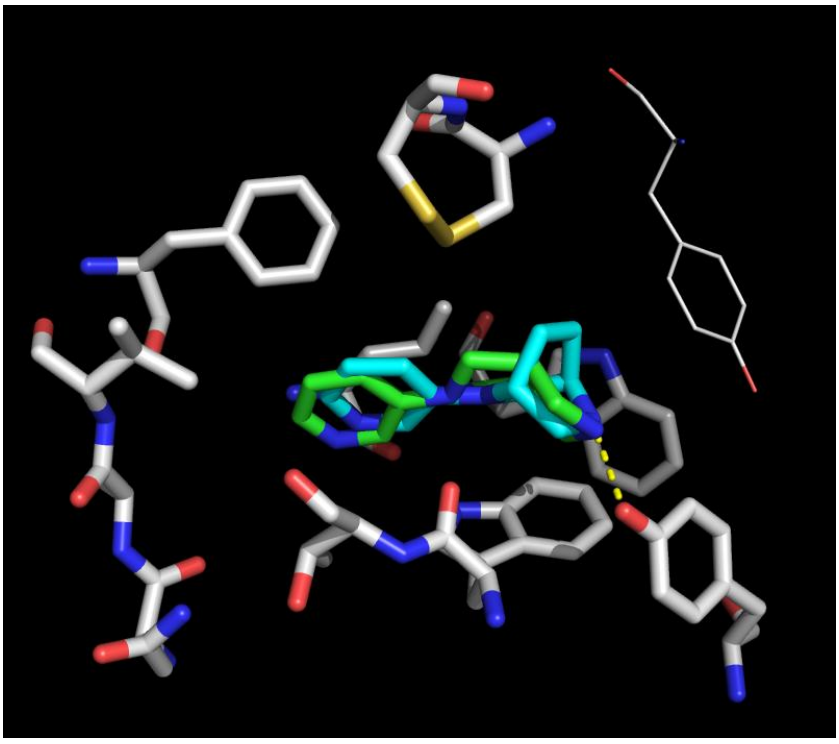

Figure 19. Model compound Bun6 **1** (green) and target compound **14** (cyan) docked within the human α4β2 LBD.

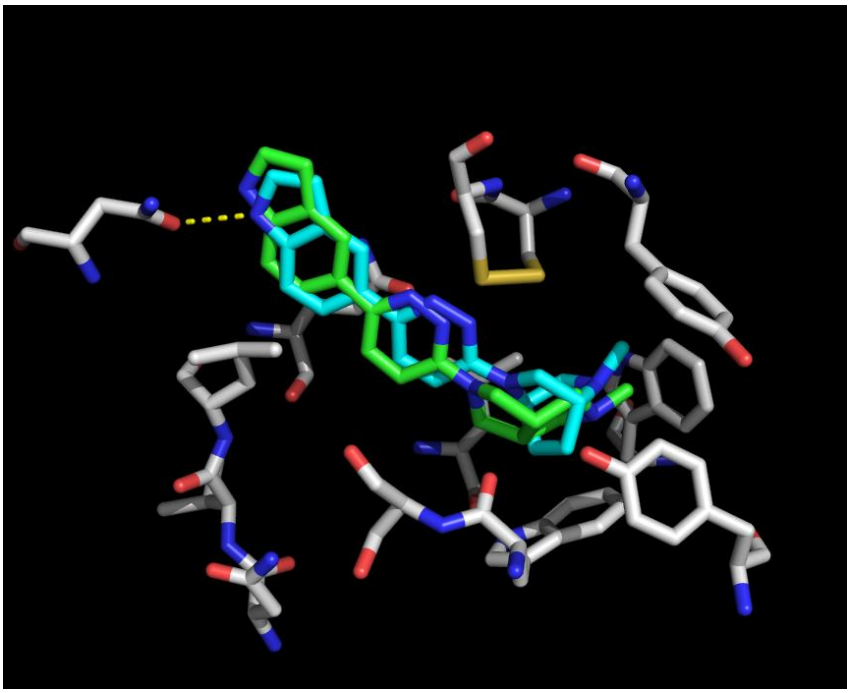

Figure 20. Model compound Bun46 **4** (green) and target compound **23** (cyan) docked within the human α7 LBD.

These results encouraged the design and synthesis of a series of target compounds characterized by the 2,5-diazabcicle[2.2.2]octane scaffold as the basic moiety, in which one nitrogen is linked to a pyridine or pyridazine heteroaromatic ring. An appropriate substitution pattern should direct selectivity towards the α4β2 or α7 nAChR subtypes. To this end, pyridine derivatives bearing alkoxy groups in *meta* position were designed, to selectively bind the heteromeric α4β2 channel. Then, *para* substituted pyridazine derivatives, aiming to enhance affinity for the α7 subtype. In order to investigate the adequate electronic properties of the charged nitrogen, some tertiary amines and quaternary salts have been prepared too.

This novel set of nicotinic ligands will aim at the validation of both the SAR study of the Abbot scientists and the computational study elaborated by our research team.[60,75] Moreover, albeit the somewhat exceptional affinity and selectivity values at the α4β2 or the α7 nicotinic channels, the Abbott model compounds were unsuccessful in the clinical trials, as shown by compound A-582841 **5**.[61] The use of a more rigid basic scaffold might improve the overall pharmacological profile of the new derivatives.

2.2. Quinuclidine-containing derivatives

The set of novel quinuclidine-containing compounds **24**-**31** (Figure 21) was designed and synthesized.

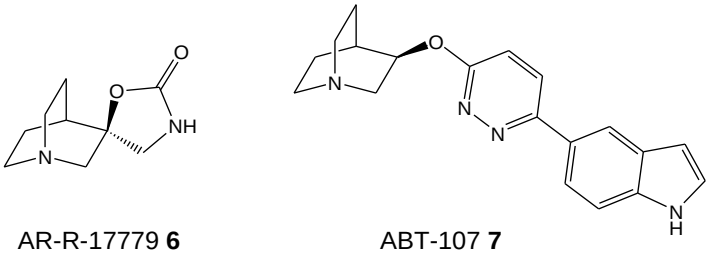

AR-R-17779 **6**

ABT-107 **7**

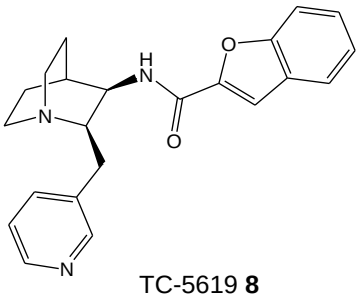

TC-5619 **8**

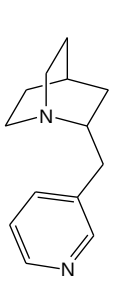

24

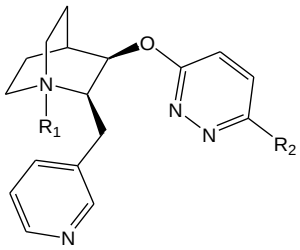

25 R_1 = H R_2 = Cl
26 R_1 = H R_2 = Ph
27 R_1 = CH_3 R_2 = Ph
28 R_1 = H R_2 = 5'-Indolyl

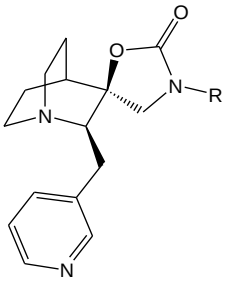

29 R = H
30 R = CH_3
31 R = Benzyl

Figure 21. Structures of target compounds based on the quinuclidine core.

As previously discussed, the quinuclidine (1-azabicyclo[2.2.2]octane) ring system is a frequent scaffold for nicotinic ligands selective for the α7 subtype. As a matter of fact, incorporation of the basic nitrogen into this bicyclic structure has been proposed to constrain the orientation of the protonation of the nitrogen in a manner that facilitates the α7 nAChR binding and activation.

However, the LBD of our α7 homology model was unable to allocate TC-5619 **8** (Figure 21), due to the presence of the bulky aromatic side pendant in position 2. The ligand induced-fit might remodel the receptor binding site creating an additional hydrophobic cleft.

Therefore, we designed a group of novel derivatives retaining both the quinuclidine ring and the 3-pyridinyl-methyl pendant in position 2, as found in the structure of TC-5619 **8**, and replacing the amide function of **8** with an ether group (**25**-**28**) or a spirooxazolidinone ring (**29**-**31**), taken from the model compounds ABT-107 **7** and AR-R-17779 **6**, respectively (Figure 21). With these target compounds we aimed at investigating if and to what extent the 3-pyridinyl-methyl substituent of reference TC-5619, now inserted in other quinuclidine-containing derivatives, should affect the affinity and functional profile at α7 nAChRs. Since the *cis* configuration of TC-5619 **8** was found to be the most favourable arrangement for binding to the α7 subtype, the same stereochemistry has been retained in the new ligands.[67]

2.3. Structural analogues of model alkaloids

As discussed in section 1.9, the isolation and the structural resolution of several AChBPs co-crystallized with natural nicotinic ligands, such as (–)-nicotine **9**, epibatidine **10** and anabaseine **11**, allowed a better characterization of the nicotinic receptor architecture, the identification of the protein residues involved in the binding process and the development of homology models for nAChRs.[68-70] The driving force of the ligand-receptor interaction process has been identified in the cation-π interaction between the protonated nitrogen of the ligands and a tryptophan residue located within the *aromatic box* region of the LBD. The basic nitrogen is further stabilized by the backbone chain of *aromatic box* amino acids. A supplementary H-bond connects some key residues belonging to both the major and the minor subunits of the LBD to an HBA region of the ligand (ester function in ACh, pyridine nitrogen in alkaloids). Albeit a full characterization of this contact is

far from being completely understood, it is well accepted that the participation of less conserved residues from the minor subunit could be crucial in affecting the selectivity profile of nicotinic ligands.

As already pointed out, the presence of water molecules in the LBD has been identified in at least two different AChBPs co-crystallized with (–)-nicotine **9** and anabaseine **11**, adding further elements to the debate on the nicotinic orthosteric binding site. A molecule of water might improve the hydrophilic properties of the LBD environment or, on the other hand, it might directly participate in the ligand-interaction process by bridging the pyridine nitrogen to some protein residues. To explore the putative role of the water molecule, we planned some new potential nicotinic ligands by modifying the structures of three natural model compounds (Figures 22 and 23).

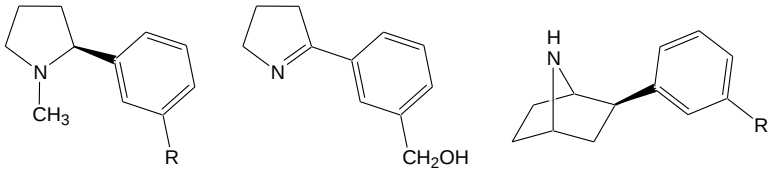

32 R = OH

33 R = CH_2OH

34

35 R = OH

36 R = CH_2OH

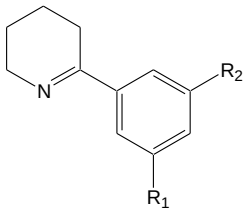

37 R_1 = OH R_2 = H

38 R_1 = CH_2OH R_2 = H

39 R_1 = CH_2OH R_2 = F

Figure 22. Structures of target compounds bearing a hydroxyl group.

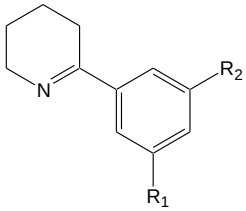

40 R_1 = H R_2 = H

41 R_1 = CH_3 R_2 = H

42 R_1 = F R_2 = H

43 R_1 = F R_2 = Br

Figure 23. Structures of target compounds bearing hydrophobic substituents.

The structures of (–)-nicotine **9**, deschloroepibatidine **13** and anabaseine **11** were modified designing new analogues which contain a hydroxyl or a hydroxymethyl group (target compounds **32**-**39**) to mimic and eventually dislocate the water molecule in the receptor-ligand interaction. In this way, a potentially similar interaction will be given by the ligand. The proposed substitution pattern on the ligand skeleton aiming to increase its binding affinity is an approach which has precedents in the literature for a series of HIV-1 protease inhibitors.[76]

The size of the basic core of anabaseine **11** was also reduced designing the lower homologue **34**. On the other hand, a few analogues potentially able to disrupt the water-ligand interaction were prepared by considering only the anabaseine basic scaffold and replacing the pyridine nitrogen with hydrophobic groups (target compounds **40**-**43**). In this way, the interaction with the water molecule would be excluded, maybe favouring a different binding mode and giving rise to a variation of the ligand functional profile.

3. Results and Discussion

3.1. Synthesis of the 2,5-diazabicycle[2.2.2]octane derivatives

The synthetic strategy adopted to accomplish the designed novel 2,5-diazabicycle[2.2.2]octane derivatives **14**-**23** required the preparation of the 2,5-diazabicycle[2.2.2]octane core, which has been the subject of various literature reports;[77-79] among them the most convenient approach is illustrated in Scheme 1.

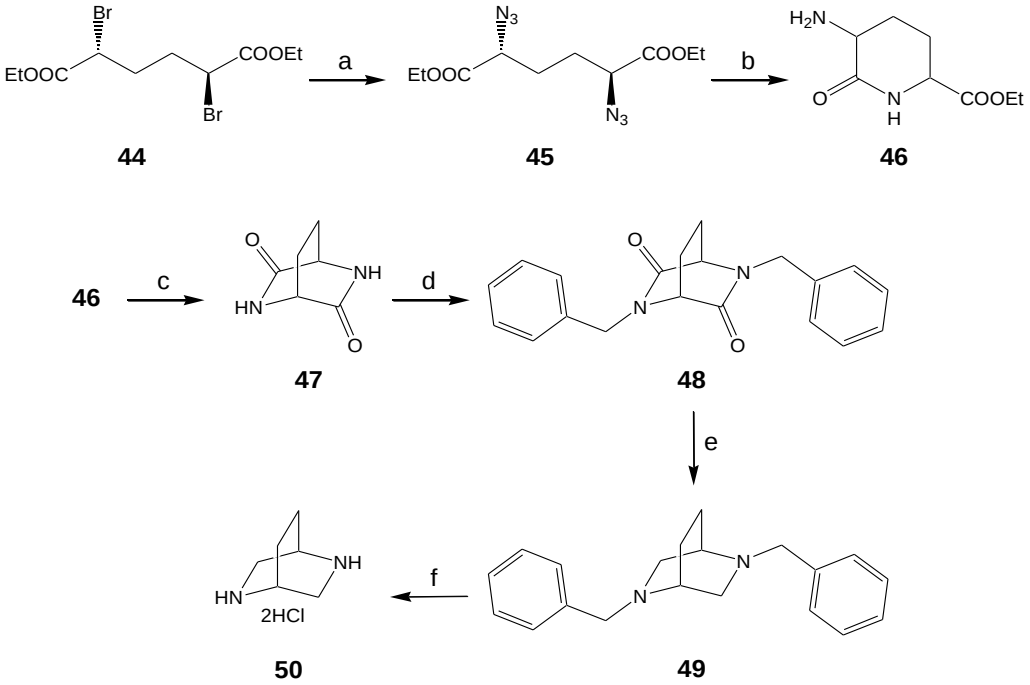

Scheme 1. *Reagents and conditions:* (a) NaN_3, EtOH, reflux, 6h; (b) i) PPh_3, THF, 0° to r.t., 3h; ii) H_2O, r.t., 16h; (c) Na, MeOH, reflux, 5h; (d) 60% NaH, BnCl, DMF, 0°C to r.t., 24h; (e) $LiAlH_4$, THF, 0° to reflux, 5h; (f) H_2, Pd/C 10%, HCl 37%, MeOH, r.t., 16h.

Following the Newman protocol[77], the linear starting material diethyl-*meso*-2,5-dibromoadipate **44** was used as the carbon source for the diazabicyclic system. The nitrogen atoms were inserted by a nucleophilic substitution using sodium azide. Several reduction procedures are already described to convert diazide **45** into the corresponding diamine. As shown in Scheme 2, a high

pressure hydrogenation with the Adam's catalyst is the strategy reported by Newman *et al.* to isolate diamine **51**.[77] However, the low yield (due mostly to the high reactivity and instability of the free diamine function, which requires to be converted into the corresponding dihydrochloride to be stabilized) and the expensive platinum dioxide catalyst, suggested the search for an alternative approach. A milder Staudinger reaction reduced efficiently the azide functions, providing the monocyclic derivative **46** in almost quantitative yield.[80] The mono-cyclization step takes place due to the basic aqueous media of the Staudinger reduction environment (the basicity is given by the secondary product triphenylphosphine oxide, Scheme 3). The subsequent sodium methoxide-assisted hydrolysis and cyclization allowed a smooth conversion of both diamine **51** and monocyclic amine **46** to the desired intermediate **47**.

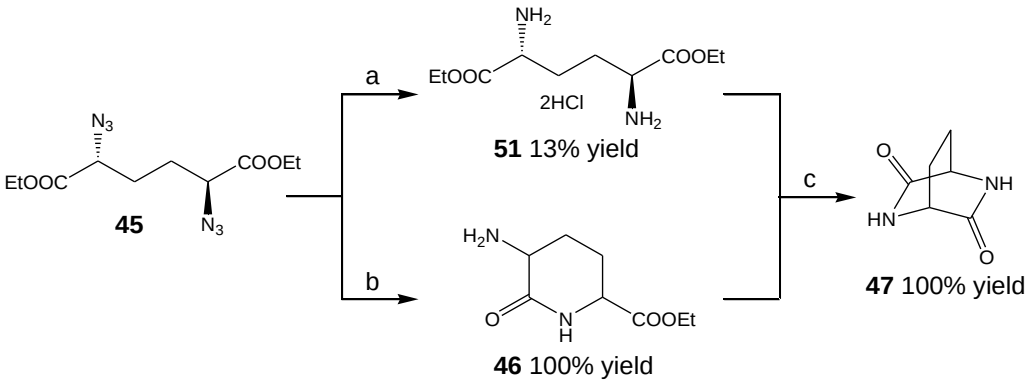

Scheme 2. Reduction and conversion of **44** to **46**. *Reagents and conditions:* (a) H_2, Pt_2O, EtOH, r.t., 4 bar, 5h; (b) i) PPh_3, THF, 0° to r.t., 3h; ii) H_2O, r.t., 16h; (c) Na, MeOH, reflux, 5h.

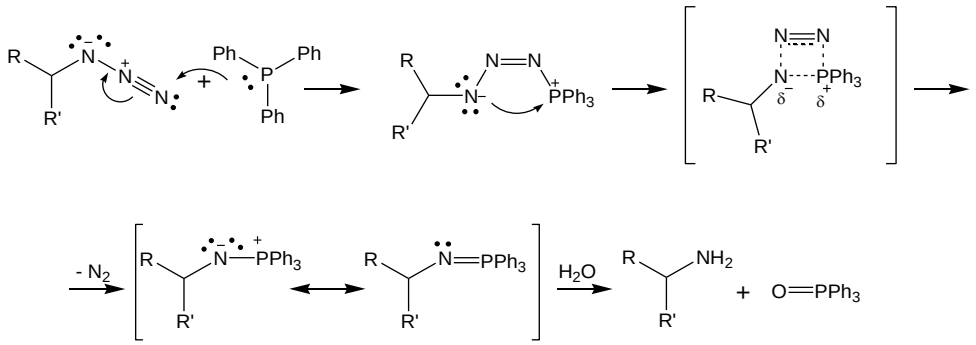

Scheme 3. Staudinger reduction mechanism.

Dilactame **47** was almost insoluble in standard organic solvents and therefore it was impossible to reduce the carbonyl groups using any hydrides in dry conditions. Protection of the amide nitrogens with benzyl groups (derivative **48**, Scheme 1) improved the solubility profile and the subsequent reduction with lithium aluminium hydride provided the protected 2,5-diazabicycle[2.2.2]octane ring **49**.[79] The instability of the free amine functions after removal of the benzyl protecting groups under standard catalytic hydrogenation conditions was overcome by adding concentrated hydrochloric acid to the reaction flask (Scheme 1), leading to the key basic core **50** as the related dihydrochloride.[81]

Next, derivative **50** was mono-Boc protected using di-*tert*-butyl dicarbonate in a sub-stoichiometric amount (0.5 eq.) to avoid protection of the second nitrogen,[81] then intermediate **51** was coupled with properly substituted pyridine bromides (Scheme 4). This functionalization was achieved through a palladium catalyzed cross-coupling protocol, due to the low electrophilic character of the *m*-pyridine bromides (intermediates **52**-**54**).[60,75]

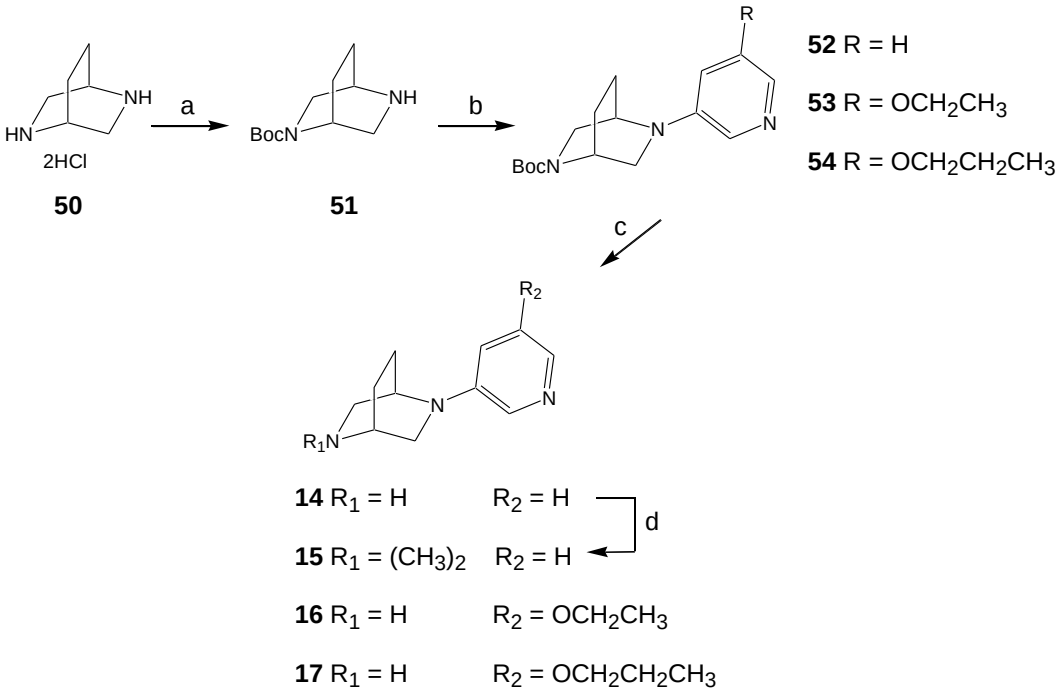

Scheme 4. Synthesis of pyridine derivatives **13**-**16**. *Reagents and conditions:* (a) Boc_2O, NaOH, H_2O/*i*PrOH, 0°C, 2h; (b) **55** or **56**, $Pd_2(dba)_3$, (±)-BINAP, *t*BuOK, THF, reflux, 5h; (c) HCl 2.0 N in Et_2O, MeOH/Et_2O, 0°C to r.t., 3h; (d) i) CH_2O, $NaBH_4$, MeOH, 0°C to r.t., 1h; ii) CH_3I, Et_2O, r.t., 3h.

The 5-alkoxylpyridine bromides **55** and **56** were prepared by reacting 3,5-dibromopyridine with the proper sodium alkoxide (Scheme 5). Deprotection in acidic media afforded the desired final compounds **14**, **16** and **17**; with a standard procedure, the secondary base **14** gave the N-Me tertiary amine, which was converted into the corresponding dimethylammonium salt **15** (Scheme 4).

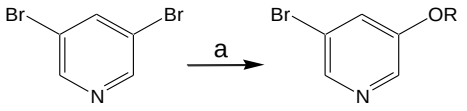

55 R = CH_2CH_3
56 R = $CH_2CH_2CH_3$

Scheme 5. Synthesis of 3-bromo-5-alkoxy-pyridines. *Reagents and conditions:* (a) NaOR, DMF, 70°C, 3h.

To obtain the desired pyridazine target compounds **18**-**23**, the mono-Boc derivative **51** was coupled with both 3,6-dichloro-pyridazine and 3-chloro-6-phenylpyridazine in the presence of DIPEA under standard thermal conditions (Scheme 6). Both intermediates **57** and **58** were deprotected to the desired secondary amines **19** and **18**. The first one underwent a standard reductive amination and the corresponding tertiary methylamine **20** was then treated with methyl iodide to provide the quaternary ammonium salt **21**. On the other hand, compound **58** was coupled with 5-indolyl boronic acid by means of a microwave-assisted Suzuki reaction to provide intermediate **59**. Deprotection with 2.0 N hydrochloric acid in diethyl ether provided the secondary amine **22**, which was converted into methylamine **23**.

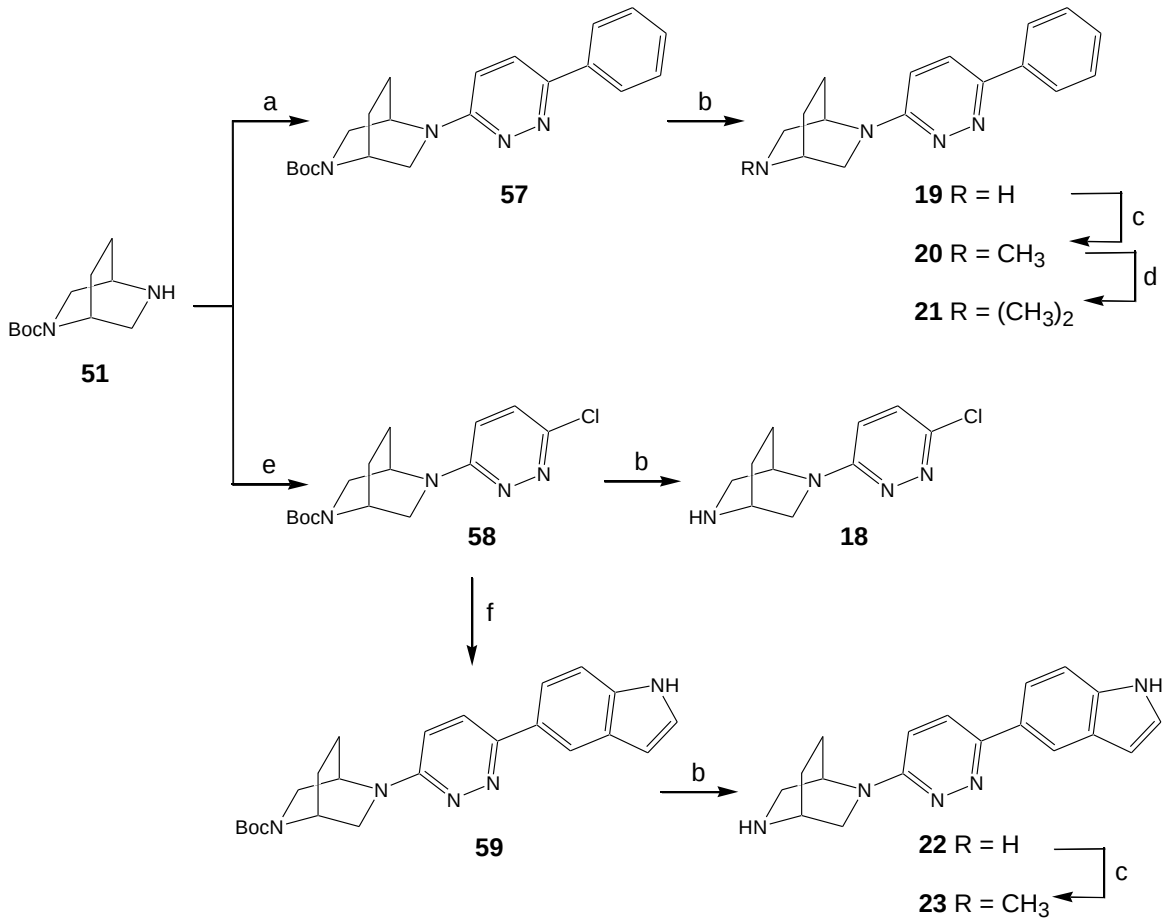

Scheme 6. Synthesis of pyridazine derivatives **17**–**22**. *Reagents and conditions:* (a) 3-chloro-6-phenyl-pyridazine, DIPEA, DMSO, 105°C, 48h; (b) HCl 2.0 N in Et_2O, MeOH/ Et_2O, 0°C to r.t., 3h; (c) CH_2O, $NaBH_4$, MeOH, 0°C to r.t., 1 h; (d) CH_3I, Et_2O, r.t., 3h; (e) 3,6-dichloro-pyridazine, DIPEA, DMSO, 105°C, 48h; (f) 5-indolyl-boronic acid, $(PPh_3)_2PdCl$, PPh_3, Na_2CO_3 1M, 1,4-1,4-dioxane/EtOH, MW irradiation, 150°C, 30 min.

3.2. Pharmacological evaluation of compounds 14–23

As shown in Table 1, derivatives **14**-**23** underwent binding experiments to evaluate their affinity at $\alpha4\beta2$, $\alpha7$ and $\alpha3\beta4$ nicotinic receptor subtypes present in rat cortex membranes, using [^{3}H]epibatidine ($\alpha4\beta2$ and $\alpha3\beta4$ subtypes) and [^{125}I]α-bungarotoxin ($\alpha7$ subtype) as reference radioligands. These pharmacological assays were performed at the Dipartimento di Farmacologia, Chemioterapia e Tossicologia Medica, University of Milan, in the research group coordinated by Dr. Cecilia Gotti.

Compound	α4β2 [^{3}H]Epi (K_i, nM)	α7 [^{125}I]α-BgTx (K_i, nM)	α3β4* [^{3}H]Epi (K_i, nM)	Selectivity ratio α4β2/α7
14	0.131 (17)	24 (18)	31 (19	183
15	3.7 (13)	12 (25)	69 (11)	3.3
16	0.368 (16)	13000 (25)	153 (22)	35000
17	0.234 (16)	21000 (26)	50 (23)	90000
18	2 (10)	118 (20)	4.1 (13)	59
19	125 (12)	132 (17)	630 (34)	1
20	2240 (22)	15.9 (40)	281 (22)	0.007
21	1000 (14)	2300 (14)	163 (20)	2.3
22	580 (15)	22 (18)	2000 (12)	0.04
23	2780 (20)	2.25 (40)	191 (19)	0.0008

Table 1. Binding data on the indicated compounds towards the α4β2, α7 and α3β4 nAChR subtypes.

The unsubstituted compound **14**, as already shown by Bunnelle and co-workers,[75] displayed high binding affinity at the α4β2 subtype with a K_i value of 131 pM (literature: K_i = 20 pM). Nevertheless, **14** showed a good affinity (K_i = 24 nM) even at the homopentameric α7 channel too, about 200-fold lower than that observed at the α4β2 receptor. The α4β2 vs. α7 selectivity ratio was massively increased when alkoxy groups were inserted in position 5. Indeed, compounds **16** and **17** reached α4β2 K_i values in the picomolar range, with barely no affinity at the α7 channel, thus displaying selectivity ratios of 35000 and 90000, respectively, the same order of magnitude compared with the α4β2-selective model ligands.[60] The presence of a hindered aliphatic chain in position 5 on the pyridine ring seems relevant to the α4β2 subtype binding selectivity, suggesting the existence of a cleft or tunnel within the α4β2 LBD,

perpendicular to the pharmacophore ground level where the protonated scaffold and the HBA ring lay.

The quaternary salt **15** showed a 100-fold decreased $\alpha4\beta2$ affinity, while it maintained, as expected, the same affinity profile at the $\alpha7$ receptor complex. This result is in agreement with the observations made by Bunnelle *et al.* on the properties of the basic nitrogen able to promote a selective binding at the $\alpha4\beta2$ subtype.[60] Derivative **18**, characterized by a pyridazine ring bearing a chlorine atom in position 6, has a similar behaviour towards both tested nAChR subtypes, with some preference for the heteromeric channel. The lack of selectivity, mainly due to a 200-fold reduction of $\alpha4\beta2$ affinity considering the parent compound **14**, confirmed that a pyridine moiety is a rather strict structural requirement for the complementary ligand-receptor recognition at this subtype. Conversely, in accordance with the results on the model compounds, the binding at the $\alpha7$ channel is less affected by the nature of the heteroaromatic ring.[60]

When a bulky aromatic substituent was introduced in *para* position on the pyridazine ring, the selectivity profile partly shifted towards the homomeric $\alpha7$ receptor. The 6-phenylpyridazine derivative **19** showed similar binding affinities at the tested receptor subtypes, whereas the indolyl-containing compound **22** exhibited a negligible 10-fold $\alpha7$ selectivity. These results are scarcely in agreement with the model substitution pattern and this could be explained by the more rigid scaffold of the target compounds which might not be able to properly fit the whole $\alpha7$ LBD. The existence of a larger $\alpha7$ orthosteric binding site compared to the $\alpha4\beta2$ active cavity is a well established feature of the homopentameric nicotinic channel, which can allocate ligands with more sterically demanding skeletons. Indeed, the binding data of tertiary amines **20** and **23** denoted a high $\alpha7$ affinity in the low nanomolar range (K_i = 15.9 and 2.25 nM, respectively) coupled with good selectivity ratios (140 and 1300, respectively). As described in section 1.7, the $\alpha7$ affinity is clearly affected by the degree of substitution of the basic nitrogen and tertiary amines generally possess the required electronic properties to fruitfully bind the homomeric $\alpha7$ channel. A different behaviour was

associated to the permanently charged dimethylammonium salt **21**, which is a low affinity ligand at both investigated nAChR subtypes.

In conclusion, our test set has validated the substitution pattern proposed by Bunnelle and coworkers as well as our *in silico* investigation, which outline the SAR able to affect affinity and subtype selectivity towards the two most abundant and pharmacologically relevant nAChRs.

Nevertheless, the target compounds underwent binding experiments also at the $\alpha3\beta4^*$ nAChR subtype, the third most expressed neuronal nicotinic channel (Table 1). Even though these compounds have been rationally designed to selectively bind the $\alpha4\beta2$ or $\alpha7$ nicotinic receptors, we believed it was interesting to explore their affinity profile also at the $\alpha3\beta4^*$ receptor complex. With the exception of compound **22**, all the tested ligands showed a meaningful binding affinity towards the $\alpha3\beta4^*$ subtype. The best affinity values were measured for compounds **14**, **15** and in particular **18**. The introduction of more hindered substituents in *para* or *meta* position led to a reduction of $\alpha3\beta4^*$ affinity, whereas the nature of the heteroaromatic ring did not affect the binding at the heteromeric channel, since pyridine and pyridazine compounds exhibited quite similar affinity values. In general, the relevant affinity at the $\alpha3\beta4^*$ nAChR subtype compromises the selectivity profile of the most promising compounds (**15**, **16** and **23**), even though the $\alpha3\beta4^*$ channel is by far less abundant within the CNS compared to the other tested receptors. Worth noting, the original report by Bunnelle *et al.* didn't mention at all the affinity profile towards the $\alpha3\beta4^*$ receptor for the model series, and we are convinced that the octahydropyrrolo[3.4.*c*]pyrrole derivatives are characterize by some, if not relevant, $\alpha3\beta4^*$ affinity as well.

3.3. Synthesis of quinuclidine-containing derivatives

The synthetic sequence applied to afford the designed novel functionalized quinuclidines **24**-**31** started with insertion of the 3-pyridinyl-methyl pendant,

found in the model compound TC-5619 **8**, into the quinuclidine scaffold (Scheme 7).[67]

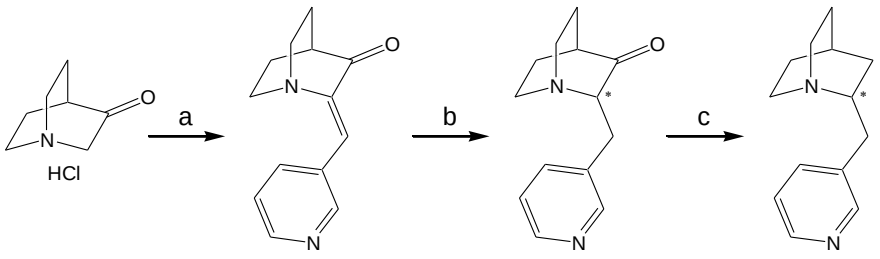

60 **61** **62** **24**

Scheme 7. Synthesis of key intermediate **62** and target compound **24**. *Reagents and conditions:* (a) 3-pyridinecarboxaldehyde, KOH, MeOH, r.t., 48h; (b) H_2, Pd/C 10%, HCl 6N, MeOH, rt, 16h; (c) $NH_2NH_2*H_2O$, KOH, DEG, 180°C, 6h.

Commercially available 3-quinuclidinone hydrochloride **60** was condensed with 3-pyridinecarboxaldehyde in a basic medium to afford the unsaturated adduct **61**. Subsequent hydrogenation in the presence of hydrochloric acid provided the corresponding intermediate **62**. To investigate the role of the heteroaromatic side pendant, we prepared compound **24**, which lacks any further substitution. To this end, the Wolff-Kishner reduction conditions were applied to **62** using hydrazine monohydrate and potassium hydroxide in diehtyleneglycol at 180°C, which provided **24** as a racemate.[82]

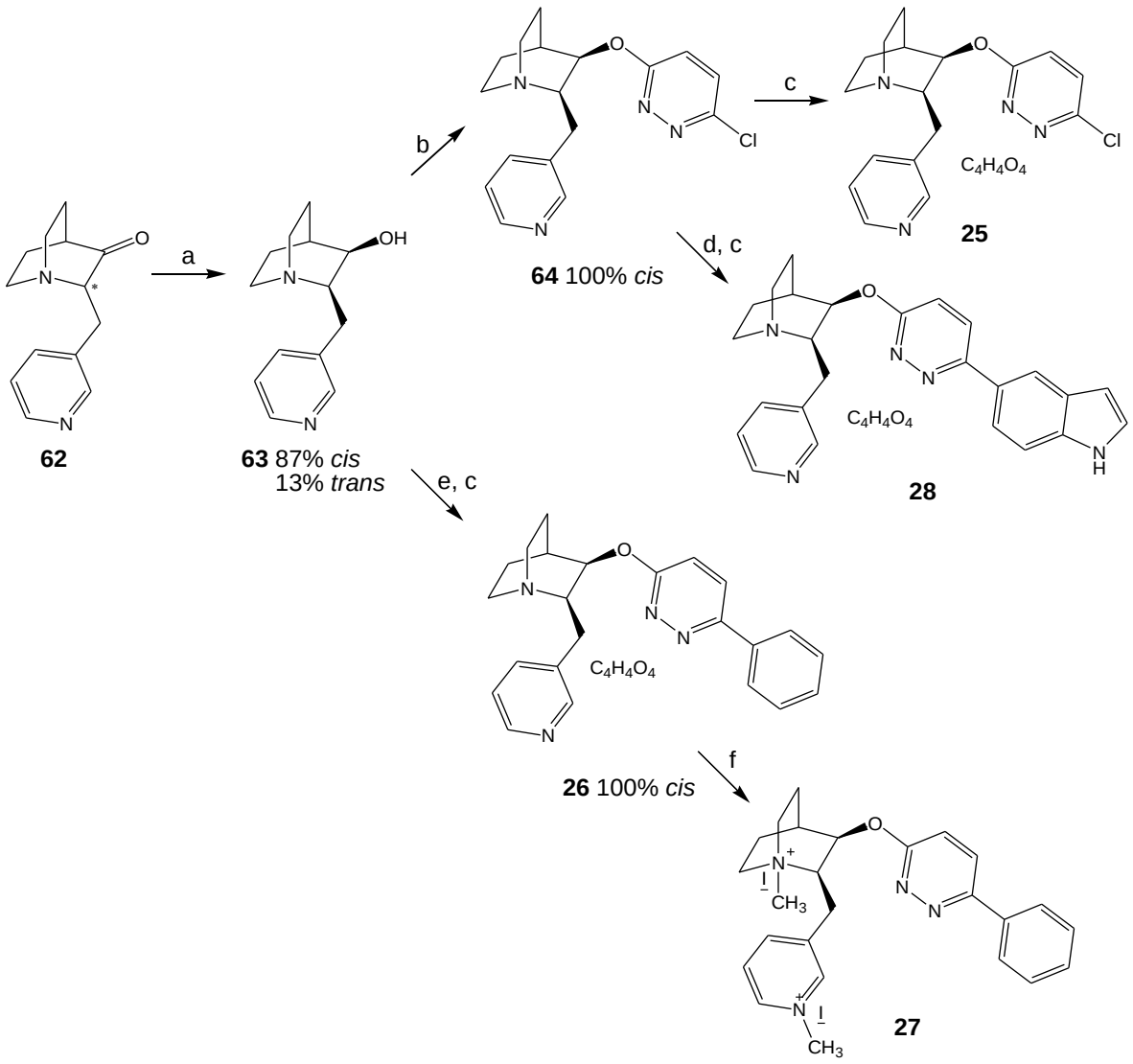

Scheme 8. Synthesis of pyridazine derivatives **25**–**28**. *Reagents and conditions:* (a) $Al(OiPr)_3$, *i*PrOH, 70°C, 6h; (b) 3,6-dichloropyridazine, NaHDMS, THF, 0°C to r.t., 5h; (c) fumaric acid, MeOH, r.t., 5h; (d) 5-indolyl-boronic acid, $(PPh_3)_2PdCl$, PPh_3, Na_2CO_3 1M, 1,4-1,4-dioxane/EtOH, MW irradiation, 150°C, 30 min; (e) 3-chloro-6-phenyl-pyridazine, NaHDMS, THF, 0°C to r.t., 5h; (f) CH_3I, MeOH, r.t., 6h.

The carbonyl function of **62** underwent two different reductive approaches. First, it was reduced to the corresponding secondary alcohol, applying the Meerwein-Pondorf-Verley (MPV) protocol, which was then reacted with a few substituted pyridazine chlorides (Scheme 8). The use of aluminium *iso*-propoxide as reductive agent allowed to obtain the desired alcohol **63** as the *cis* predominant isomer (*cis*/*trans* ratio: 87:13, evidenced by ^{1}H-NMR analysis).[67] As illustrated in Scheme 9, the MPV reaction consists of the aluminium-catalyzed hydride shift from the α-carbon of an alcohol component

to the carbonyl carbon of a second component, through a six-membered transition state, referred to as the Meerwein-Ponndorf-Verley reduction or the Oppenauer oxidation, depending on which is the desired reaction product.[83] The major *cis* isomer is obtained due to the steric hindrance of the 3-pyridinyl-methyl substituent, which forces the hydride attack from the opposite side.

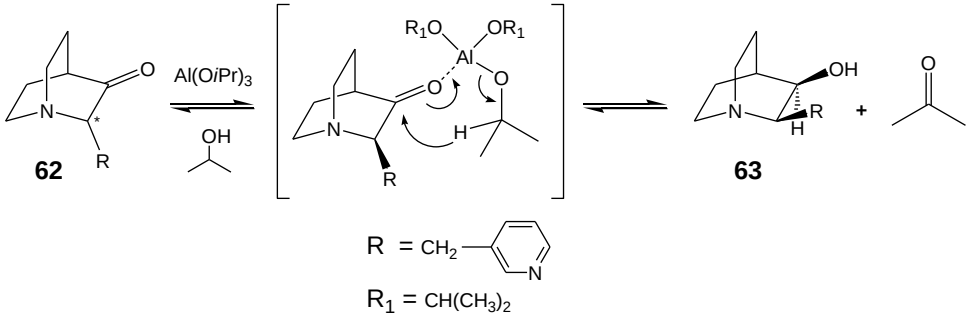

Scheme 9. MPV reduction mechanism.

Alcohol **63** was then coupled with substituted pyridazine chlorides, using the strong base sodium bis(trimethylsilyl)amide, which promoted the nucleophilic attack of the corresponding alkoxide. The chromatographic purification of the adducts allowed complete separation of the *cis* isomer from the *trans* minor component. Intermediate **64**, bearing a chlorine atom in position 6 of the pyridazine ring, was treated first with fumaric acid to isolate the crystalline target compound **25**, then with 5-indolyl-boronic acid in a microwave-assisted Suzuki coupling, to introduce the indole ring. Salification with fumaric acid provided the desired compound **28**. Coupling with 3-chloro-6-phenylpyridazine led directly to the desired phenyl-substituted derivative **26**, which was then reacted with methyl iodide. Unfortunately, we weren't able to selectively methylate the tertiary nitrogen without affecting the pyridine ring: the bis-quaternary salt **27** was thus isolated and characterized.

A second reductive approach performed on ketone **62** is illustrated in Scheme 10. The introduced spirocyclic epoxide was hence transformed into the corresponding spirooxazolidinone derivatives **29**-**31**.

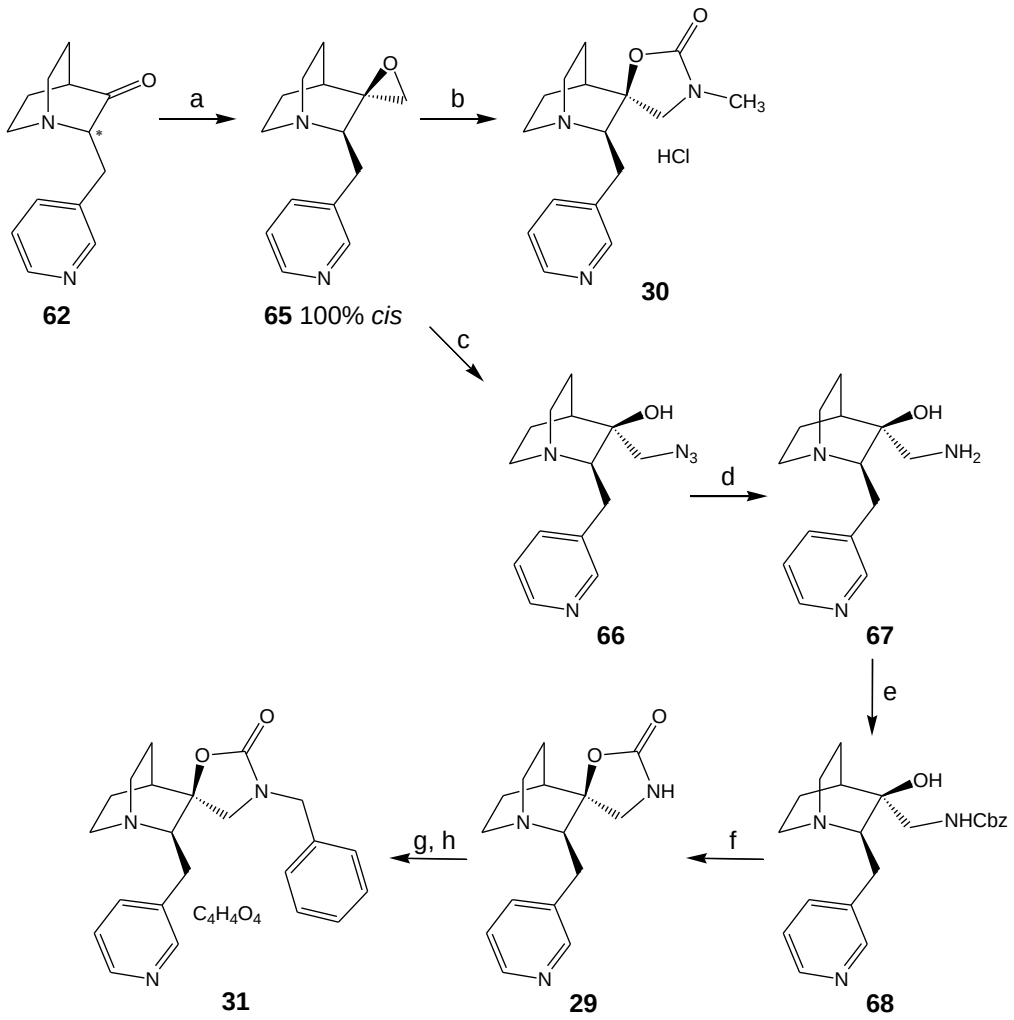

Scheme 10. Synthesis of spirooxazolidinone derivatives **29**-**31**. *Reagents and conditions:* (a) TMSOI, 60% NaH, DMSO, r.t., 24h; (b) i) CH_3NH_2, MeOH, r.t., 24h; ii) DCI, THF, reflux, 3h; (c) NaN_3, NH_4Cl, MeOH/H_2O, r.t., 24h; (d) $LiAlH_4$, THF, 0°C to r.t., 3h; (e) CbzCl, DIPEA, DCM, 0°C to r.t., 3h; (f) 60% NaH, THF, 0°C to r.t., 3h; (g) Benzyl chloride, 60% NaH, DMF, 70°C, 12h; (h) fumaric acid, MeOH, r.t., 5h.

Ketone **62** was converted into spirocyclic epoxide **65** applying the Johnson-Corey-Chaykovsky reaction conditions.[84] As illustrated in Scheme 11, trimethylsulfoxonium iodide (TMSOI), treated with sodium hydride, generated the active species dimethyloxosulfonium methylide, whose negatively charged carbon attacked the carbonyl carbon of **62**. Again, the bulky 3-pyridinyl-methyl substituent directed the diastereoselectivity of the carbon coupling, leading to the racemic *cis* isomer **65**, and no sign of *trans* isomer formation, based on ^{1}H-NMR analysis.[85] The ring-closure is facilitated by the presence of the sulfonium cation which is a good leaving group.

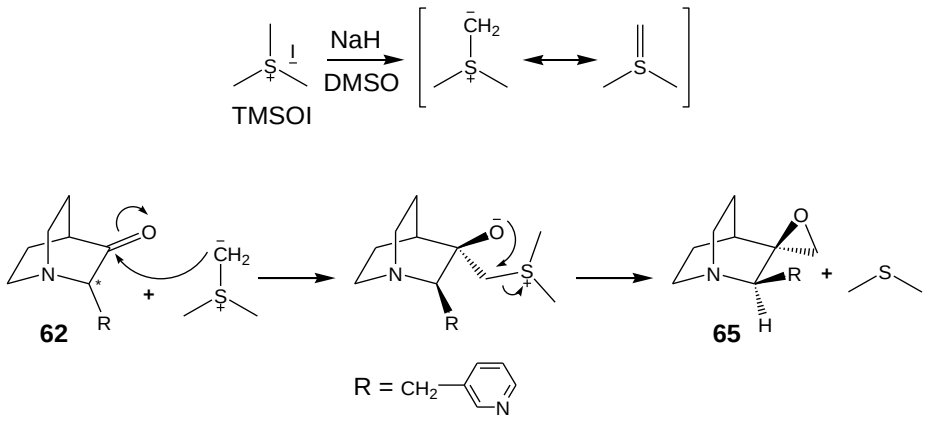

Scheme 11. Johnson-Corey-Chaykovsky reaction mechanism.

At this stage, the high reactivity of the tensioned three-membered spirocyclic ring was exploited to generate the spirooxazolidinone function.[86] Ring-opening with gaseous methylamine (with no isolation of the intermediate) and subsequent cyclization in the presence of *N-N'*-diisopropylcarbodiimide (DCI) as the carbonyl source afforded the target compound **30**. At the same time, several unsuccessful attempts were made to perform ring-opening of the epoxide **65** with aqueous ammonia. Therefore, intermediate **65** was treated with sodium azide and the corresponding β-azido alcohol was reduced with lithium aluminium hydride at room temperature to the primary amine **67** (Scheme 10). The amine function of β-amino alcohol **67** was protected with benzyl chloroformate (intermediate **68**). Treatment with sodium hydride allowed the nucleophilic ring-closure affording compound **29**.

At variance with the other compounds of this set, the target derivative **29** precipitated as a colourless crystalline derivative, which was slightly soluble in polar standard organic solvents such as DMSO or MeOH. Its amino acid-like behaviour precluded any further derivations. Indeed, we tried to functionalize the carbamate nitrogen with several aromatic moieties (e.g., pyridine, thiophene, benzothiophene), but the 3-pyridinyl-methyl side chain sterically inhibited all the couplings. We achieved better results by using reactants (i.e., benzyl chloride) able to overcome the hindrance of the pyridyl side chain. In this way, the final ligand **31** was prepared and tested.

3.4. Pharmacological evaluation of compounds 24-31

Compounds **24**-**31** underwent pharmacological experiments to evaluate their affinity at $\alpha4\beta2$ and $\alpha7$ nicotinic receptor subtypes present in rat cortex membranes by binding studies using, as radioligands, [^{3}H]epibatidine ($\alpha4\beta2$ subtype) and [^{125}I]α-bungarotoxin ($\alpha7$ subtype) and the results are shown in Table 2. Binding affinity studies were performed again by the research group coordinated by Dr. Cecilia Gotti.

Unfortunately, the compounds under study showed K_i values at the $\alpha7$ receptor significantly lower than the reference compound **8**. The unsubstituted compound **24** is the only ligand already known from the literature, and it was described as an $\alpha4\beta2$ (K_i = 16 nM) and $\alpha6\beta2$* (K_i = 85 nM) full agonist, with some $\alpha7$ affinity (K_i = 450 nM).[87] In spite of the differences in the absolute K_i values, we observed for compound **24** an $\alpha4\beta2$ vs. $\alpha7$ selectivity ratio comparable to that found in the literature.[87]

Compound	α4β2 [^{3}H]Epi (K_i, nM)	α7 [^{125}I]α-BgTx (K_i, nM)	Selectivity ratio α4β2/α7
TC-5619 **8**	2300[67]	1.0[67]	2300
24	114 (12)	3400 (36)	0.03
25	1200 (12)	763 (23)	1.6
26	740 (12)	68 (23)	11
27	1000 (13)	13000 (40)	0.08
28	291 (11)	21 (20)	14
29	9000 (17)	21000 (35)	0.4
30	14000 (13)	11000 (27)	1.3
31	2400 (12)	11000 (31)	0.2

Table 2. Binding data on the indicated compounds towards the α4β2 and α7 nAChR subtypes.

The introduction of biaromatic rings in position 3, such as in compounds **26** and **28**, reverted the selectivity profile of **24** leading to good α7 binding affinity values in the high nanomolar range, in line with our purpose when these analogues of TC-5619 **8** and ABT-107 **7** were designed. However, a modest α7 vs. α4β2 selectivity (11 and 14, respectively) was detected. These observations are also in agreement with the results published by Bunnelle *et al.*[60] and with the binding data obtained for the set of 2,5-diazabicyle[2.2.2]octane derivatives (Section 3.2). The replacement of the aromatic ring in position 6 of the pyridazine nucleus with a chlorine atom (compound **25**) and the bis-quaternarization of the nitrogen atoms (compound **27**) caused a massive drop of α4β2 and α7 affinity.

The very low affinity showed by the spirooxazolidinone derivatives **29**-**31** at the tested nAChRs could be explained by the rigidity of the spirocyclic system, which might force the 3-pyridinyl-methyl chain in an unfavourable interaction

with the nicotinic channels. This substituent, when inserted in more rigid molecular skeleton, might not be able to properly align within the α7 orthosteric site. In this regard, we recently found out that the Targacept researchers published an exhaustive overview on the binding affinity and pharmacological profile of TC-5619 **8** and its four stereoisomers.[88] In this paper, quite surprisingly, the authors reported the *trans* isomers as the eutomers (α7 K_i = 1.40 and 4.98 nM, respectively), whereas the *cis* series was described by having only a high nanomolar binding affinity (α7 K_i = 0.4 and 0.8 μM). Curiously, the same authors, in the first TC-5619 series paper dating back to 2005[67], described the *cis* configuration as the most favourable in the recognition by the α7 nAChR subtype, with an α7 K_i value of 1.0 nM for the *cis* isomers of TC-5619 **8** (compounds **8l** in that article). Based on this amazing report, we certainly chose the wrong structural model to build our quinuclidine-containing derivatives and, maybe, the *trans* isomers would lead to a stronger interaction with the target α7 nAChR subtypes.

3.5. Synthesis of derivatives structurally related to (*S*)-nicotine, deschloroepibatidine and anabaseine

The synthetic strategy applied to afford the designed novel (–)-nicotine **9** variants **32** and **33** is shown below in Scheme 12.

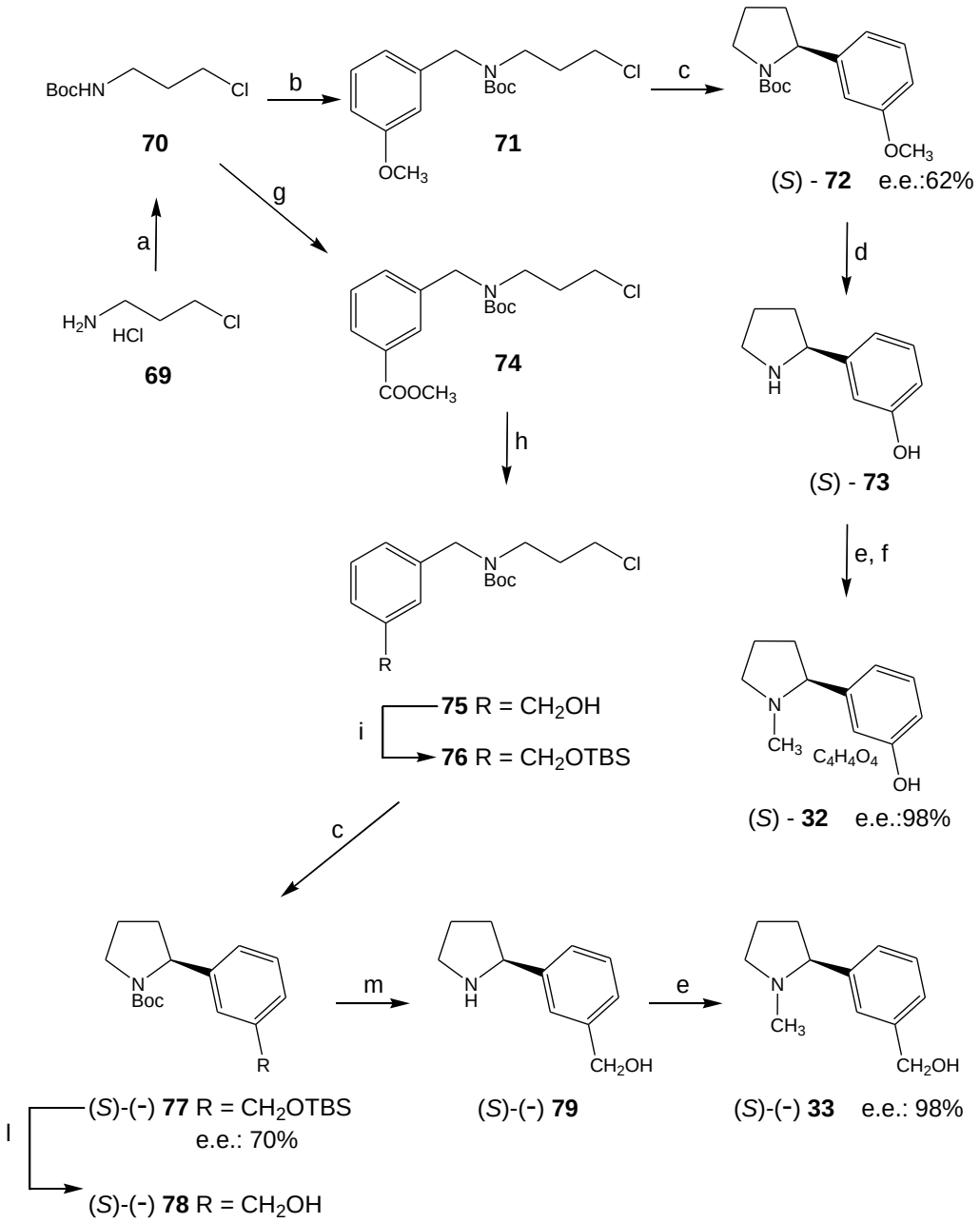

Scheme 12. Synthesis of (*S*)–nicotine **9** derivatives **33** and **33**. *Reagents and conditions:* (a) Boc_2O, TEA, THF, r.t., 20h; (b) 3-Methoxy-bromomethylbenzene, 60% NaH, THF, reflux, 5h; (c) (–)-Sparteine, *s*-BuLi, toluene, -78°C, 5h; (d) BBr_3, DCM, -78°C to r.t., 2h; (e) CH_2O, $NaBH_4$, MeOH, 0°C to r.t., 1h; (f) Fumaric acid, MeOH, r.t., 5h; (g) Methyl 3-(bromomethyl)benzoate, 60% NaH, THF, reflux, 5h; (h) $LiBH_4$, THF, reflux, 30h; (i) TBSCl, imidazole, DMF, 35°C, 8h; (l) TBAF, THF, r.t., 1h; (m) 4.0 N HCl in 1,4-dioxane, Et_2O, 0°C to r.t., 3h.

Commercially available 3-chloropropylamine hydrochloride **69** was *N*-Boc-protected and coupled with two suitably substituted benzyl bromides. Linear intermediate **71** underwent an asymmetric cyclization using (–)-sparteine as

the chiral enantiopure catalyst. As shown in Scheme 13, two mechanisms may account for the role of (–)-sparteine in affecting the enantioselectivity of the process.[89] On one hand, (–)-sparteine might co-ordinate the *s*-BuLi-mediated lithiation step: an asymmetric deprotonation of the benzyl carbon provides the enantio-enriched lithiated intermediate, which then undergoes cyclization. On the other hand, the chiral base might operate during the cyclization step, promoting an asymmetric ring-closure of the racemic lithiated intermediate, thus leading to the same enantio-enriched protected pyrrolidine. The cyclic product **72** was obtained with an e.e. of 62%, based on chiral HPLC analysis.

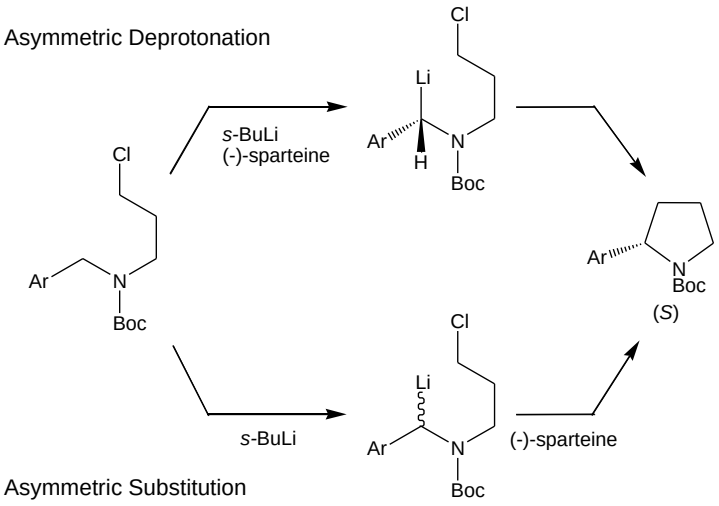

Scheme 13. Asymmetric cyclization of intermediate **71**.

Both methoxy group and protected nitrogen of intermediate **72** were liberated by treatment with boron tribromide, and the subsequent reductive amination provided the tertiary amine **32**, which was crystallized and isolated as the corresponding fumarate. Chiral HPLC analysis on the free base of **32** allowed to detect few traces only of the minor enantiomer (e.e.: 98%). This can be explained by the mutual loss of two components in a mixture after several reaction/purification/crystallization steps: the ratio between the two isomers increases, if the minor component is decreasing. In fact, two enantiomers can have different kinetics of reaction (either considering the

wanted chemical transformation or an undesired side reaction) or of purification/crystallization processes, as known from the theory of the kinetic resolution of racemic mixtures.

Due to the unavailability of commercial benzyl bromides bearing a hydroxymethyl group in *meta* position, we prepared methyl benzoate **74** as the precursor of the desired primary alcohol. The altered electronic properties of the linear intermediate **74**, due to the presence of an electron-withdrawing ester group, led to an unsuccessful ring-closure. The ester function was thus reduced to the corresponding alcohol, which was protected with *tert*-butyldimethylsilyl chloride (TBSCl). Asymmetric cyclization of protected alcohol **76** provided the cyclic intermediate **77** in 70% e.e. Deprotection of both hydroxyl and amine functions, followed by the usual reductive amination step, led to the desired target compound **33** as the pure (*S*)-enantiomer (e.e.: 98%).

A different approach was followed to obtain target compound **34**, that can be considered a molecular hybrid of both (–)-nicotine **9** and anabaseine **12**. In fact, it contains the same five-membered basic ring of (–)-nicotine **9** and an unsaturation which deletes the stereocenter. The iminocyclic system of **34** can be considered as a lower ring-size analogue of anabaseine **12** as well. A palladium(0)-catalyzed copper(I)-assisted Liebeskind-Srogl cross-coupling between pyrrolidin-thione **80** and the proper boronic acid gave the desired cyclic derivative **34** (Scheme 14).[90]

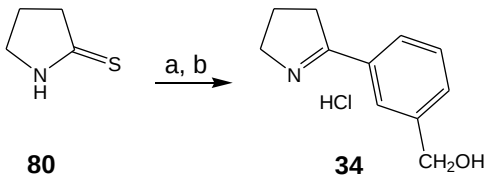

80 **34**

Scheme 14. Synthesis of target compound **34**. *Reagents and conditions:* (a) 3-(hydroxymethyl)phenylboronic acid, copper(I) thiophene-2-carboxilate, $Pd(PPh_3)_4$, THF, MW irradiation, 100°C, 2h; (b) HCl 2.0N in Et_2O, r.t., 3h.

The synthesis of the deschloroepibatidine-related molecules **35** and **36** took advantage of the key intermediate **88**, which was prepared using literature procedures (Scheme 15).[91]

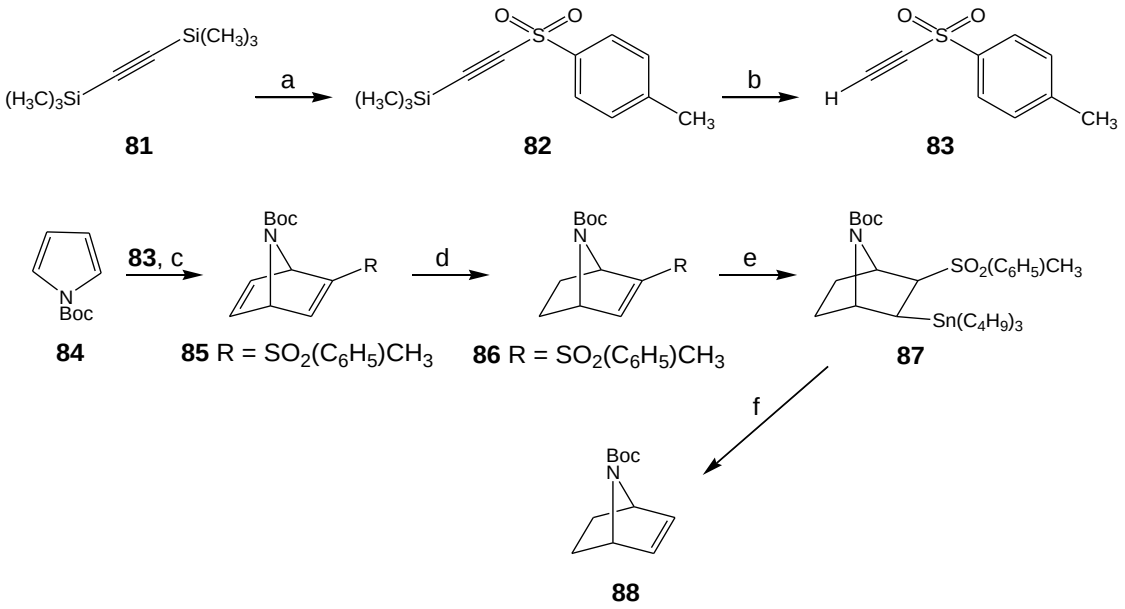

Scheme 15. Synthesis of key intermediate **88**. *Reagents and conditions:* (a) Tosyl chloride, $AlCl_3$, DCM, 0°C to r.t., 6h; (b) K_2CO_3, $NaHCO_3$, DCM/H_2O, r.t., 24h; (c) 80°C, 3 days; (d) $NiCl_2$, $NaBH_4$, HCl 37%, EtOH/THF, r.t., 1h; (e) Tributyltin hydride, AIBN, toluene, reflux, 6h; (f) TBAF, THF, reflux, 16h.

One of the two silyl groups of bis(trimethylsilyl)acetylene **81** was replaced with a tosyl function. Desilylation in a basic medium afforded alkyne **83**, which underwent a Diels-Alder reaction with Boc-pyrrole **84** to obtain the protected bicyclic intermediate **85**. Selective reduction of the less substituted double bond was achieved by using nickel boride as the reductive agent (generated *in situ* by addition of sodium borohydride to nickel chloride). Finally, radical addition of tributyltin hydride at the residual unsaturated bond and subsequent elimination of both tosyl and organostannic functions generated the required alkene **88**.

At this stage, alkene **88** was coupled with the properly substituted phenyl bromides in a reductive palladium acetate-catalyzed Heck reaction variant (Scheme 16).[92] ^{1}H-NMR analysis on products **89** and **90** evidenced a racemic mixture of *exo* epimers, which reflects the active configuration of the model compounds epibatidine **10** and deschloroepibatidine **13**. The preferential *syn* over *anti* diastereoselection has been already rationalized in the literature.[93,94] Treatment with boron tribromide of **89** allowed deprotection

of the phenol oxygen, then the secondary amine functions were generated in acidic media, thus providing the target compounds **35** and **36**.

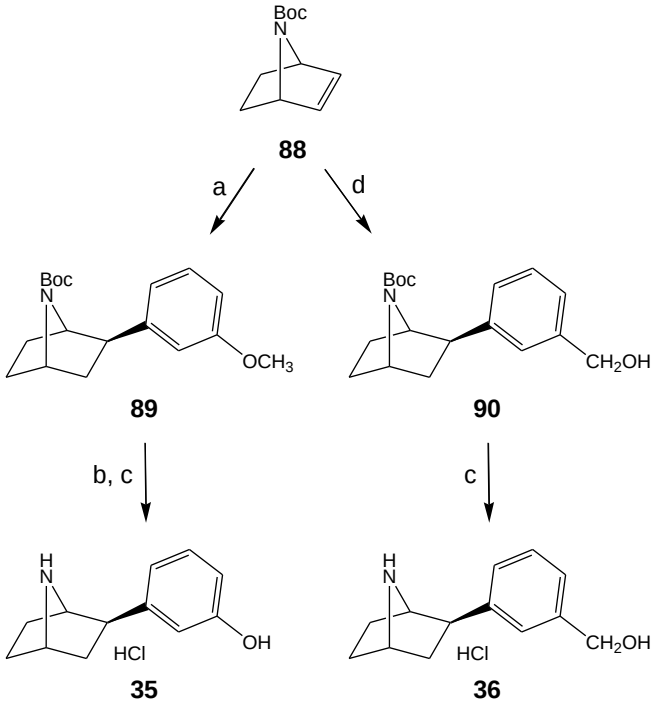

Scheme 16. Synthesis of deschloroepibatidine-related derivatives **35** and **36**. *Reagents and conditions:* (a) 3(Methoxy)phenyl bromide, $Pd(OAc)_2$, TBAC, KCHO, DMF, 80°C, 5h; (b) (i) BBr_3, DCM, -78°C to 0°C, 2h; (ii) Boc_2O, TEA, DCM, r.t., 2h; (c) 4.0 N HCl in 1,4-dioxane, Et_2O, 0°C to r.t., 4h; (d) 3(Bromophenyl)methanol, $Pd(OAc)_2$, TBAC, KCHO, DMF, 80°C, 5h.

The preparation of the anabaseine analogues **37**-**43** required different synthetic approaches. In particular, to synthesize compounds **37** and **38**, commercially available 2-piperidone **91** was used as starting reagent (Scheme 18).[95] Protection of the amide nitrogen with Boc and subsequent treatment with Grignard reagents led to the isolation of the linear intermediates **92** and **94**, bearing a methoxy group and an iodine atom in *m*-position, respectively. The primary amine function of **92** was obtained after acid treatment, then a spontaneous cyclization occurred which provided the iminocyclic intermediate **93**. Demethylation with 48% hydrobromic acid afforded the desired compound **37** (Scheme 17). Since the attempts to prepare Grignard reagents in the presence of a hydroxymethyl or a carboxylate function were unsuccessful, δ-valerolactame **91** was treated with

3-(iodo)benzyl magnesium bromide. The substituted iodobenzene **95** was then submitted to a microwave-assisted carbonylation reaction using molybdenum hexacarbonyl as carbon oxide source.[96,97] Application of this protocol allowed isolation of the corresponding methyl ester **96**, which was selectively reduced with sodium *bis*(2-methoxyethoxy)aluminium hydride (Red-Al) to produce the primary alcohol **38**.[98] (Scheme 18).

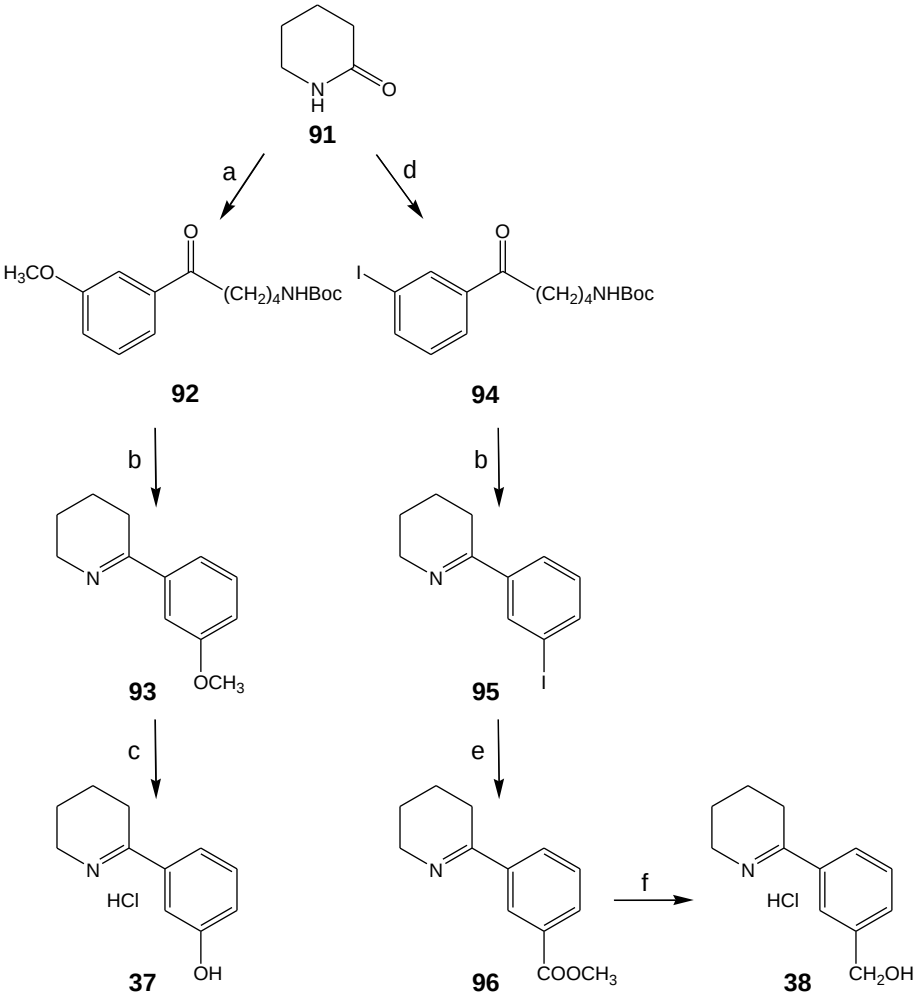

Scheme 17. Synthesis of anabaseine-related derivatives **37** and **38**. *Reagents and conditions:* (a) (i) *n*-BuLi, THF, -78°C, 30 min; (ii) Boc_2O, THF, -78°C, 3h; (iii) 3-(Methoxy)benzylMgBr, THF, -78°C, 3h; (b) (i) TFA, r.t., 3h; (ii) NaOH 30%, r.t., 30 min; (c) HBr 48%, reflux, 2h; (d) (i) *n*-BuLi, THF, -78°C, 30 min; (ii) Boc_2O, THF, -78°C, 3h; (iii) 3-(Iodo)benzylMgBr, THF, -78°C, 3h; (e) $Mo(CO)_6$, Pd/C 10%, DIPEA, DMAP, MeOH, 1,4-dioxane, MW irradiation, 130°C, 1h; (f) Red-Al, THF, r.t., 1h.

The remaining anabaseine analogues **39**-**43** were prepared by reacting 5-bromovaleronitrile **97** and various organolithium and Grignard reagents

(Scheme 18).[99] 1,3-Dibromo-5-fluorobenzene **98** was treated with butyllithium and the corresponding lithiated intermediate was reacted with 5-bromovaleronitrile **97** to provide the cyclic dihalogenated derivative **43**. In this case, the carbonylation-reduction approach illustrated before involved the bromine atom of **43**, giving the desired compound **39**.[96-98] The anabaseine-related derivatives **40**-**42** were easily obtained by reacting 5-bromovaleronitrile **97** with the proper organolithium or Grignard reagent.[99]

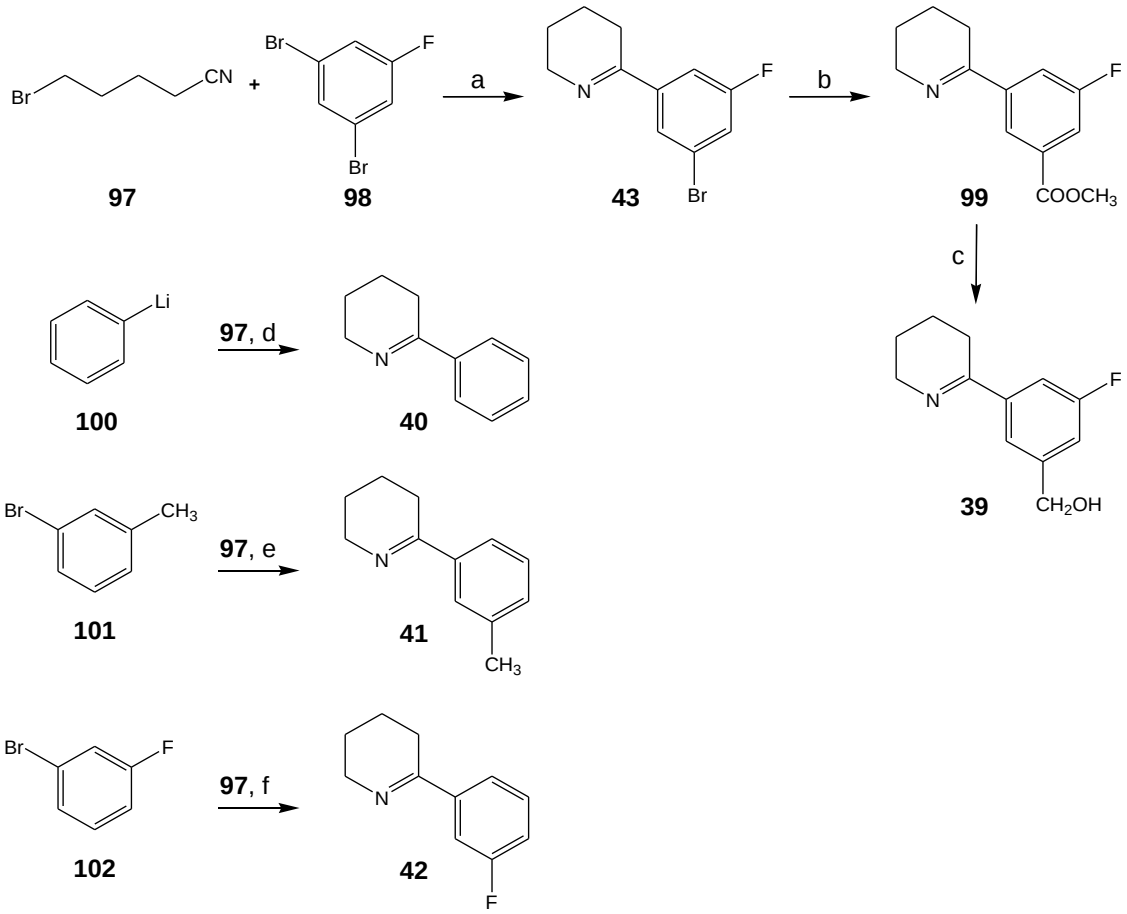

Scheme 18. Synthesis of anabaseine-related **11** derivatives **39** - **43**. *Reagents and conditions:* (a) 1. *n*-BuLi, Et_2O, -78°C, 2h; 2. THF, r.t., 90 min; (b) $Mo(CO)_6$, Pd/C 10%, DIPEA, DMAP, MeOH, 1,4-dioxane, MW irradiation, 130°C, 2h; (c) Red-Al, THF, r.t., 24h; (d) THF, reflux, 3h; (e) Mg, THF, r.t., 20 min; 2. THF, r.t., 1h; (f) *n*-BuLi, Et_2O, -78°C, 1h; 2. THF, r.t., 16h.

3.6. Pharmacological evaluation of compounds 32-44

Compounds **32**-**44** underwent binding experiments to evaluate their affinity at α4β2, α7 and α3β4* nicotinic receptor subtypes in rat cortex membranes, using [^{3}H]epibatidine (α4β2 and α3β4* subtypes) and [^{125}I]α-bungarotoxin (α7 subtype) as radioligands (Table 3).

Compound	α4β2 [^{3}H]Epi (K_i, nM)	α7 [^{125}I]α-BgTx (K_i, nM)	α3β4* [^{3}H]Epi (K_i, nM)	Selectivity ratio α3β4*/α4β2	Selectivity ratio α3β4*/α7
(*S*)-Nicotine **9**	11.1	1600	481	0.02	3.33
Epibatidine **10**	0.06	4.2	0.15	0.40	28
Anabaseine **11**	32	58	660	0.05	0.09
32	703 (14)	10000 (41)	4900 (22)	0.14	14
33	6200 (9)	15000 (43)	4800 (16)	1.29	2.41
34	2060 (21)	590 (48)	1550 (18)	1.33	0.38
35	127 (11)	609 (36)	80 (13)	1.59	7.61
36	429 (14)	1800 (35)	92 (16)	4.66	20
37	32000 (8)	9300 (42)	680 (23)	47	14

38	35000 (13)	158 (35)	80 (35)	438	2
39	744 (38)	82 (73)	80 (24)	9.3	10.3
40	2080 (20)	2400 (53)	115 (18)	18	21
41	1450 (37)	384 (53)	155 (20)	9.4	2
42	2040 (23)	2370 (57)	108 (20)	19	2.5
43	1770 (21)	204 (44)	48 (17)	37	4.2

Table 3. Binding data on the indicated compounds towards the $\alpha4\beta2$, $\alpha7$ and $\alpha3\beta4$ nAChR subtypes

Binding affinity studies were performed, as indicated above, at the Dipartimento di Farmacologia, Chemioterapia e Tossicologia Medica, University of Milan.

As discussed in section 1.9, the putative role of the water molecule in the binding mode of epibatidine **10** and deschloroepibatidine **13** was investigated through molecular dynamics simulations, revealing that a solvated active cavity would allow a better allocation of the ligand pyridine ring, particularly if the chlorine atom of epibatidine is missing, as it is in **13**. In the set of studied compounds, the deschloroepibatidine variants **35** and **36** behaved as nicotinic ligands characterized by a high nanomolar affinity range at the $\alpha4\beta2$ channel, with about a 2000-fold and 7000-fold decrease in affinity compared with the super agonist epibatidine **10**. Their interaction within the LBD of the $\alpha4\beta2$ nAChR was analyzed through molecular dynamics. The two compounds were docked into the active site of the $\alpha4\beta2$ nAChR subtype homology model using the Gold 5.1 program. The docking protocol generated, for compound **35**, two possible binding modes: in the first cluster the phenol OH group is oriented

towards the α4 *C*-loop (Figure 24, left panel) whereas, in the second cluster**,** the OH should be able to displace the putative water molecule, since it directly interacts with the β2-Asn108 residue (Figure 24, right panel).

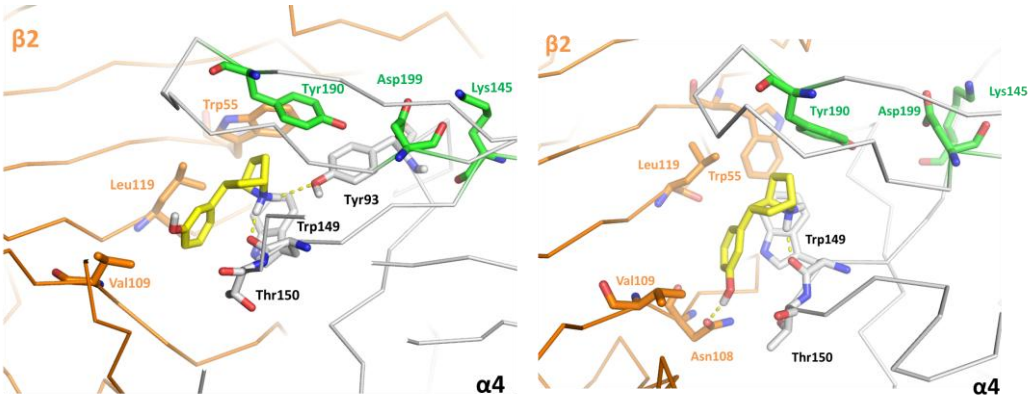

Figure 24. The two different binding modes of compound **35** docked within the α4β2 homology model: on the left, the OH is oriented towards the *C*-loop of the α4-chain; on the right, it reaches the residue Asn108 on the β2-subunit.

Subsequently, through free energy calculations, we observed that, in the most likely binding mode of **35**, the aryl moiety is flipped by 180° compared to the model ligands, with the OH group towards the *C*-loop of the major subunit (Figure 24, left panel). Therefore, compound **35** seems to adopt a different interaction pattern with the receptor compared to that of epibatidine **10** and, in this orientation, its OH group is unable to displace the water molecule. The distance between the aromatic carbon atom, which has replaced the pyridine nitrogen, and the oxygen atom is 1.4 Å, which is too short to mimic the water-assisted H-bond. As a consequence, compound **35** is not able to reproduce the same molecular interactions of the model compound with the target receptor and, after the recognition of the basic scaffold by the *aromatic box* (which is the driving force for binding), the aryl moiety shows stabilizing interactions with different amino acids compared to epibatidine **10**. Indeed, this hypothetical difference in the binding mode of **35** with respect to the reference agonists could be associated, on one hand and, with a considerable loss in binding affinity and, on the other, with the electrophysiological data reported in Figure 25, which are indicative also of a variation in the pharmacological profile.

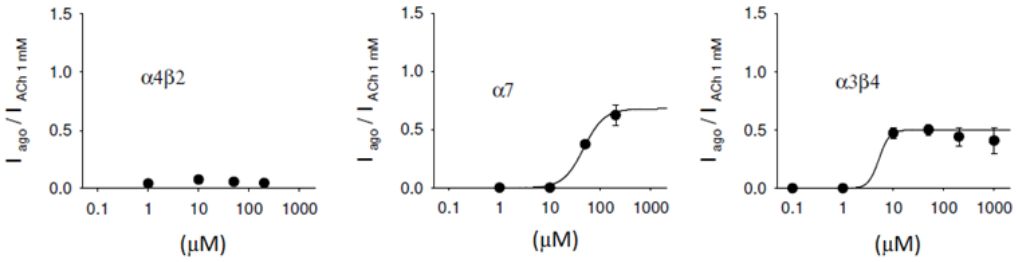

Figure 25. Functional evaluations of compound **35** at the α4β2, α7 and α3β4* nAChRs. The electrophysiological experiments were performed by prof. Sergio Fucile, Dipartimento di Fisiologia e Farmacologia, Università di Roma La Sapienza.[100] Human α4β2, α7 and α3β4 nAChRs were expressed by stable transfection in the human HEK 293 (α4β2 and α3β4* subtypes) or rat anterior pituitary GH4C1 cell line (α7 subtype). Whole-cell current recordings were performed and whole-cell capacitance and patch series resistance were estimated from slow transient compensations. Then, dose-response relationships were constructed by sequentially applying different concentrations of ligands and normalizing the resulting current amplitudes to the value obtained by applying 1 mM ACh to the same cell, as appropriate.

Indeed, epibatidine **10** and deschloroepibatidine **13** are full agonists at the α4β2 nAChRs, whereas **35** behaves as an antagonist at the same receptor subtype. When considering the other tested nicotinic receptors (α7 and α3β4 subtypes) **35** shows a partial agonist profile (Figure 25).

Compound **36**, due to the bulkier hydroxymethyl group, shows an increased distance between the alcohol OH and the carbon atom replacing the pyridine nitrogen up to 2.4 Å. Based on molecular dynamics simulations, in the most favourable binding mode the ligand is able to directly create a hydrogen bond with β2-Leu119, thus displacing and mimicking the putative water molecule (Figure 26). Hence, based on these theoretical results, the hydroxymethyl group attached to the phenyl ring is able to displace the hypothetical water molecule from the α4β2 receptor binding site and, consequently, the relatively low affinity shown by **36** (with a K_i value about 4-fold higher than that of its lower homologue **35**) could be attributed to the reduction of the contribution of the electrostatic terms to the overall value of free energy of binding. In fact, through energy calculations on **36**, we found that the electrostatic contribution to the binding of deschloroepibatidine **13** and **35** is more relevant than that of **36**, and this could suggest that the water

molecule, although not directly involved in a hydrogen bond with the pyridine nitrogen of epibatidine **10**, might influence the weight of the electrostatic terms in the free energy of binding. Moreover, taking into account that the electrostatic interaction is the first driving force of the ligand-receptor recognition process, it is reasonable to assume that the solvent molecules direct the correct placement of the pyridine moiety of epibatidine **10** within the binding site.

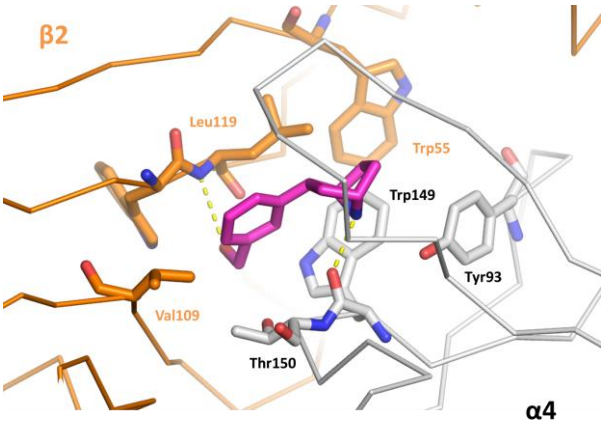

Figure 26. Compound **36** docked within the α4β2 homology model.

As expected, the OH groups of the target compounds have affected the binding affinity at the other tested nAChR subtypes as well. The epibatidine-related compounds **35** and **36** are characterized by a substantial drop of affinity at all the tested nicotinic channels compared to the model ligands, with a decrease of affinity at the α4β2 receptor subtype higher than 2000-fold, whereas at the α7 and α3β4* channels the reduction of affinity is less pronounced (higher than 200-fold and 500-fold, respectively). The hydroxyl groups of compounds **35** and **36**, whether mimicking the water bridge or not, led to a more relevant perturbation of affinity towards the α4β2 nAChR subtype rather than the other tested nicotinic channels and, indeed, compound **35** is still able to partly activate the α7 and α3β4* nAChR subtypes (Figure 25).

The (–)-nicotine **9** variants **32**-**34** show a dramatic drop of affinity at all the tested receptor subtypes. However, a further analysis reveals that the

reduction of binding affinity is again more pronounced for the heteromeric α4β2 channel compared to the α7 and α3β4* subtypes (higher than 100-fold vs. 5-fold and 10-fold), the same trend observed for the epibatidine analogues.

On the contrary, the anabaseine derivatives **37**-**43** are characterized by an overall high affinity at the α3β4* receptors, with some selectivity towards the other channels. As a matter of fact, compounds **38**-**43** modestly increase the α3β4* affinity of anabaseine **12** (from 4- to 14-fold), while their affinity is substantially reduced at the other nAChR subtypes. In general, the selectivity profile of anabaseine **12** has been completely reversed by replacing the pyridine nitrogen with the hydroxyl and hydroxymethyl groups.

The binding affinity at the α4β2 nAChR subtype was highly affected by the absence of the pyridine nitrogen: an average reduction of about 300-fold was achieved, even more pronounced for compounds **37** and **38** with a higher than 1000-fold decrease. (–)-Nicotine **9** and anabaseine **12** have very similar affinity values at the α4β2 receptor and the reduction in affinity of their modified analogues followed a similar trend. Conversely, the binding at the α7 nAChR subtype was reduced only by 40-fold on average. On the whole, the anabaseine-related set of compounds displays a decreased affinity at both α4β2 and α7 receptors, more marked again for the heteromeric subtype, while possessing a remarkable increase of affinity at the α3β4* nAChR.

Compound **38**, bearing the hydroxymethyl group in *meta* position, increases the anabaseine α3β4* vs. α4β2 selectivity by 8000-fold, while it still retains some α7 affinity. We studied the binding mode of **38** within the α3β4* LBD trough a docking analysis into the active site of the homology model of this subtype (Figure 27). A hydrogen bond interaction between the hydroxymethyl group and β4-Thr107 could suggest the displacing of the water molecule and therefore the creation of a less hydrophilic environment of the active cavity. A reduced contribution of the electrostatic terms in the free energy of binding could be one of the reasons for the decreased binding affinity at the α4β2 and α7 nAChRs subtypes, whereas the same component could be less relevant for the α3β4* orthosteric site. However, a more in depth

analysis of the α3β4* active site properties is still required to support this hypothesis.

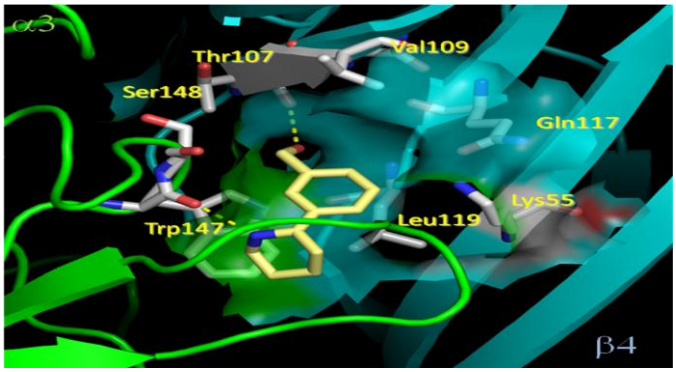

Figure 27. Compound **38** docked within the α3β4 homology model.

Electrophysiological experiments on compound **38** elucidated its α3β4* partial agonist and α7 full agonist profiles (Figure 28). In addition, this compound hasn't been able to evoke any current at the α4β2 channel.

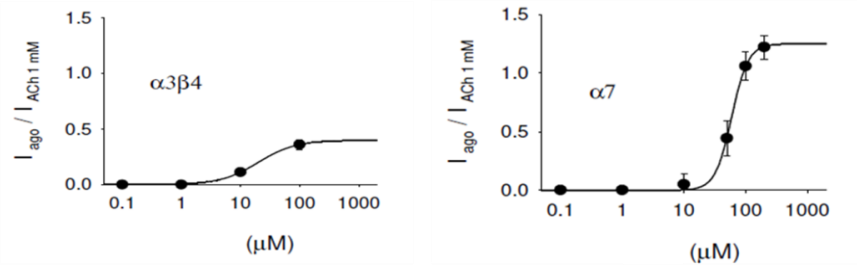

Figure 28. Functional evaluations of compound **38** at the α3β4 and α7 nAChRs (see legend to Figure 25).

Further comments should be spent on the compounds related to **38**. The phenol-containing analogue **37** remarkably improved the α3β4* vs. α7 selectivity profile compared to **38**, although a relevant reduction of α3β4* affinity was observed. On the contrary, the affinity at the α3β4* nAChR subtype is not affected if an extra substituent is inserted in *meta* position: compound **39**, which is characterized by a hydroxymethyl group and a fluorine on the aromatic ring, displayed the same affinity at the α3β4* channel compared to **38**, with an 8-fold decrease of affinity at the homomeric α7

receptor and a 40-fold regain at the $\alpha4\beta2$ subtype compared to **38**. A broader study is required to better clarify the effect of the substitution pattern on the affinity/selectivity profile at the $\alpha3\beta4$* subtype for these analogues of **38**.

Interestingly, even compounds bearing only hydrophobic substituents (**40**-**43**) are characterized by a high affinity at the $\alpha3\beta4$* nAChR subtype. In general, these novel nicotinic ligands show promising affinity at the $\alpha3\beta4$* channel (the best value is displayed by compound **43** with a value of K_i = 48 nM), with some selectivity towards the other tested nAChRs. These affinity data could imply a quite different binding mode with respect to anabaseine **12** and, as a consequence, a putative change in the pharmacological profile at this subtype. The hydrophobic aryl moieties might interact with different amino acids within the LBD and the water molecule might not interfere at all with the binding recognition process. As a result of different binding modes, electrophysiological data on the most interesting among the anabaseine-related compounds could point out a progressive modulation of the pharmacological behaviour, passing from full agonism, typical of the natural model compound, to partial agonism or antagonism of these more “hydrophobic” ligands.

4. Conclusions

Two groups of novel bicycloctane- and quinuclidine-containing derivatives **14**-**31** (Figure 29) were initially designed, synthesized, and assayed to study and validate a substitution pattern able to direct the selectivity profile towards the $\alpha4\beta2$ or $\alpha7$ nAChR subtypes.

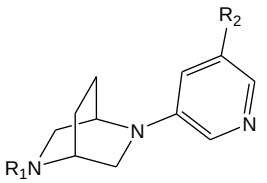

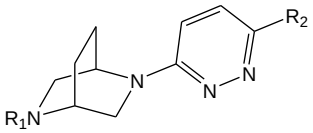

14 R_1 = H R_2 = H

15 R_1 = $(CH_3)_2$ R_2 = H

16 R_1 = H R_2 = OCH_2CH_3

17 R_1 = H R_2 = $OCH_2CH_2CH_3$

18 R_1 = H R_2 = Cl

19 R_1 = H R_2 = Ph

20 R_1 = CH_3 R_2 = Ph

21 R_1 = $(CH_3)_2$ R_2 = Ph

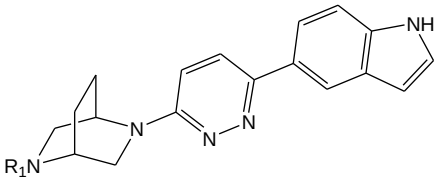

22 R_1 = H

23 R_1 = CH_3

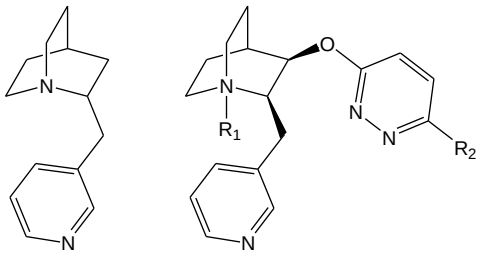

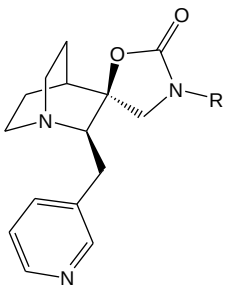

24

25 R_1 = H R_2 = Cl

26 R_1 = H R_2 = Ph

27 R_1 = CH_3 R_2 = Ph

28 R_1 = H R_2 = 5'-Indolyl

29 R = H

30 R = CH_3

31 R = Benzyl

Figure 29. Bicyclooctane- and quinuclidine-containing derivatives.

Some of the investigated compounds **14-23** were characterized as potent and selective $\alpha4\beta2$ or $\alpha7$ nAChR ligands, as a function of the substituents on the heteroaromatic moiety as well as the nature of the charged nitrogen atom. Conversely, in the set of analogues of quinuclidine (**24-31**), a drop in affinity and selectivity was observed with respect to the reference $\alpha7$-selective ligands.

Next, a third group of quite novel nicotinic ligands (compound **32**-**43**, Figure 30) was generated by modifying the structure of selected natural nicotinic agonists. Our initial goal was to investigate the putative role of water molecules in the LBD of the most studied nAChRs subtypes.

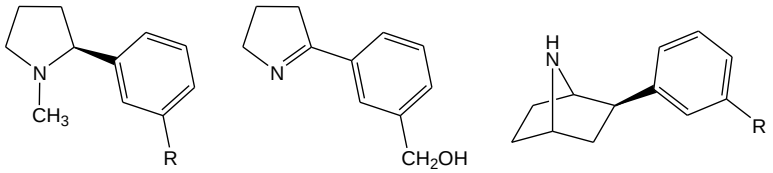

32 R = OH **34** **35** R = OH

33 R = CH_2OH **36** R = CH_2OH

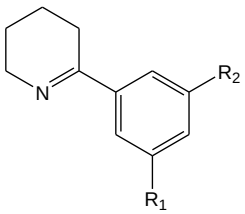

37 R_1 = OH R_2 = H

38 R_1 = CH_2OH R_2 = H

39 R_1 = CH_2OH R_2 = F

40 R_1 = H R_2 = H

41 R_1 = CH_3 R_2 = H

42 R_1 = F R_2 = H

43 R_1 = F R_2 = Br

Figure 30. Novel nicotinic ligands based on the structures of natural nicotinic agonists.

We studied this group of new compounds by means of binding affinity assays, functional (electrophysiological) experiments, and computational analysis (molecular docking, molecular dynamics simulations and free energy calculations). Our conclusion is that the molecule of water, rather than being directly involved in a hydrogen bond with the ligand participating to the stabilization of the ligand-receptor complex, could influence the weight of the

electrostatic terms in the free energy of binding. The skeleton of known natural nicotinic agonists was modified adding substituents able to mimic or disrupt the water molecule in the receptor-ligand interaction, leading to a remarkable perturbation of the binding affinity, subtype selectivity and pharmacological profile. This last set of compounds represents a new class of anabaseine-related analogues characterized as $\alpha 3\beta 4$*-preferring ligands, in which the agonist pharmacological profile of the natural model derivative has been shifted towards partial agonism or, maybe, antagonism. In the light of these data, the study of the most interesting among the latter compounds will be extended, aiming at better defining relevant structural requirements able to address nicotinic ligands towards a subtype, the $\alpha 3\beta 4$* nAChR, which still lacks an in depth characterization.

5. Experimental

5.1. General Procedures

Procedures that resulted in the recovery or decomposition of starting material are not described in this section. All reactions that involve air/moisture sensitive compounds were performed under an atmosphere of dry argon with flame dried glassware. Reactions were stirred using a Teflon® coated magnetic stirrer bar and a stirrer hot plate.

NMR Spectroscopy

Proton and carbon magnetic resonance spectra were recorded at the specified field strength and in the solvent indicated using standard pulse techniques on Varian Mercury 300 (300 MHz) spectrometer at ambient temperatures.

Chemical shifts (δ_H) are reported in parts per million (ppm) and are referenced to TMS or the residual solvent peak. Coupling constants (*J*) are quoted to the nearest 0.1 Hz.

Mass Spectrometry

Mass spectra were recorded by the University of Milan mass spectrometry service using a VG Autospec (EI/CI mode). Only molecular ions (M^+), and fragments from the molecular ions and other major peaks are reported.

Microwave Reactor

Where microwave irradiation was used, reactions were carried out in a CEM Focused Microwave Synthesis System, Model Discovery.

Chiral HPLC

Chiral HPLC was performed eluiting with the specified eluent at the specified flowrate using a Kromasil Amycoat column (0.46 cm x 25 cm, 5μm), using a

Jasco PU-980 HPLC pump achieving detection using a Jasco UV-975 Detector.

Optical Rotation

Optical rotation measurements were performed using a Jasco P-1010 Polarimeter.

5.2. Experimental Procedures

Diethyl *meso*-2,5-diazidohexanedioate [45]

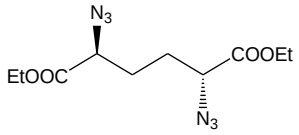

To a solution of diethyl *meso*-2,5-dibromoadipate **44** (25 g, 69.43 mmol) in absolute EtOH (150 mL), NaN_3 was added (12.37 g, 190.25 mmol) and the mixture was stirred under reflux for 5 h. The reaction was then diluted with water (100 mL) and extracted with Et_2O (3 x 50 mL). The organic layers were dried over Na_2SO_4, filtered and concentrated in *vacuo* to afford 20.25 g of clean product (100% yield).

45: yellow oil.

***R*f**: 0.3 (CyHex/AcOEt 9:1); UV, $KMnO_4$.

^{1}H-NMR ($CDCl_3$): δ 1.32 (t, *J* = 7.2 Hz, 6H), 1.80-2.00 (m, 4H), 3.91 (m, 2H), 4.27 (q, *J* = 7.2 Hz, 4H).

Ethyl 5-amino-6-oxopiperidine-2-carboxylate [46]

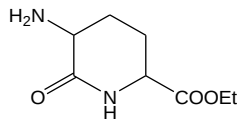

To an ice-cold solution of diethyl *meso*-2,5-diazidohexanedioate **45** (19.734 g, 79.5 mmol) in THF (134 mL), PPh_3 (43.79 g, 166.9 mmol) was cautiously added and the mixture stirred at room temperature for 3 h. Then, water (5.8 mL) was added and the reaction was stirred overnight at room temperature.
The solvent was evaporated in *vacuo* and the crude material purified by flash chromatography (DCM/MeOH 95:5 $\rightarrow$ 80:20) to give 11.85 g of monocyclic amide (80% yield).

46: yellow solid.

***R*$_f$**: 0.4 (DCM/MeOH 9:1); $KMnO_4$.

^{1}H-NMR ($CDCl_3$): δ 1.29 (t, *J* = 7.2 Hz, 3H), 1.59-1.71 (m, 1H), 1.76-1.89 (m, 1H), 2.01 (bs, 2H), 2.15 (m, 1H), 2.24-2.39 (m, 1H), 3.33 (m, 1H), 4.10 (m, 1H), 4.20 (q, *J* = 7.2 Hz, 2H), 6.20 (bs, 1H).

MS (ESI): *m/z* 187.1 $[M+H]^+$, calc. for $C_8H_{14}N_2O_3$ 186.21.

2,5-Diazabicyclo[2.2.2]octane-3,6-dione [47]

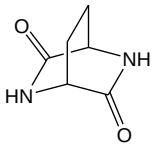

Sodium (1.6 g, 69.344 mmol) was added in an argon atmosphere to dry MeOH (250 mL). Once MeONa was completely formed (clean solution), a solution of ethyl 5-amino-6-oxopiperidine-2-carboxylate **46** (11.85 g, 63.04 mmol) in dry MeOH was added (250 mL) and the resulting mixture was heated at reflux for 4 h (pH $\geq$ 10).

The solvent was evaporated in *vacuo* and the resulting white solid was digested with Et_2O (two times) and AcOEt (one time) to give 8.84 g of the bicyclic amide (100% yield).

47: colourless solid.

m.p.: 245-249° C dec.

***R*$_f$**: 0.1 (DCM/MeOH 9:1 + 1% TFA).

^{1}H-NMR (CD_3OD): δ 1.89 (m, 2H), 2.06 (m, 2H), 3.90 (m, 2H).

2,5-Dibenzyl-2,5-diazabicyclo[2.2.2]octane-3,6-dione [48]

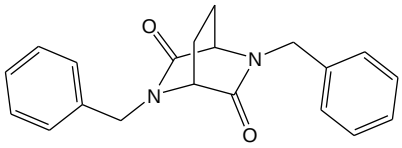

To a suspension of 2,5-diazabicyclo[2.2.2]octane-3,6-dione **47** (8.84 g 63.04) in dry DMF (200 mL) in an argon atmosphere, 60% NaH was added portionwise (5 g, 126 mmol) and the mixture was stirred at room temperature for 1 h.

Once cooled with an ice-bath, benzyl chloride (18.1 mL, 157.6 mmol) was added dropwise and the mixture stirred overnight at room temperature.

The reaction was poured into a mixture of water and ice (300 mL) and extracted with $CHCl_3$ (3 x 50 mL). The organic layers were washed with water and brine, then dried over Na_2SO_4, filtered and concentrated. The crude product was treated with Et_2O to crash out 13.307 g of protected amide as colourless crystals (66% yield).

48: colourless solid.

m.p.: 165-167° C.

$\boldsymbol{R_f}$: 0.25 (CyHex/AcOEt 5:5); UV, $KMnO_4$.

^{1}H-NMR ($CDCl_3$): δ 1.69-1.81 (m, 4H), 4.01 (s, 2H), 4.37 (d, *J* = 14.9 Hz, 2H), 4.73 (d, *J* = 14.9 Hz, 2H), 7.24 (m, 4H), 7. 32 (m, 6H).

MS (ESI): *m/z* 321.1 $[M+H]^+$, calc. for $C_{20}H_{20}N_2O_2$ 320.39.

2,5-Dibenzyl-2,5-diazabicyclo[2.2.2]octane [49]

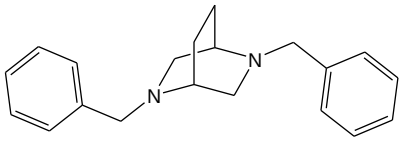

To a solution of 2,5-dibenzyl-2,5-diazabicyclo[2.2.2]octane-3,6-dione **48** (5.688 g, 17.754 mmol) in dry THF (132 mL) in an argon atmosphere, $LiAlH_4$ (2.7 g, 71.01 mmol) was added slowly and the mixture stirred under reflux for 4 h.

The reaction was ice-cooled, diluted with Et_2O (20 mL) and quenched with AcOEt (15 mL) and water (10 mL). The suspension was filtered through a celite-septum and the solvent removed in *vacuo* to provide 4.891 g of protected amine (94% yield).

49: yellow oil.

***R*f**: 0.3 (CyHex/AcOEt 2:8); UV, $KMnO_4$, Dragendorff reagent.

^{1}H-NMR ($CDCl_3$): δ 1.65 (m, 2H), 1.98 (m, 2H), 2.61 (bs, 2H), 2.74 (d, *J* = 10.3 Hz, 2H), 3.08 (d, *J* = 10.3 Hz, 2H), 3.76 (s, 4H), 7.21-7.40 (m, 10H).

MS (ESI): *m/z* 293.2 $[M+H]^+$, calc. for $C_{20}H_{24}N_2$ 292.42.

2,5-Diazabicyclo[2.2.2]octane dihydrochloride [50]

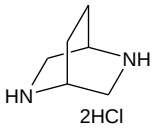

A solution of 2,5-dibenzyl-2,5-diazabicyclo[2.2.2]octane **49** (1.546 g, 5.287 mmol) in MeOH (180 mL) was treated with concentrated HCl (3.8 mL) and then Pd/C 10% (0.35 g) was added. The mixture was hydrogenated at room temperature for 16 h.
The resulting suspension was filtered through a celite-septum and the solvent evaporated in *vacuo* to afford 0.937 g of pure crystalline diamine dihydrochloride (96% yield).

50: yellow solid.

m.p.: 200°C dec.

R_f: 0.0; $KMnO_4$.

^{1}H-NMR (D_2O): δ 1.83-1.93 (m, 2H), 2.09-2.19 (m, 2H), 3.48 (m, 4H), 3.83 (bs, 2H).

MS (ESI): *m/z* 112.9 $[M+H]^+$, calc. for $C_6H_{12}N_2$ 112.17.

tert-Butyl 2,5-diazabicyclo[2.2.2]octane-2-carboxylate [51]

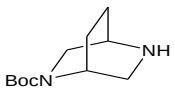

To a solution of 2,5-diazabicyclo[2.2.2]octane dihydrochloride **50** (0.937 g, 5.062 mmol) in *i*-PrOH/H_2O/NaOH 1.0 M (70 mL/24.3 mL/4.6 mL) at 0° C, a solution of Boc_2O (0.552 g, 2.531 mmol) in 2-propanol (12 mL) was added dropwise and the mixture was stirred at 0° C for 2 h.
The solvent was removed in *vacuo* and the crude material was treated with brine (30 mL) and 2.0 N NaOH in water (pH = 10), then extracted with AcOEt (5 x 20 mL). The pooled organic layers were washed with brine, dried over Na_2SO_4, filtered and concentrated to provide 0.535 g of pure mono-Boc-protected amine (50% yield).

51: yellow oil.

***R*$_f$**: 0.45 (DCM/MeOH 8:2); $KMnO_4$.

^{1}H-NMR ($CDCl_3$): δ 1.45 (s, 9H), 1.64-1.84 (m, 2H), 1.86-2.04 (m, 2H), 2.98-3.10 (m, 2H), 3.20-3.32 (m, 1H), 3.36-3.48 (m, 1H), 3.50-3.62 (m, 1H), 3.90-4.08 (m, 1H).

MS (ESI): *m/z* 213.2 $[M+H]^+$, calc. for $C_{11}H_{20}N_2O_2$ 212.29.

tert-Butyl 5-(pyridin-3-yl)-2,5-diazabicyclo[2.2.2]octane-2-carboxylate [52]

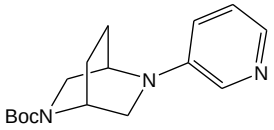

A solution of (±)-BINAP (62 mg, 0.1 mmol) e $Pd_2(dba)_3$ (46 mg, 0.05 mmol) in dry toluene (20 mL) was heated at reflux in an argon atmosphere for 10 min. Once the solution was cooled to 40°C, a solution of *tert*-butyl 2,5-diazabicyclo[2.2.2]octane-2-carboxylate **51** (535 mg, 2.52 mmol) in dry toluene (7 mL), *t*-BuONa (388 g, 4.032 mmol), 3-bromo-pyridine (0.246 mL, 2.52 mmol) was added and the resulting mixture was stirred at 80°C for 5 h.
The mixture was cooled to ambient and filtered through a celite-septum. The solvent was removed in *vacuo* and the residue purified by flash chromatography (CyHex/AcOEt 20:80 $\rightarrow$ 10:90) to obtain 790 mg of pure product (67% yield).

52: yellow oil.

***R*f:** 0.25 (AcOEt); UV, $KMnO_4$, Dragendorff reagent.

^{1}H-NMR ($CDCl_3$): δ 1.43 (s, 9H), 1.75-1.86 (m, 2H), 2.00-2.08 (m, 2H), 3.32-3.38 (m, 1H), 3.45-3.53 (m, 1H), 3.60-3.64 (m, 2H), 4.02 (m, 1H), 4.24-4.38 (m, 1H), 6.86 (m, 1H), 7.09 (m, 1H), 7.92 (m, 1H), 8.04 (m, 1H).

MS (ESI): *m/z* 290.2 $[M+H]^+$, calc. for $C_{16}H_{23}N_3O_2$ 289.37.

2-(Pyridin-3-yl)-2,5-diazabicyclo[2.2.2]octane dihydrochloride [14]

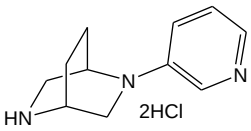

To a solution of *tert*-butyl 5-(pyridin-3-yl)-2,5-diazabicyclo[2.2.2]octane-2-carboxylate **52** (139 mg, 0.480 mmol) in Et_2O (1 mL) at 0°C, 2.0 M HCl in Et_2O (1 mL) was added dropwise and the mixture stirred at room temperature for 3 h.
The precipitate was filtered and washed with Et_2O to provide 99 mg of the title compound (79% yield).

14: dark-yellow solid.

^{1}H-NMR (CD_3OD): δ 1.82-1.91 (m, 2H), 2.03-2.07 (m, 2H), 3.38-3.53 (m, 3H), 3.68-3.73 (m, 1H), 3.89 (m, 1H), 4.23 (m, 1H), 7.65 (m, 2H), 7.86 (m, 1H), 7.96 (s, 1H).

MS (ESI): *m/z* 190.1 $[M+H]^+$, calc. for $C_{11}H_{15}N_3$ 289.26.

2,2-Dimethyl-5-(pyridin-3-yl)-5-aza-2-azoniabicyclo[2.2.2]octane iodide [15]

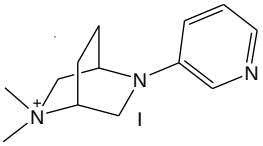

To a solution of *tert*-butyl 5-(pyridin-3-yl)-2,5-diazabicyclo[2.2.2]octane-2-carboxylate **52** (420 mg, 1.451 mmol) in formic acid (3.5 mL), 37% formaldehyde in water was added (0.622 mL) and the solution was stirred at 90°C for 1 h.

The mixture was cooled to ambient and quenched with saturated $NaHCO_3$ solution (5 mL). The aqueous layer was basified with NaOH 5.0 M (pH > 10) and extracted with DCM (6 x 3 mL). The pooled organic layers were dried over Na_2SO_4, filtered and concentrated to afford 292 mg of pure tertiary amine (99% yield).

To a solution of 2-methyl-5-(pyridin-3-yl)-2,5-diazabicyclo[2.2.2]octane (182 mg, 0.895 mmol) in Et_2O (4 mL), methyl iodide (0.167 mL 2.69 mmol) was added and the mixture stirred at room temperature for 6 h.

The mixture was filtered and the solid was treated with hot MeOH until a clean solution was observed. Once cooled to ambient, the precipitate was filtered off, and the clean solution was concentrated in *vacuo* to obtain 87 mg of the title compound (28% yield).

15: yellow solid.

m.p.: 220-222°C dec.

^{1}H-NMR (CD_3OD): δ 2.03-2.12 (m, 3H), 2.47-2.57 (m, 1H), 3.35 (s, 3H), 3.38 (s, 3H), 3.50-3.54 (m, 1H), 3.70-3.74 (m, 1H), 3.81-3.86 (m, 1H), 3.94 (m, 1H), 4.2 (dt, *J* = ? Hz, 1H), 4.39 (m, 1H), 7.30 (m, 1H), 7.96 (m, 1H), 8.12 (d, *J* = 2.48 Hz, 1H).

^{13}C-NMR (CD_3OD): δ 20.31, 21.49, 44.70, 46.56, 53.50, 54.05, 63.28, 68.03, 120.09, 124.537, 133.88, 138.23, 143.63.

MS (ESI): *m/z* 218.2 $[M+H]^+$, calc. for $C_{13}H_{20}N_3$ 218.32.

3-Bromo-5-ethoxypyridine [55]

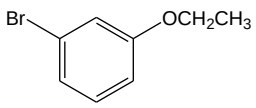

Sodium (0.146 g, 6.33 mmol) was added in an argon atmosphere to dry EtOH (5 mL). Once EtONa was completely formed (clean solution), the solvent was removed in *vacuo* , the residue was taken in dry DMF (6 mL) and 3,5-dibromopyridine (1 g, 4.22 mmol) was added. The mixture was stirred in an argon atmosphere at 70°C for 3 h.

The reaction was poured into ice/water (25 mL) and extracted with Et_2O (3 x 10 mL). The pooled organic layers were washed with water and brine, dried over Na_2SO_4 and concentrated. The crude product was purified by flash chromatography (CyHex/AcOEt 90:10) to afford 690 mg of the desired compound (78% yield)

55: yellow oil.

^{1}H-NMR ($CDCl_3$): δ 1.44 (t, *J* = 7.15 Hz, 3H), 4.06 (q, *J* = 7.15 Hz, 2H), 7.34 (t, *J* = 1.92; 2.48 Hz, 1H), 8.22 (d, *J* = 2.47; Hz, 1H), 8.26 (d, *J* = 1.92 Hz, 1H).

tert-Butyl 5-(5-ethoxypyridin-3-yl)-2,5-diazabicyclo[2.2.2]octane-2-carboxylate [53]

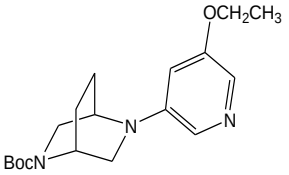

A solution of (±)-BINAP (32 mg, 0.05 mmol) and $Pd_2(dba)_3$ (23 mg, 0.03 mmol) in dry toluene (10 mL) was heated at reflux in an argon atmosphere for 10 min. Once the solution was cooled to 40°C, a solution of *tert*-butyl 2,5-diazabicyclo[2.2.2]octane-2-carboxylate **51** (269 mg, 1.27 mmol) in dry toluene (3.6 mL), *t*-BuONa (195 g, 2.03 mmol), 3-bromo-5-ethoxypyridine **55** (267 mg, 1.27 mmol) were added and the resulting mixture was stirred at 80°C for 4 h.

The mixture was cooled to ambient and filtered through a celite-septum. The solvent was removed in *vacuo* and the residue purified by flash chromatography (CyHex/AcOEt 20:80) to obtain 138 mg of pure product (33% yield).

53: yellow oil.

***R*$_f$:** 0.17; UV, $KMnO_4$.

^{1}H-NMR ($CDCl_3$): δ 1.39-1.44 (m, 3H), 1.47 (s, 9H), 1.80-1.88 (m, 2H), 2.03-2.09 (m, 2H), 3.33-3.39 (m, 1H), 3.46-3.55 (m, 1H), 3.61-3.67 (m, 2H), 4.02-4.13 (m, 3H), 4.25-4.40 (m, 1H), 6.41 (m, 1H), 7.67 (m, 1H), 7.73 (m, 1H).

^{13}C-NMR ($CDCl_3$): δ 14.80, 25.26, 25.92, 28.71, 29.93, 44.22, 50.30, 53.85, 64.10, 80.03, 104.81, 124.56, 127.06, 145.43, 154.78, 156.23.

MS (ESI): *m/z* 334.2 $[M+H]^+$, calc. for $C_{18}H_{27}N_3O_3$ 333.43.

2-(5-Ethoxypyridin-3-yl)-2,5-diazabicyclo[2.2.2]octane dihydrochloride [16]

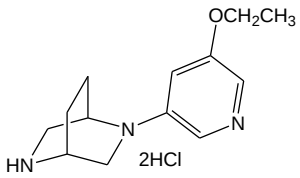

To a solution of t*ert*-butyl 5-(5-ethoxypyridin-3-yl)-2,5-diazabicyclo[2.2.2] octane-2-carboxylate **53** (120 mg, 0.232 mmol) in MeOH/Et_2O 1:1 (0.8/0.8 mL) at 0°C, 2.0 M HCl in Et_2O (2.14 mL) was added dropwise and the mixture stirred at room temperature for 6 h.
The solvent was removed in *vacuo* and the residue digested with Et_2O to obtain 81 mg of the desired compound (73% yield).

16: colourless solid.

m.p.: 240°C dec.

^{1}H-NMR (CD_3OD): δ 1.46 (t, *J* = 7.16 Hz, 3H), 2.03-2.07 (m, 2H), 2.11-2.20 (m, 2H), 3.47-3.67 (m, 3H), 3.85-3.89 (m, 1H), 3.98 (m, 1H), 4.26 (q, *J* = 7.16 Hz, 1H), 4.43 (m, 1H), 7.34 (m, 1H), 7.86 (d, *J* = 1.65 Hz, 1H), 7.94 (d, *J* = 1.65 Hz, 1H).

^{13}C-NMR (CD_3OD): δ 13.53, 20.81, 23.20, 43.57, 46.12, 46.27, 65.83, 111.16, 117.58, 118.40, 147.13, 158.76.

MS (ESI): *m/z* 234.2 $[M+H]^+$, calc. for $C_{13}H_{19}N_3O$ 233.31.

3-Bromo-5-propoxypyridine [56]

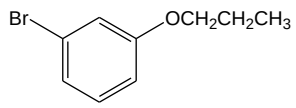

Sodium (0.437 g, 19 mmol) was added in an argon atmosphere to dry 1-propanol (15 mL). Once *n*-PrONa was completely formed (clean solution), the solvent was removed in *vacuo* , the residue was taken in dry DMF (18 mL) and 3,5-dibromopyridine (3 g, 12.66 mmol) was added. The mixture was stirred in an argon atmosphere at 70°C for 4 h.

The reaction was poured into ice/water (50 mL) and extracted with Et_2O (3 x 20 mL). The pooled organic layers were washed with water and brine, dried over Na_2SO_4 and concentrated. The crude product was purified by flash chromatography (CyHex/AcOEt 90:10) to afford 1.817 g of the desired compound (66% yield).

56: yellow oil.

^{1}H-NMR ($CDCl_3$): δ 1.04 (t, *J* = 7.43 Hz, 3H), 1.82 (sex, *J* = 6.33; 7.43 Hz, 2H), 3.95 (t, *J* = 6.33 Hz, 2H), 7.34 (t, *J* = 1.65; 2.48 Hz, 1H), 8.22 (d, *J* = 2.48; Hz, 1H), 8.26 (d, *J* = 1.65 Hz, 1H).

tert-Butyl 5-(5-propoxypyridin-3-yl)-2,5-diazabicyclo[2.2.2]octane-2-carboxylate [54]

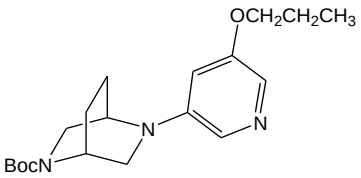

A solution of (±)-BINAP (27 mg, 0.04 mmol) and $Pd_2(dba)_3$ (20 mg, 0.02 mmol) in dry toluene (8.5 mL) was heated at reflux in an argon atmosphere for 10 min. Once the solution was cooled to 40°C, a solution of *tert*-butyl 2,5-diazabicyclo[2.2.2]octane-2-carboxylate **51** (227 mg, 1.07 mmol) in dry toluene (3 mL), *t*-BuONa (165 g, 1.71 mmol), 3-bromo-5-propoxypyridine **56** (231 mg, 1.07 mmol) was added and the resulting mixture was stirred at 80°C for 4 hours.

The mixture was cooled to ambient and filtered through a celite-septum. The solvent was removed in *vacuo* and the residue purified by flash chromatography (CyHex/AcOEt 10:90) to obtain 276 mg of pure product (74% yield).

54: yellow oil.

***R*$_f$:** 0.21; UV, $KMnO_4$.

^{1}H-NMR ($CDCl_3$): δ 1.03 (t, *J* = 7.42 Hz, 3H), 1.46 (s, 9H), 1.75-1.88 (m, 4H), 2.05-2.11 (m, 2H), 3.34-3.39 (m, 1H), 3.47-3.55 (m, 1H), 3.61-3.65 (m, 2H), 3.93-4.04 (m, 3H), 4.25-4.40 (m, 1H), 6.40 (m, 1H), 7.68-7.72 (m, 2H).

^{13}C-NMR (DMSO-d6): δ 11.08, 22.77, 25.77, 25.09, 25.83, 28.79, 44.36, 45.14, 45.98, 50.47, 69.77, 79.36, 104.04, 125.68, 127.34, 145.70, 154.38, 156.27.

MS (ESI): *m/z* 348.2 $[M+H]^+$, calc. for $C_{19}H_{29}N_3O_3$ 347.45.

2-(5-Propoxypyridin-3-yl)-2,5-diazabicyclo[2.2.2]octane dihydrochloride [17]

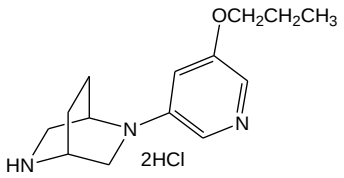

To a solution of *tert*-butyl 5-(5-propoxypyridin-3-yl)-2,5-diazabicyclo[2.2.2] octane-2-carboxylate **54** (276 mg, 0.79 mmol) in MeOH/Et_2O 1:1 (1.75/1.75 mL) at 0°C, 2.0 M HCl in Et_2O (3.2 mL) was added dropwise and the mixture stirred at room temperature for 5 h.
The solvent was removed in *vacuo* and the residue digested with Et_2O to obtain 202 mg of the wanted compound (80% yield).

17: yellow solid.

m.p.: 240-242°C dec.

^{1}H-NMR (CD_3OD): δ 1.07 (t, *J* = 7.43 Hz, 3H), 1.87 (sex, *J* = 6.32; 7.43 Hz, 2H), 2.02-2.07 (m, 2H), 2.09-2.26 (m, 2H), 3.52-3.67 (m, 3H), 3.85-3.89 (m, 1H), 3.98 (m, 1H), 4.16 (t, *J* = 6.32 Hz, 2H), 4.43 (m, 1H), 7.36 (m, 1H), 7.87 (d, *J* = 1.92 Hz, 1H), 7.93 (d, *J* = 2.2 Hz, 1H).

^{13}C-NMR (CD_3OD): □ 9.45, 20.81, 22.14, 23.20, 43.56, 46.12, 46.28, 71.52, 111.15, 117.56, 118.40, 147.12, 158.94.

MS (ESI): *m/z* 248.2 $[M+H]^+$, calc. for $C_{14}H_{21}N_3O$ 247.34.

tert-Butyl 5-(6-phenylpyridazin-3-yl)-2,5-diazabicyclo[2.2.2]octane-2-carboxylate [57]

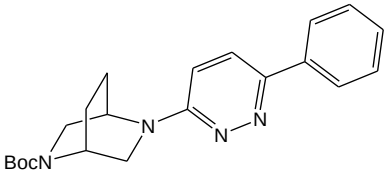

To a solution of *tert*-butyl 2,5-diazabicyclo[2.2.2]octane-2-carboxylate **51** (165 mg, 0.777 mmol) in dry DMSO (0.5 mL) in an argon atmosphere, dry DIPEA (0.474 mL, 2.719 mmol) and 3-chloro-6-phenylpyridazine (148 mg, 0.777 mmol) were added and the mixture was stirred at 105°C for 30 h.
The mixture was cooled to ambient and quenched with saturated $NaHCO_3$ solution (5 mL). The aqueous layer was extracted with AcOEt (3 x 3 mL) and the resulting organic layers were dried over Na_2SO_4, filtered and concentrated. The residue was purified by flash chromatography (CyHex/AcOEt 90:10 $\rightarrow$ 70:30) to provide 99 mg of clean product (35% yield).

57: yellow solid.

m.p.: 175-177°C

***R*$_f$:** 0.10 (CyHex/AcOEt 8:2); UV, $KMnO_4$.

^{1}H-NMR ($CDCl_3$): δ 1.47 (bs, 9H), 1.86-1.94 (m, 2H), 2.05-2.13 (m, 2H), 3.50-3.59 (m, 2H), 3.69-3.76 (m, 2H), 4.42 (m, 1H), 5.15 (m, 1H), 6.73 (d, *J* = 9.35 Hz, 1H), 7.36-7.47 (m, 3H), 7.67 (d, *J* = 9.35 Hz, 1H), 7.98-8.00 (m, 2H).

^{13}C-NMR ($CDCl_3$): δ 25.29, 25.99, 28.71, 29.94, 44.18, 50.46, 52.21, 80.05, 111.60, 125.62, 125.98, 128.76, 129.03, 137,13, 150.68, 154.92, 157.57.

MS (ESI): *m/z* 367.2 $[M+H]^+$, calc. for $C_{21}H_{26}N_4O_2$ 366.46.

2-(6-Phenylpyridazin-3-yl)-2,5-diazabicyclo[2.2.2]octane dihydrochloride [19]

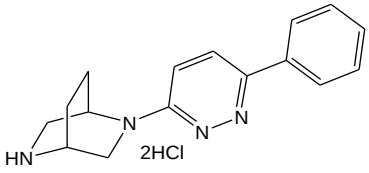

To a solution of *tert*-butyl 5-(6-phenylpyridazin-3-yl)-2,5-diazabicyclo [2.2.2]octane-2-carboxylate **57** (128 mg, 0.350 mmol) in MeOH/Et_2O 2:1 (1.40/0.78 mL) at 0°C, 2.0 M HCl in Et_2O (2.1 mL) was added dropwise and the mixture stirred at room temperature for 6 h.
The solvent was removed in *vacuo* and the residue digested with Et_2O to obtain 87 mg of the title compound (73% yield).

17: yellow solid.

m.p.: 224-225°C dec.

^{1}H-NMR (CD_3OD): δ 2.10-2.14 (m, 2H), 2.25-2.29 (m, 2H), 3.57-3.64 (m, 1H), 3.69-3.73 (m, 1H), 3.92-3.96 (m, 1H), 4.10-4.14 (m, 2H), 4.82 (m, 1H), 7.62-7.64 (m, 3H), 7.96-7.99 (m, 2H), 8.03 (d, *J* = 9.9 Hz, 1H), 8.53 (d, *J* = 9.9 Hz, 1H).

^{13}C-NMR (CD_3OD): δ 20.50, 22.85, 45.78, 122.95, 127.05, 129.52, 129.56, 131.81, 132,50.

MS (ESI): *m/z* 267.2 $[M+H]^+$, calc. for $C_{16}H_{18}N_4$ 266.15.

2-Methyl-5-(6-phenylpyridazin-3-yl)-2,5-diazabicyclo[2.2.2]octane fumarate [20]

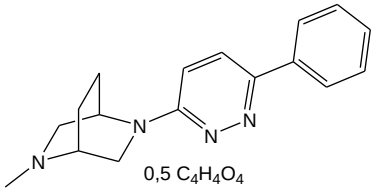

To a solution of 2-(6-phenylpyridazin-3-yl)-2,5-diazabicyclo[2.2.2]octane **19** (34 mg, 0.128 mmol) in MeOH (1.5 mL), 37% formaldehyde in water (0.062 mL, 0.756 mmol) was added and the mixture was stirred at room temperature for 30 min. Then $NaBH_4$ (11 mg, 0.27 mmol) was added at 0°C and the mixture stirred at room temperature for further 30 min.

The mixture was quenched with a saturated $NaHCO_3$ solution (3 mL) and extracted with DCM (4 x 2 mL). The organic layers were dried over Na_2SO_4, filtered and concentrated to afford 36 mg of clean tertiary amine (100% yield).

To a solution of the free tertiary amine (82 mg, 0.292 mmol) in MeOH (2 mL), fumaric acid (34 mg, 0.292 mmol) was added and the mixture was stirred at room temperature for 2 h.

The solvent was removed in *vacuo* and the crude product was crystallized from 2-propanol to provide the title compound (94% yield).

20: colourless solid.

^{1}H-NMR (CD_3OD): δ 1.85-2.05 (m, 2H), 2.03-2.18 (m, 1H), 2.22-2.38 (m, 1H), 2.80 (s, 3H), 3.46-3.53 (m, 1H), 3.64 (dd, *J* = 2.15; 12.10 Hz, 1H), 4.06 (dt, *J* = 2.83; 11.83 Hz, 1H), 4.76-4.83 (m, 1H), 6.66 (s, 1H), 7.18 (d, *J* = 9.36 Hz, 1H), 7.39-7.52 (m, 3H), 7.84-7.93 (m, 3H).

^{13}C-NMR (CD_3OD): δ 21.10, 23.41, 24.04, 40.75, 43.12, 45.89, 53.86, 57.39, 63.57, 113.41, 125.98, 126.70, 128.77, 128.85, 135.16, 136.69, 151,54, 157.31, 170.65.

MS (ESI): *m/z* 267.2 $[M+H]^+$, calc. for $C_{17}H_{20}N_4$ 280.37.

2,2-Dimethyl-5-(6-phenylpyridazin-3-yl)-5-aza-2-azoniabicyclo[2.2.2]octane iodide [21]

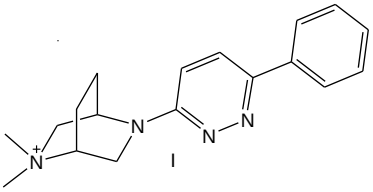

To a solution of 2-methyl-5-(6-phenylpyridazin-3-yl)-2,5-diazabicyclo[2.2.2] octane **20** (36 mg, 0.128 mmol) in MeOH/Et_2O 1:3 (0.15/0.50 mL), methyl iodide (0.25 mL 4 mmol) was added and the mixture stirred at room temperature for 2 h.
The solvent was removed in *vacuo* and the residue digested with Et_2O to obtain 42 mg of the title compound (78% yield).

21: yellow solid.

m.p.: 228-230°C dec.

^{1}H-NMR (CD_3OD): δ 2.09-2.15 (m, 3H), 2.54-2.63 (m, 1H), 3.37 (s, 3H), 3.41 (s, 3H), 3.79-3.86 (m, 3H), 4.01 (m, 1H), 4.37 (dt, *J* = 3.03; 6.05; 13.48 Hz, 1H), 5.03 (m, 1H), 7.25 (d, *J* = 9.63 Hz, 1H), 7.44-7.52 (m, 3H), 7.92-7.98 (m, 3H).

^{13}C-NMR (CD_3OD): δ 20.26, 21.81, 43.44, 45.36, 53.75, 54.06, 63.43, 68.10, 113.90, 126.10, 126.89, 128.86, 129.04, 136,53, 152.31, 157.03.

MS (ESI): *m/z* 295.2 $[M+H]^+$, calc. for $C_{18}H_{23}N_4$ 295.40.

tert-Butyl 5-(6-chloropyridazin-3-yl)-2,5-diazabicyclo[2.2.2]octane-2-carboxylate [58]

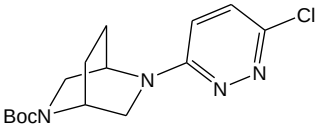

To a solution of *tert*-butyl 2,5-diazabicyclo[2.2.2]octane-2-carboxylate **51** (227 mg, 1.07 mmol) in dry DMSO (0.7 mL) in an argon atmosphere, dry DIPEA (0.652 mL, 3.745 mmol) and 3,6-dichloropyridazine (160 mg, 1.07 mmol) were added and the mixture was stirred at 105°C for 48.
The mixture was cooled to ambient and quenched with saturated $NaHCO_3$ solution (5 mL). The aqueous layer was extracted with AcOEt (4 x 3 mL) and then the organic layers were dried over Na_2SO_4, filtered and concentrated. The residue was purified by flash chromatography (CyHex/AcOEt 80:20) to provide 193 mg of clean product (55% yield).

58: colourless solid.

m.p.: 152-154°C

***R*$_f$:** 0.19; UV, $KMnO_4$.

^{1}H-NMR ($CDCl_3$): δ 1.46 (bs, 9H), 1.79-1.96 (m, 2H), 2.03-2.11 (m, 2H), 3.41-3.56 (m, 2H), 3.63-3.67 (m, 2H), 4.40 (m, 1H), 5.00 (m, 1H), 6.63 (d, *J* = 9.62 Hz, 1H), 7.23 (d, *J* = 9.62 Hz, 1H).

^{13}C-NMR ($CDCl_3$): δ 25.15, 25.86, 28.68, 29.93, 44.04, 45.65, 50.27, 52.33, 80.15, 113.88, 129.17, 146.21, 154.83, 157,69.

MS (ESI): *m/z* 325.2 $[M+H]^+$, calc. for $C_{15}H_{21}Cl\ N_4O_2$ 324.81.

2-(6-Chloropyridazin-3-yl)-2,5-diazabicyclo[2.2.2]octane dihydrochloride [18]

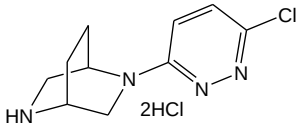

To a solution of *tert*-butyl 5-(6-chloropyridazin-3-yl)-2,5-diazabicyclo[2.2.2] octane-2-carboxylate **58** (240 mg, 0.739 mmol) in MeOH/Et_2O 2:1 (3/1.5 mL) at 0°C, 2.0 M HCl in Et_2O (4.5 mL) was added dropwise and the mixture stirred at room temperature for 7 h.
The precipitate was collected by filtration and washed with Et_2O to get 166 mg of clean white solid (75% yield).

18: colourless solid.

m.p.: 187-189°C dec.

^{1}H-NMR (CD_3OD): δ 2.08-2.13 (m, 2H), 2.26-2.28 (m, 2H), 3.57-3.61 (m, 1H), 3.70-3.75 (m, 1H), 4.11-4.14 (m, 2H), 4.74 (m, 1H), 7.96-7.98 (m, 2H).

^{13}C-NMR (CD_3OD): δ 20.25, 22.61, 45.33, 45.56, 46.28, 123.83, 135.18, 146.02, 151.85.

MS (ESI): *m/z* 225.0 $[M+H]^+$, calc. for $C_{10}H_{13}ClN_4$ 224.69.

tert-Butyl 5-(6-(1H-indol-5-yl)pyridazin-3-yl)-2,5-diazabicyclo[2.2.2]octane-2-carboxylate [59]

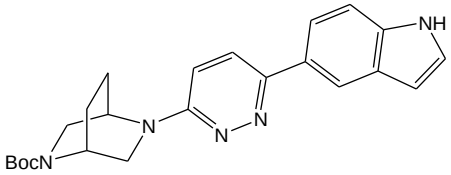

To a solution of t*ert*-butyl 5-(6-chloropyridazin-3-yl)-2,5-diazabicyclo[2.2.2] octane-2-carboxylate **58** (136 mg, 0.42 mmol) in 1,4-dioxane/EtOH 1:1 (6.8 mL), 5-indolylboronic acid (147 mg, 0.913 mmol), $(PPh_3)_2PdCl$ (6.5 mg, 0.01 mmol), triphenylphosphine (8 mg, 0.03 mmol) and Na_2CO_3 1.0 M (0.25 mL) were added, and the mixture was sealed in a tube and heated under MW irradiation (250 W) at 150°C for 30 min.

The mixture was filtered through a celite-septum and the solvent removed in *vacuo*. The residue was taken with water (3 mL) and 2.0 N HCl in water (3 mL), then the aqueous layer washed with Et_2O (3 x 3mL), basified with $NaHCO_3$ and extracted with DCM (8 x 3 mL). The pooled organic layers were dried over Na_2SO_4, filtered and concentrated and the crude product was finally purified by flash chromatography (CyHex/AcOEt 50:50) to afford 85 mg of the title compound (50% yield).

59: yellow solid.

m.p.: 133-135°C.

***R*$_f$:** 0.15; UV, $KMnO_4$, CAM.

^{1}H-NMR ($CDCl_3$): δ 1.48 (bs, 9H), 1.83-1.93 (m, 2H), 2.05-2.17 (m, 2H), 3.47-3.59 (m, 2H), 3.71-3.81 (m, 2H), 4.41 (m, 1H), 5.12 (m, 1H), 6.61 (m, 1H), 6.70-6.76 (m, 1H), 7.23-7.26 (m, 1H), 7.47 (d, *J* = 8.52 Hz, 1H), 7.71-7.74 (m, 1H), 7.93 (d, *J* = 8.52 Hz, 1H), 8.19 (m, 1H), 8.51 (bs, 1H).

^{13}C-NMR ($CDCl_3$): δ 25.32, 26.03, 28.74, 43.71, 44.25, 50.51, 52.25, 80.02, 103.45, 111.72, 118.48, 120.74, 125.25, 125.83, 128.45, 129.25, 136.43, 152.04, 154.98, 157.28.

MS (ESI): *m/z* 406.3 $[M+H]^+$, calc. for $C_{23}H_{27}N_5O_2$ 405.49.

2-(6-(1*H*-indol-5-yl)pyridazin-3-yl)-2,5-diazabicyclo[2.2.2]octane [22]

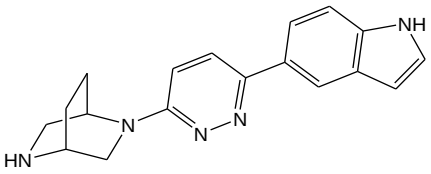

To a solution of *tert*-butyl 5-(6-(1H-indol-5-yl)pyridazin-3-yl)-2,5-diazabicyclo [2.2.2]octane-2-carboxylate **59** (94 mg, 0.232 mmol) in MeOH/Et_2O 1:1 (0.72/0.72 mL) at 0°C, 2.0 M HCl in Et_2O (0.93 mL) was added dropwise and the mixture stirred at room temperature for 5 h.
The solvent was removed in *vacuo* and the residue purified by acid/base extraction and digested with Et_2O to obtain 34 mg of secondary amine (48% yield).

23: colourless solid.

m.p.: 124-125°C dec.

^{1}H-NMR ($CDCl_3$): δ 1.70-1.90 (m, 2H), 1.97-2.11 (m, 2H), 3.22-3.26 (m, 2H), 3.39-3.43 (m, 1H), 3.61-3.64 (m, 1H), 3.73-3.77 (m, 1H), 4.84 (m, 1H), 6.62 (m, 1H), 6.76 (d, *J* = 9.35 Hz, 1H), 7.24 (m, 1H), 7.48 (d, *J* = 8.52 Hz, 1H), 7.72 (d, *J* = 9.35 Hz, 1H), 7.96 (d, *J* = 8.52 Hz, 1H), 8.19 (m, 1H), 8.43 (bs, 1H).

^{13}C-NMR ($CDCl_3$): δ 25.76, 27.16, 29.94, 43.17, 45.28, 48.83, 103.46, 111.66, 111.79, 118.37, 120.78, 125.14, 125.62, 128.43, 129.47, 136.36, 151.58, 157.36.

MS (ESI): *m/z* 306.2 $[M+H]^+$, calc. for $C_{18}H_{19}N_5$ 305.38.

2-(6-(1*H*-indol-5-yl)pyridazin-3-yl)-5-metyl-2,5-diazabicyclo[2.2.2]octane [23]

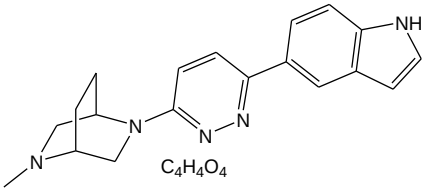

To a solution of 2-(6-(1*H*-indol-5-yl)pyridazin-3-yl)-2,5-diazabicyclo[2.2.2] octane **21** (21 mg, 0.069 mmol) in DCM/MeOH 9:1 (2.5 mL), 37% formaldehyde in water (0.032 mL, 0.423 mmol) was added and the mixture was stirred at room temperature for 30 min. Then $NaBH(OAc)_3$ (30 mg, 0.138 mmol) was added at 0°C and the mixture stirred at room temperature for 2 h.
The mixture was quenched with a saturated $NaHCO_3$ solution (3 mL) and extracted with DCM (4 x 2 mL). The organic layers were dried over Na_2SO_4, filtered and concentrated to afford 17 mg of clean tertiary amine (77% yield).
To a solution of the free tertiary amine (17 mg, 0.053 mmol) in MeOH (1.7 mL), fumaric acid (6 mg, 0.053 mmol) was added and the mixture was stirred at room temperature for 2 h.
The solvent was removed in *vacuo* and the crude product was crystallized from 2-propanol to provide the title compound (97% yield).

23: colourless solid.

m.p.: 124-125°C dec.

^{1}H-NMR (CD_3OD): δ 2.01-2.10 (m, 2H), 2.15-2.19 (m, 1H), 2.30-2.43 (m, 1H), 3.02 (s, 3H), 3.20-3.26 (m, 2H), 3.61-3.62 (m, 2H), 3.78-3.82 (m, 1H), 4.11-4.15 (m, 1H), 6.54-6.55 (m, 1H), 6.71 (s, 2H), 7.21 (d, *J* = 9.35 Hz, 1H), 7.29 (m, 1H), 7.50 (d, *J* = 8.53 Hz, 1H), 7.70 (d, *J* = 8.53 Hz, 1H), 7.97 (d, *J* = 9.35 Hz, 1H), 8.09 (bs, 1H).

^{13}C-NMR (CD_3OD): δ 22.94, 40.53, 42.56, 45.24, 54.07, 77.20, 88.14, 101.98, 111.53, 113.96, 118.41, 119.73, 125.67, 127.43, 128.72, 134.64, 137.11, 153.70, 156.72, 168.82.

MS (ESI): *m/z* 320.1 $[M+H]^+$, calc. for $C_{19}H_{21}N_5$ 319.40.

2-((Pyridin-3-yl)methylene)quinuclidin-3-one [61]

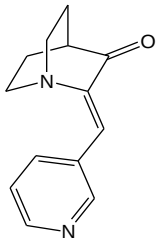

To a solution of KOH (0.5 g, 8.91 mmol) in methanol (2.8 mL), quinuclidinone hydrochloride **60** (5 g, 30.93 mmol) was added and the mixture stirred for 45 min. Then 3-pyridinecarboxaldehyde (2.9 mL, 30.93 mmol) was added and the mixture stirred until complete disappearance of the aldehyde (TLC monitoring, 72 h).
The reaction was diluted with water (45 mL) and the crashed-out solid was filtered to afford 4.768 g of pure product as a bright yellow solid (72% yield).

61: yellow solid.

m.p.: 107-108° C.

***R*$_f$:** 0.17 (CyHex/AcOEt 4:6); UV; Dragendorff reagent.

^{1}H-NMR ($CDCl_3$): δ 2.00-2.07 (m, 4H), 2.64 (m, 1H), 2.95-2.99 (m, 2H), 3.12-3.17 (m, 2H), 6.98 (s, 1H), 7.28 (m, 1H), 8.45-8.53 (m, 2H), 9.04 (d, *J* = 1.93 Hz, 1H).

^{13}C-NMR ($CDCl_3$): δ 25.89, 40.34, 47.63, 121.70, 123.59, 130.20, 138.75, 146.75, 150.13, 153.17, 205.84.

MS (ESI): *m/z* 215.1 $[M+H]^+$, calc. for $C_{13}H_{14}N_2O$ 214.26.

2-((Pyridin-3-yl)methyl)quinuclidin-3-one [62]

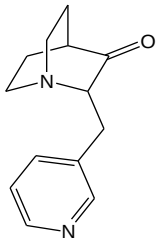

To a solution of 2-((pyridin-3-yl)methylene)quinuclidin-3-one **61** (2.5 g, 11.668 mmol) in methanol (26 mL), 6.0 N HCl in water (6.1 mL) and palladium on activated charcoal 10% (202 mg) were added and the mixture sealed and hydrogenated at room temperature and 25 psi for 16 h.
The solvent was removed in *vacuo*, the residue taken with chloroform (20 mL) and 2.0 N NaOH in water (20 mL) and the mixture stirred for 1 hour. After dilution with brine and DCM, the two layers were separated and the aqueous layer extracted with DCM (3 x 30 mL). The organic phase was dried over Na_2SO_4, filtered, concentrated and the crude material crystallized with Et_2O to provide 1.731 g of clean product (69% yield).

62: yellow solid.

m.p.: 92° C.

***R*$_f$:** 0.23 (AcOEt/MeOH 9:1); UV; Dragendorff reagent.

^{1}H-NMR ($CDCl_3$): δ 1.94-2.05 (m, 4H), 2.46 (m, 1H), 2.71-2.91 (m, 3H), 3.03-3.21 (m, 3H), 3.28-3.33 (m, 1H), 7.21 (m, 1H), 7.57-7.59 (m, 1H), 8.43-8.50 (m, 2H).

^{13}C-NMR ($CDCl_3$): δ 25.08, 27.14, 30.87, 40.17, 41.23, 49.05, 71.04, 121.70, 123.54, 134.74, 136.48, 148.07, 150.46, 220.91.

MS (ESI): *m/z* 217.0 $[M+H]^+$, calc. for $C_{13}H_{16}N_2O$ 216.26

$[\alpha]^{20}_{D}$: – 0.9 (c 1, $CHCl_3$)

2-((Pyridin-3-yl)methyl)quinuclidine dihydrochloride [24]

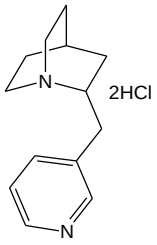

To a solution of 2-((pyridin-3-yl)methyl)quinuclidin-3-one **62** (250 mg, 1.156 mmol) in diethylene glycol (2 mL) in an argon atmosphere, KOH (1.264 g, 22.542 mmol) and hydrazine hydrate (1.121 mL, 23.12 mmol) were added, and the mixture was stirred at 100°C for 2.5 h and at 180 °C for further 2.5 h.
The reaction was cooled to ambient, diluted with water (12 mL) and conc. HCl (pH = 1), washed with Et_2O (10 mL), basified with NaOH 20% (pH = 11/12) and extracted with DCM (3 x 20 mL). The organic layers were dried over Na_2SO_4, filtered, concentrated in *vacuo* to obtain 100 mg of the desired compound (43% yield).
The free base (100 mg, 0.495 mmol) was treated with 1.25 M HCl in methanol for 1 hour. The solvent was removed in *vacuo* and the residue crystallized with 2-propanol to give 114 mg of the title compound (84% yield).

24: colourless solid.

m.p.: 272-273° C dec.

^{1}H-NMR (CD_3OD): δ 1.67 (m, 1H), 1.91-2.07 (m, 5H), 2.17 (m, 1H), 3.33-3.53 (m, 5H), 3.59-3.69 (m, 1H), 4.03 (m, 1H), 8.11 (dd, *J* = 5.77; 8.75 Hz, 1H), 8.70 (m, 1H), 8.84 (d, *J* = 5.77 Hz, 1H), 8.98 (m, 1H).

^{13}C-NMR (D_2O): δ 20.04, 21.71, 22.58, 29.44, 34.60, 42.11, 49.07, 57.70, 127.74, 136.17, 140.62, 141.63, 147.91.

MS (ESI): *m/z* 203.1 $[M+H]^+$, calc. for $C_{13}H_{18}N_2$ 202.30.

cis-2-((Pyridin-3-yl)methyl)quinuclidin-3-ol [63]

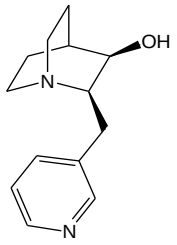

To a solution of 2-((pyridin-3-yl)methyl)quinuclidin-3-one **62** (200 mg, 0.925 mmol) in dry 2-propanol (3.8 mL) in an argon atmosphere, aluminium *iso*-propoxide (567 mg, 2.774 mmol) was added and the mixture stirred at 72°C for 2 h.

The reaction was cooled to ambient and concentrated in *vacuo*, the residue taken with NaOH 20% (5mL) and extracted with DCM (3 x 3 mL). The organic layers were dried over Na_2SO_4, filtered, concentrated in *vacuo* to provide 201 mg of the title compound (99% yield) as a 87/13 mixture of *cis*/*trans* isomers (^{1}H-NMR analysis).

63: yellow oil.

***R*$_f$:** 0.08 (DCM/MeOH 9:1); UV; $KMnO_4$; Dragendorff reagent.

^{1}H-NMR ($CDCl_3$): δ 1.25-1.37 (m, 1H), 1.44-1.52 (m, 1H), 1.60-1.66 (m, 1H), 1.91 (m, 2H), 2.68-2.87 (m, 4H), 3.04-3.20 (m, 3H), 3.90 (m, 1H), 7.20 (dd, *J* = 4.68; 7.98 Hz, 1H), 7.62 (m, 1H), 8.42 (m, 1H), 8.55 (m, 1H).

^{13}C-NMR ($CDCl_3$): δ 19.19, 24.88, 29.52, 31.09, 41.79, 49.04, 62.05, 69.05, 123.48, 136.47, 136.85, 147.51, 150.80.

MS (ESI): *m/z* 219.1 $[M+H]^+$, calc. for $C_{13}H_{18}N_2O$ 218.29.

$[\alpha]^{20}_D$: – 0.1 (c 1,1, $CHCl_3$)

cis-3-(6-Chloropyridazin-3-yloxy)-2-((pyridin-3-yl)methyl)quinuclidine [64]

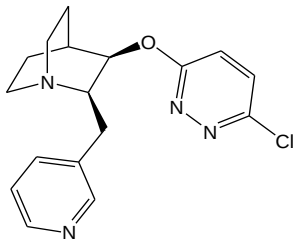

To a solution of *cis*-2-((pyridin-3-yl)methyl)quinuclidin-3-ol **63** (461 mg, 2.112 mmol) in dry THF (2.3 mL) at 0°C in an argon atmosphere, NaHDMS 1.5 M in THF (1.83 mL, 2.746 mmol) was added and the mixture stirred at 0°C for 1 h. Then, 3,6-dichloropyridazine (355 mg, 2.387 mmol) was added and the mixture stirred at 0°C for 3 h and at room temperature for further 24 h.

The reaction was quenched with water (5 mL) and NaOH 2N (5 mL) and extracted with AcOEt (6 x 8 mL). The combined organic layers were dried over Na_2SO_4, filtered, concentrated in *vacuo*, and the residue purified by flash chromatography (DCM/MeOH 90:10 → 80:20) to provide 196 mg of a dark-red oil. Filtration through a short basic aluminium oxide pad afforded 116 mg of pure title compound as a racemic mixture of *cis* isomers (^{1}H-NMR analysis, 17% yield).

64: yellow oil.

***R*$_f$:** 0.15 (DCM/MeOH 9:1); UV; $KMnO_4$; Dragendorff reagent.

^{1}H-NMR ($CDCl_3$): δ 1.33-1.43 (m, 1H), 1.62-1.80 (m, 3H), 2.42-2.44 (m, 1H), 2.78-2.93 (m, 3H), 2.95-3.07 (m, 2H), 3.19-3.29 (m, 1H), 3.37-3.46 (m, 1H), 5.48 (dd, *J* = 4.4; 7.7 Hz, 1H), 6.99 (d, *J* = 9.35 Hz, 1H), 7.14 (dd, *J* = 4.95; 7.7 Hz, 1H), 7.37 (d, *J* = 9.35, 1H), 7.53 (m, 1H), 8.35 (dd, *J* = 1.37; 4.95 Hz, 1H), 8.41 (m, 1H).

^{13}C-NMR ($CDCl_3$): δ 19.51, 24.07, 25.65, 31.02, 41.76, 49.09, 60.92, 74.91, 120.32, 123.50, 131.40, 135.36, 136.33, 147.65, 150.63, 151.18, 164.24.

MS (ESI): *m/z* 331.1 $[M+H]^+$, calc. for $C_{17}H_{19}ClN_4O$ 330.81.

$[\alpha]^{20}_D$: – 0.1 (c 0.75, $CHCl_3$)

cis-3-(6-Chloropyridazin-3-yloxy)-2-((pyridin-3-yl)methyl)quinuclidine fumarate [25]

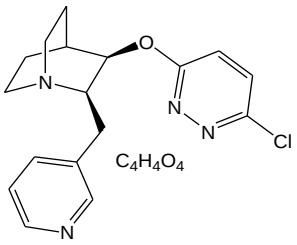

To a solution of c*is*-3-(6-chloropyridazin-3-yloxy)-2-((pyridin-3-yl)methyl) quinuclidine **64** (20 mg, 0.06 mmol) in methanol (0.2 mL), fumaric acid (7 mg, 0.06 mmol) in methanol (0.1 mL) was added and the solution was stirred at room temperature for 4 h.
The solvent was removed in *vacuo* and the solid crystallized from 2-propanol to obtain 21 mg of pure product (84% yield).

25: colourless solid.

m.p.: 168-171° C dec.

^{1}H-NMR (CD_3OD): δ 1.78-1.89 (m, 1H), 2.02-2.08 (m, 3H), 2.71 (m, 1H), 3.18-3.25 (m, 2H), 3.36-3.46 (m, 2H), 3.54 (dd, *J* = 10.46; 14.31 Hz, 1H), 3.65-3.76 (m, 1H), 4.31-4.39 (m, 1H), 5.56 (dd, *J* = 4.95; 7.43 Hz, 1H), 6.68 (s, 1.5H), 7.31 (dd, *J* = 4.95; 7.97 Hz, 1H), 7.37 (d, *J* = 9.08, 1H), 7.71 (d, *J* = 9.08, 1H), 7.83 (m, 1H), 8.33 (m, 1H), 8.47 (m, 1H).

^{13}C-NMR (CD_3OD): δ 16.97, 19.81, 24.53, 28.45, 42.12, 61.13, 70.78, 121.07, 124.17, 132.33, 132.45, 134.87, 137.59, 147.55, 149.67, 151.87, 163.60, 169.67.

MS (ESI): *m/z* 331.1 $[M+H]^+$, calc. for $C_{17}H_{19}ClN_4O$ 330.81.

cis- 3-(6-(1_H_-Indol-5-yl)pyridazin-3-yloxy)-2-((pyridin-3-yl)methyl)quinuclidine fumarate [28]

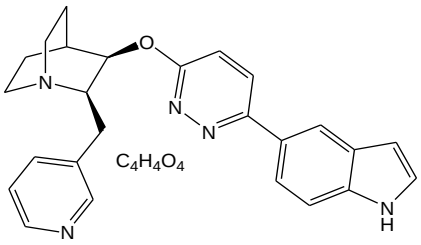

To a solution of c*is*-3-(6-chloropyridazin-3-yloxy)-2-((pyridin-3-yl)methyl) quinuclidine **64** (97 mg, 0.293 mmol) in 1,4-dioxane/EtOH 1:1 (5 mL), 5-indolylboronic acid (102 mg, 0.636 mmol), $(PPh_3)_2PdCl$ (5 mg, 0.0067 mmol), triphenylphosphine (5 mg, 0.02 mmol) and Na_2CO_3 1.0 M (2.3 mL) were added, and the mixture was sealed in a tube and heated under MW irradiation (250 W) at 150°C for 1 h.

The mixture was filtered through a celite-septum washing with methanol and the solvent was removed in *vacuo*. The residue was purified by flash chromatography (DCM/MeOH 90:10 → 90:10 + NH_3 1%) to get 100 mg of pure compound (83% yield).

To a solution of the free base (120 mg, 0.292 mmol) in methanol (0.9 mL), fumaric acid (34 mg, 0.292 mmol) in methanol (0.6 mL) was added and the solution was stirred at room temperature for 2 h. The solvent was removed in *vacuo* and the solid crystallized from 2-propanol to obtain 117 mg of the title compound (73% yield).

28: colourless solid.

m.p.: 230-232° C dec.

^{1}H-NMR (CD_3OD): δ 1.85-1.93 (m, 1H), 2.06-2.16 (m, 3H), 2.81 (m, 1H), 3.20-3.27 (m, 2H), 3.37-3.51 (m, 2H), 3.62 (dd, *J* = 10.18; 14.03 Hz, 1H), 3.72-3.81 (m, 1H), 4.36-4.42 (m, 1H), 5.63 (dd, *J* = 4.68; 7.7 Hz, 1H), 6.56 (d, *J* = 3.3 Hz, 1H), 6.70 (s, 2H), 7.30-7.35 (m, 2H), 7.38 (d, *J* = 9.35 Hz, 1H), 7.50 (m,

1H), 7.69 (dd, *J* = 1.65; 8.52 Hz, 1H), 7.86 (m, 1H), 8.11 (m, 1H), 8.12 (d, *J* = 9.35, 1H), 8.32 (m, 1H), 8.52 (m, 1H).

^{13}C-NMR (CD_3OD): δ 16.98, 19.76, 24.06, 24.63, 28.50, 42.30, 61.44, 69.95, 102.11, 111.65, 118.59, 119.20, 120.03, 124.20, 125.92, 126.77, 128.73, 129.47, 132.42, 134.83, 137.46, 137.66, 147.57, 149.75, 158.19, 162.73, 169.52.

MS (ESI): *m/z* 412.2 $[M+H]^+$, calc. for $C_{25}H_{25}N_5O$ 411.50.

cis-3-(6-Phenylpyridazin-3-yloxy)-2-((pyridin-3-yl)methyl)quinuclidine fumarate [26]

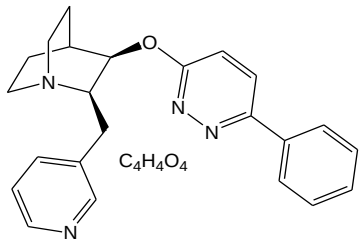

To a solution of *cis*-2-((pyridin-3-yl)methyl)quinuclidin-3-ol **63** (300 mg, 1.374 mmol) in dry THF (1.5 mL) at 0°C in an argon atmosphere, NaHDMS 1.5 M in THF (1.5 mL, 2.25 mmol) was added and the mixture stirred at 0°C for 1 hour. Then, 3-chloro-6-phenylpyridazine (296 mg, 1.553 mmol) was added and the mixture stirred between 0 and 10°C for 5 h.

The reaction was quenched with water (3 mL) and 2.0 N NaOH in water (3 mL) and extracted with AcOEt (3 x 5 mL). The organic layers were dried over Na_2SO_4, filtered, concentrated in *vacuo*, and the residue purified then by flash chromatography (DCM/MeOH 90:10 → 80:20) to provide 173 mg of the title compound as a racemic mixture of *cis* isomers (^{1}H-NMR analysis, 34% yield).

To a solution of the free base (173 mg, 0.464 mmol) in methanol (1.4 mL), fumaric acid (54 mg, 0.464 mmol) in methanol (1 mL) was added and the solution was stirred at room temperature for 4 h.

The white precipitate was filtered and washed with Et_2O to obtain 185 mg of the title compound (93% yield).

26: colourless solid.

m.p.: 219-221° C dec.

^{1}H-NMR (CD_3OD): δ 1.72-1.82 (m, 1H), 1.97-2.06 (m, 3H), 2.70 (m, 1H), 3.18-3.29 (m, 4H), 3.50-3.66 (m, 2H), 4.18-4.26 (m, 1H), 5.57-5.61 (m, 1H), 6.68 (s, 1H), 7.29 (dd, *J* = 5.22; 7.97 Hz, 1H), 7.41 (d, *J* = 9.08, 1H), 7.49-7.53 (m,

3H), 7.85 (m, 1H), 7.91-7.94 (m, 2H), 8.09 (d, *J* = 9.08, 1H), 8.27 (m, 1H), 8.48 (m, 1H).

^{13}C-NMR (CD_3OD): δ 17.65, 20.89, 24.95, 29.23, 41.93, 60.97, 71.28, 118.68, 124.06, 126.65, 128.93, 129.13, 129.70, 133.65, 135.10, 135.93, 137.63, 147.12, 149.70, 156.37, 163.63, 172.43.

MS (ESI): *m/z* 373.1 $[M+H]^+$, calc. for $C_{23}H_{24}N_4O$ 372.46.

cis-1-Methyl-2-((1-methylpyridinium-3-yl)methyl)-3-(6-phenylpyridazin-3-yloxy)-1-azoniabicyclo[2.2.2]octane diiodide [27]

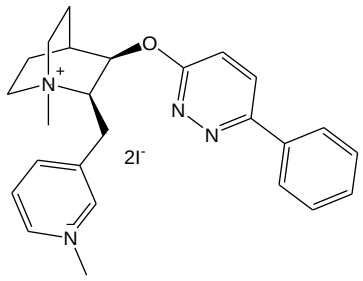

To a solution of c*is*-3-(6-phenylpyridazin-3-yloxy)-2-((pyridin-3-yl)methyl) quinuclidine **26** (122 mg, 0.328 mmol) in EtOH (1.3 mL) and MeOH (0.5 mL), methyl iodide (0.61 mL, 9.827 mmol) was added and the solution was stirred at room temperature for 1 h.
The solvent was removed in *vacuo* and the solid digested with Et_2O to give 164 mg of the title compound (76% yield).

27: yellow solid.

m.p.: 176-178° C.

^{1}H-NMR (CD_3OD): δ 2.00-2.07 (m, 1H), 2.18-2.33 (m, 3H), 2.88 (m, 1H), 3.29 (s, 3H), 3.50-3.58 (m, 1H), 3.72-4.06 (m, 5H), 4.35 (s, 3H), 5.04-5.06 (m, 1H), 5.71-5.75 (m, 1H), 7.50-7.54 (m, 3H), 7.58 (d, *J* = 9.36, 1H), 7.85 (m, 1H), 7.92-7.95 (m, 2H), 8.15 (d, *J* = 9.36 Hz, 1H), 8.63-8.66 (m, 2H), 9.37 (m, 1H).

^{13}C-NMR (CD_3OD): δ 18.50, 20.22, 24.01, 26.49, 48.91, 53.58, 59.74, 67.70, 70.34, 118.79, 126.70, 127.47, 129.00, 129.37, 129.92, 135.67, 137.15, 144.06, 146.08, 146.29, 156.95, 162.80.

MS (ESI): *m/z* 401.2 $[M]^+$, calc. for $C_{25}H_{30}N_4O^{2+}$ 402.53.

cis-2'-((Pyridin-3-yl)methyl)-1'-azaspirooxirane-2,3'-bicyclo[2.2.2]octane [65]

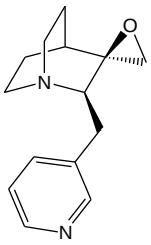

To a solution of trimethyl sulfoxide iodide (2.646 g, 12.022 mmol) in dry DMSO (10 mL) in an argon atmosphere, 60% NaH (492 mg, 12.3 mmol) was added and the mixture was stirred at room temperature for 30 min. Then, 2-((pyridin-3-yl)methyl)quinuclidin-3-one **62** (2 g, 9.248 mmol) was added and the mixture stirred at 70°C for 1.5 h.

The reaction was cooled to ambient, quenched with water (15 mL) and extracted with DCM (6 x 8 mL). The pooled organic layers were washed with water (4 x 10 mL), dried over Na_2SO_4, filtered, concentrated in *vacuo* to afford 1.877 g of the title compound as a racemic mixture of *cis* isomers (based on ^{1}H-NMR analysis, 68% yield).

65: yellow solid.

m.p.: 104-105° C.

***R*$_f$:** 0.42 (DCM/MeOH 9:1); UV; Dragendorff reagent.

^{1}H-NMR ($CDCl_3$): δ 1.34-1.38 (m, 1H), 1.48-1.58 (m, 1H), 1.72-1.84 (m, 2H), 1.93-2.02 (m, 1H), 2.44 (d, *J* = 4.68 Hz, 1H), 2.63-2.99 (m, 6H), 3.17-3.31 (m, 2H), 7.18 (dd, *J* = 4.95: 7.70 Hz, 1H), 7.55 (dt, *J* = 1.65; 2.20; 7.70 Hz, 1H), 8.41 (dd, *J* = 1.65; 4.95 Hz, 1H), 8.46 (d, *J* = 2.20 Hz, 1H).

^{13}C-NMR ($CDCl_3$): δ 22.97, 25.22, 30.64, 30.90, 41.25, 49.36, 52.27, 61.75, 62.26, 123.38, 135.40, 136.82, 147.62, 150.70.

MS (ESI): *m/z* 231.0 $[M+H]^+$, calc. for $C_{14}H_{18}N_2O$ 230.31.

$[\alpha]^{20}_D$: – 0.27 (c 1.1, $CHCl_3$)

cis-3-Methyl-2'-((pyridin-3-yl)methyl)-1'-azaspirooxazolidine-5,3'-bicyclo[2.2.2]octan-2-one hydrochloride [30]

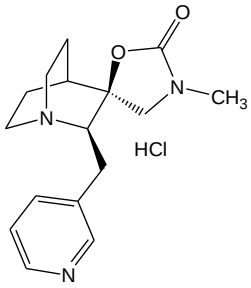

To a solution of c*is*-2'-((pyridin-3-yl)methyl)-1'-azaspirooxirane-2,3'-bicyclo [2.2.2]octane **65** (200 mg, 0.868 mmol) in MeOH (1.2 mL), excess gaseous methylamine was added and the mixture was sealed in a steel-tube and stirred at room temperature for 24 h.
The solvent and the excess of the amine were removed in *vacuo*, the residue was taken with THF (1.5 mL), 1,1'-carbonyldiimidazole (169 mg, 1.042 mmol) was added and the mixture stirred under reflux for 3 h.
The solvent was removed in *vacuo*, then the residue was treated with 1.25 M HCl in MeOH for 1 h. Concentration in *vacuo* and crystallization with 2-propanol gave 174 mg of pure title compound (62% yield).

30: colourless solid.

m.p.: 222-224° C dec.

^{1}H-NMR (CD_3OD): δ 1.92-2.07 (m, 3H), 2.28-2.34 (m, 2H), 2.47 (s, 3H), 2.85 (d, *J* = 9.9 Hz, 1H), 3.20-3.26 (m, 1H), 3.34-3.57 (m, 5H), 3.63 (d, *J* = 9.9 Hz, 1H), 4.25 (m, 1H), 7.45 (dd, *J* = 5.22; 7.97 Hz, 1H), 7.91-7.94 (m, 1H), 8.49-8.51 (m, 1H), 8.59 (m, 1H).

^{13}C-NMR (CD_3OD): δ 17.83, 18.03.28, 24.04, 28.39, 29.31, 31.99, 42.08, 55.02, 65.93, 77.69, 124.28, 131.30, 138.55, 148.23, 150.12, 156.62.

MS (ESI): *m/z* 288.2 $[M+H]^+$, calc. for $C_{16}H_{21}N_3O_2$ 287.36.

cis-3-(Azidomethyl)-2-((pyridin-3-yl)methyl)quinuclidin-3-ol [66]

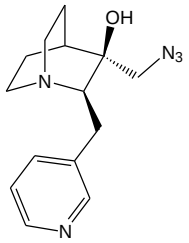

To a solution of c*is*-2'-((pyridin-3-yl)methyl)-1'-azaspirooxirane-2,3'-bicyclo[2.2.2]octane **65** (851 mg, 3.695 mmol) in MeOH (30 mL) and water (3.4 mL), sodium azide (1.201 g, 18.475 mmol) and ammonium chloride (435 mg, 8.129 mmol) were added, and the mixture stirred at 80°C for 16 h.

The reaction was cooled to ambient and concentrated in *vacuo*, the residue was taken with 2.0 N NaOH in water (20mL) and extracted with AcOEt (6 x 8 mL). The combined organic layers were dried over Na_2SO_4, filtered and concentrated in *vacuo* to provide 882 mg of β-azido alcohol (87% yield).

66: yellow oil.

***R*$_f$:** 0.16 (DCM/MeOH 9:1); UV; $KMnO_4$; Dragendorff reagent.

^{1}H-NMR ($CDCl_3$): δ 1.27-1.36 (m, 1H), 1.50-1.59 (m, 2H), 1.92-2.04 (m, 2H), 2.55-2.73 (m, 3H), 2.78-3.02 (m, 3H), 3.11-3.18 (m, 1H), 3.21 (d, *J* = 12.1 Hz, 1H), 3.44 (d, *J* = 12.1 Hz, 1H), 7.19 (m, 1H), 7.60 (m, 1H), 8.42 (m, 1H), 8.50 (m, 1H).

^{13}C-NMR ($CDCl_3$): δ 21.48, 24.06, 30.71, 41.10, 49.08, 58.68, 65.80, 73.28, 123.39, 136.49, 137.20, 147.48, 150.87.

MS (ESI): *m/z* 274.1 $[M+H]^+$, calc. for $C_{14}H_{19}N_5O$ 273.33.

$[\alpha]^{20}_D$: – 0.1 (c 1, $CHCl_3$)

cis-3-(Aminomethyl)-2-((pyridin-3-yl)methyl)quinuclidin-3-ol [67]

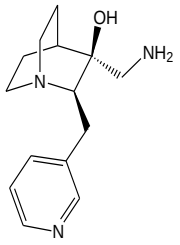

To a suspension of $LiAlH_4$ (496 mg, 13.061 mmol) in dry THF (4.1 mL) at 0°C in an argon atmosphere, a solution of c*is*-3-(azidomethyl)-2-((pyridin-3-yl)methyl)quinuclidin-3-ol **66** (1.19 g, 4.354 mmol) in dry THF (4.1 mL) was added dropwise, and the mixture stirred at room temperature for 3 h.

The reaction was cooled to 0°C, diluted with Et_2O (5 mL), then quenched with AcOEt (10 mL) and water (3 mL); the residue was taken with 2.0 N NaOH in water (20mL) and extracted with AcOEt (6 x 8 mL). The suspension was filtered through a celite-septum and the solvent removed in *vacuo* to give 885 mg of β-amino alcohol (77% yield).

67: yellow oil.

***R*f:** 0.05 (DCM/MeOH 9:1); UV; $KMnO_4$; Dragendorff reagent.

^{1}H-NMR ($CDCl_3$): δ 1.27-1.37 (m, 1H), 1.45-1.74 (m, 4H), 1.99-2.09 (m, 1H), 2.31 (d, *J* = 12.65 Hz, 1H), 2.54 (m, 1H), 2.61-2.73 (m, 2H), 2.76-3.00 (m, 3H), 3.13-3.24 (m, 1H), 3.63 (bs, 1H), 7.18 (dd, *J* = 4.95; 7.98 Hz, 1H), 7.58 (m, 1H), 8.39 (dd, *J* = 1.65; 4.95 Hz, 1H), 8.49 (d, *J* = 1.65 Hz, 1H).

^{13}C-NMR ($CDCl_3$): δ 21.46, 24.05, 30.70, 41.10, 49.09, 58.62, 65.79, 73.29, 123.37, 136.41, 137.16, 147.58, 150.94.
MS (ESI): *m/z* 248.2 $[M+H]^+$, calc. for $C_{14}H_{21}N_3O$ 247.34.

cis-Benzyl-(3-hydroxy-2-((pyridin-3-yl)methyl)quinuclidin-3-yl)methylcarbamate [68]

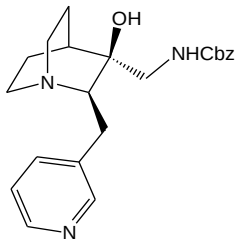

To a solution of *cis*-3-(aminomethyl)-2-((pyridin-3-yl)methyl)quinuclidin-3-ol **67** (400 mg, 1.617 mmol) in dry DCM (16 mL) at 0°C, DIPEA (0.34 mL, 1.941 mmol) and benzyl chloroformate (0.28 mL, 1.941 mmol) were added, and the mixture stirred at room temperature for 3 h.

The reaction was quenched with water (10 mL) and 5% H_3PO_4 (pH < 3), washed with DCM (2 x 6 mL), then basified with Na_2CO_3 (pH > 9) and extracted with DCM (5 x 8 mL). The organic layers were dried over Na_2SO_4, filtered and concentrated in *vacuo* to provide 291 mg of the protected β-amino alcohol (47% yield).

68: colourless solid.

m.p.: 110-113° C.

***R*$_f$:** 0.09 (DCM/MeOH 9:1); UV; CAM; Dragendorff reagent.

^{1}H-NMR ($CDCl_3$): δ 1.25-1.33 (m, 1H), 1.52-1.63 (m, 2H), 1.82 (m, 1H), 1.96 (m, 1H), 2.62-2.69 (m, 2H), 2.74-2.88 (m, 3H), 3.10-3.31 (m, 3H), 5.07 (s, 2H), 5.53 (m, 1H), 7.14 (m, 1H), 7.26-7.36 (m, 5H), 7.53 (m, 1H), 8.36 (m, 1H), 8.45 (m, 1H).

^{13}C-NMR ($CDCl_3$): δ 21.40, 24.17, 30.71, 31.11, 41.08, 48.66, 49.09, 66.07, 67.33, 73.84, 123.49, 128.40, 128.49, 128.79, 136.44, 136.74, 137.17, 147.26, 150.76, 157.99.

MS (ESI): *m/z* 382.2 $[M+H]^+$, calc. for $C_{22}H_{27}N_3O_3$ 381.47.

cis-2'-((Pyridin-3-yl)methyl)-1'-azaspirooxazolidine-5,3'-bicyclo[2.2.2]octan-2-one [29]

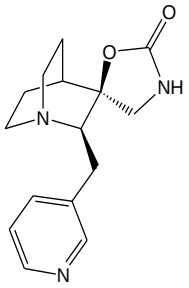

To a solution of c*is*-benzyl-(3-hydroxy-2-((pyridin-3-yl)methyl)quinuclidin-3-yl)methylcarbamate **68** (505 mg, 1.324 mmol) in dry THF (13 mL) at 0°C, 60 % NaH (64 mg, 1.589 mmol) was added, and the mixture stirred at room temperature for 3 h.

The reaction was quenched with water (8 mL) and H_3PO_4 5% (pH < 3), washed with Et_2O (3 x 4 mL), then basified with Na_2CO_3 (pH > 9) and extracted with DCM (8 x 6 mL). The pooled organic layers were dried over Na_2SO_4, filtered and concentrated in *vacuo* to afford 331 mg of the desired compound (91% yield).

29: colourless solid.

m.p.: 254-256° C dec.

***R*$_f$:** 0.15 (DCM/MeOH 9:1); UV; CAM; Dragendorff reagent.

^{1}H-NMR (CD_3OD): δ 1.48-1.58 (m, 1H), 1.65-1.70 (m, 2H), 2.04 (m, 2H), 2.73-2.85 (m, 3H), 2.91-2.99 (m, 1H), 3.03-3.25 (m, 4H), 5.58 (d, *J* = 9.35 Hz, 1H), 7.35 (m, 1H), 7.79-7.82 (m, 1H), 8.36-8.38 (m, 1H), 8.50 (m, 1H).

^{13}C-NMR (CD_3OD): δ 20.61, 21.28, 30.17, 32.77, 40.95, 49.28, 66.32, 83.94, 123.90, 135.59, 138.23, 146.72, 149.90, 159.93.

MS (ESI): *m/z* 274.2 $[M+H]^+$, calc. for $C_{15}H_{19}N_3O_2$ 273.33.

cis-3-Benzyl-2'-((pyridin-3-yl)methyl)-1'-azaspirooxazolidine-5,3'-bicyclo[2.2.2]octan-2-one [31]

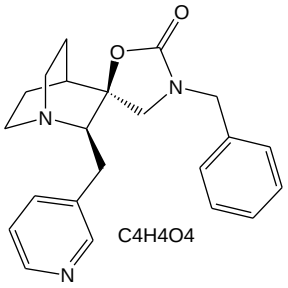

To a solution of c*is*-2'-((pyridin-3-yl)methyl)-1'-azaspirooxazolidine-5,3'-bicyclo[2.2.2]octan-2-one **29** (160 mg, 0.585 mmol) in DMF dry (3 mL) at 0°C, 60% NaH (71 mg, 1.777 mmol) was added and the mixture stirred at room temperature for 30 min. Benzyl chloride (0.074 mL, 0.651 mmol) was then added at 0°C and the mixture stirred again at room temperature for 3 h and at 45°C overnight.

The reaction was cooled to ambient, quenched with water (5 mL), saturated $NaHCO_3$ (5 mL) and extracted with DCM (3 x 6 mL). The organic layers were dried over Na_2SO_4, filtered and concentrated in *vacuo*. The residue was purified by flash chromatography (DCM →DCM/MeOH 95:05) to obtain 57 mg of the desired compound (27% yield).

To a solution of the free base (57 mg, 0.157 mmol) in MeOH (0.5 mL), fumaric acid (23 mg, 0.198 mmol) in methanol (0.4 mL) was added and the solution was stirred at room temperature for 4 h.

The solvent was removed in *vacuo* and the solid crystallized from 2-propanol to obtain 62 mg of the title compound (73% yield).

31: colourless solid.

m.p.: 190-192° C dec.

^{1}H-NMR (CD_3OD): δ 1.80-1.95 (m, 3H), 2.21-2.29 (m, 2H), 2.76 (m, 1H), 3.11-3.20 (m, 2H), 3.31-3.49 (m, 5H), 3.93-3.96 (m, 1H), 4.06-4.18 (m, 2H), 6.73 (s, 3H), 7.02-7.04 (m, 2H), 7.29-7.34 (m, 4H), 7.79 (m, 1H), 8.70 (m, 2H).

^{13}C-NMR ($CDCl_3$): δ 21.21, 22.24, 30.77, 33.36, 41.41, 48.29, 48.55, 53.59, 67.92, 80.66, 123.47, 128.22, 128.28, 129.13, 135.02, 135.65, 137.29, 147.84, 150.65, 157.54.

MS (ESI): *m/z* 364.1 $[M+H]^+$, calc. for $C_{22}H_{25}N_3O_2$ 363.4.

tert-Butyl 3-chloropropylcarbamate [70]

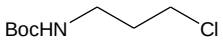

To an ice-cold solution of Boc_2O (7.78 g, 38.5 mmol) and TEA (5.9 mL, 42.7 mmol) in THF (70 mL), 3-chloropropylamine hydrochloride **69** (5 g, 38.5 mmol) was added and the mixture stirred for 20 h.
The reaction was diluted with a saturated $NaHCO_3$ solution (100 mL) and extracted with AcOEt (3 x 60 mL). The combined organic layers were dried over Na_2SO_4, filtered and concentrated in *vacuo* to afford 6.276 g of clean product (84% yield).

70: yellow oil.

***R*$_f$:** 0.32 (CyHex/AcOEt 9:1); PMA.

^{1}H-NMR ($CDCl_3$): δ 1.42 (s, 9H), 1.91 (m, 2H), 3.25 (m, 2H), 3.59 (t, *J* = 6.33 Hz, 2H), 4.70 (m, 1H).

tert-Butyl 3-chloropropyl(3-methoxybenzyl)carbamate [71]

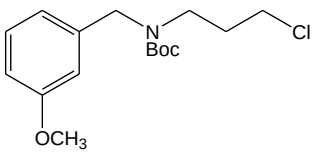

To a suspension of 60% NaH (558 mg, 13.952 mmol) in dry THF (21 mL) in an argon atmosphere, a solution of *tert*-butyl 3-chloropropylcarbamate **70** (1.351 g, 6.976 mmol) in dry THF (7 mL) and 3-methoxybromobenzene (1.465 mL, 10.464 mmol) were added, and the mixture heated at reflux for 5 h.
The reaction was cooled to 0°C and quenched with water (20 mL), then extracted with Et_2O (2 x 15 mL). The organic layers were dried over Na_2SO_4, filtered and the solvent was removed in *vacuo*. The crude material was purified by flash chromatography (CyHex → CyHex/AcOEt 95:05) to give 966 mg of pure product (44% yield).

71: yellow oil.

***R*$_f$:** 0.36 (CyHex/AcOEt 9:1); UV, PMA.

^{1}H-NMR ($CDCl_3$): δ 1.47 (bs, 9H), 1.97 (m, 2H), 3.32 (m, 2H), 3.52 (m, 2H), 3.79 (s, 3H), 4.42 (m, 2H), 6.81 (m, 3H), 7.24 (m, 1H).

(*S*)-(–)-*tert*-Butyl 2-(3-methoxyphenyl)pyrrolidine-1-carboxylate [72]

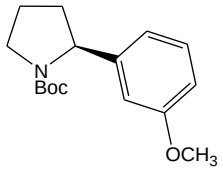

To a solution of (–)-sparteine (1.084 g, 4.625 mmol) in dry toluene (10 mL) in an argon atmosphere at −78°C, a solution of 1.4 M *sec*-butyllithium in cyclohexane (3.43 mL, 4.81 mmol) was added dropwise. A solution of *tert*-butyl 3-chloropropyl(3-methoxybenzyl)carbamate **71** (966 mg, 3.084 mmol) in dry toluene (15 mL) was added and the mixture was stirred at −78°C for 5 h.
The reaction was warmed to ambient and quenched with water (20 mL), then extracted with Et_2O (3 x 25 mL). The pooled organic layers were washed once with H_3PO_4 5%, twice with water, then dried over Na_2SO_4, filtered and concentrated in *vacuo*. The crude material was purified by flash chromatography (CyHex/AcOEt 95:05 → CyHex/AcOEt 90:10) to obtain 611 mg of clean product (71% yield).

72: yellow oil.

***R*$_f$:** 0.33 (CyHex/AcOEt 7:3); UV, PMA, $KMnO_4$.

^{1}H-NMR ($CDCl_3$): δ 1.44 (bs, 9H), 1.84 (m, 3H), 2.27 (m, 1H), 3.59 (m, 2H), 3.79 (s, 3H), 4.76 (m, 1H), 6.71 (m, 1H), 6.75 (m, 2H), 7.22 (m, 1H).

$[\alpha]^{20}_D$: − 50.86 (c 1, $CHCl_3$)

E.e.: 62%; Kromasil 5-Amycoat column, eluited with 5% 2-propanol in hexane, 1.0 mL/min flow.
Rt minor peak = 5.3 min (19%)
Rt major peak = 6.3 min (81%)

(*S*)-(–)-3-(Pyrrolidin-2-yl)phenol [73]

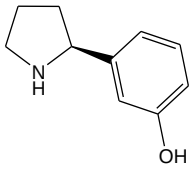

To a solution of (*S*)-(–)-*tert*-butyl 2-(3-methoxyphenyl)pyrrolidine-1-carboxylate **72** (421 mg, 1.518 mmol) in dry DCM (18 mL) in an argon atmosphere at −78°C, a solution of 1.0 M BBr_3 in hexane (3.8 mL, 3.415 mmol) was added dropwise. The solution was stirred at −78°C for 1 h and for further 4 h at −10°C.

The reaction was warmed to ambient and quenched with MeOH (20 mL), then concentrated in *vacuo*. The crude material was purified by acid/base extraction. The basic water layer was concentrated under *vacuum* and the resulting mixture was taken with DCM and filtered through a celite-septum. The organic layers were dried over Na_2SO_4, filtered and then concentrated in *vacuo* to afford 133 mg of clean secondary amine (60% yield).

73: yellow oil.

***R*$_f$:** 0.18 (AcOEt/MeOH 8:2); UV, Dragendorff reagent, $KMnO_4$.

^{1}H-NMR ($CDCl_3$): δ 1.72 (m, 1H), 1.88 (m, 2H), 2.13 (m, 1H), 2.92 (m, 1H), 3.15 (m, 1H), 3.95 (dd, *J* = 7.15; 8.8 Hz, 1H), 6.48 (bs, 2H), 6.7 (m, 3H), 7.1 (t, *J* = 7.98 Hz, 1H).

^{13}C-NMR ($CDCl_3$): δ 25.47, 33.36, 46.32, 62.92, 114.59, 115.81, 117.70, 130.03, 142.69, 158.37.

MS (ESI): *m/z* 164.0 $[M+H]^+$, calc. for $C_{10}H_{13}NO$ 163.22.

(*S*)-(–)-3-(1-Methylpyrrolidin-2-yl)phenol fumarate [32]

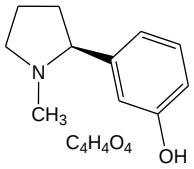

To a solution of (*S*)-(–)-3-(pyrrolidin-2-yl)phenol **73** (133 mg, 0.815 mmol) in MeOH (9 mL), 37% formaldehyde in water (0.39 mL, 4.808 mmol) was added and the solution was stirred at room temperature for 30 min. Once cooled to 0°C, $NaBH_4$ was added and the mixture stirred at room temperature for 30 min.

The reaction was quenched with water (10 mL) and extracted with DCM (4 x 8 mL). The organic layers were dried over Na_2SO_4, filtered and then concentrated in *vacuo* to get 132 mg of pure tertiary amine (91% yield).

To a solution of the free base (105 mg, 0.6 mmol) in methanol (1.8 mL), a solution of fumaric acid (76 mg, 0.652 mmol) in MeOH (1.2 mL) was added and the resulting mixture was stirred at room temperature for 5 h.

The solvent was removed in *vacuo* and the residue crystallized from 2-propanol/Et_2O to obtain 94 mg of the title compound (53% yield).

32: colourless solid.

m.p.: 100-101° C.

^{1}H-NMR (D_2O): δ 2.14 (m, 3H), 2.40 (m, 1H), 2.63 (s, 3H), 3.17 (m, 1H), 3.70 (m, 1H), 4.15 (m, 1H), 6.59 (s, 2H), 6.89 (m, 3H), 7.26 (t, *J* = 7.97 Hz, 1H).

^{13}C-NMR (D_2O): δ 21.37, 30.72, 37.60, 55.67, 72.54, 115.04, 116.95, 119.07, 130.53, 134.16, 134.71, 158.53, 169.09.

MS (ESI): *m/z* 178.1 $[M+H]^+$, calc. for $C_{11}H_{15}NO$ 177.24.

$[\alpha]^{20}_{D}$: −64.20 (c 0.6, MeOH)

E.e.: 98%; Kromasil 5-Amycoat column, elated with 10% 2-propanol in hexane, 1.0 mL/min flow.
Rt minor peak = 4.9 min (1%)
Rt major peak = 5.4 min (99%)

Methyl 3-((*tert*-butoxycarbonyl(3-chloropropyl)amino)methyl)benzoate [74]

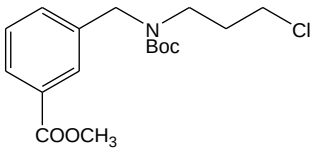

To a suspension of 60% NaH (619 mg, 15.5 mmol) in dry THF (23 mL) in an argon atmosphere, a solution of tert-butyl-3-chloropropylcarbamate **70** (1.5 g, 7.75 mmol) in dry THF (7.8 mL) and methyl-3-bromobenzoate (2.66 g, 11.63 mmol) were added, and the mixture was heated at reflux for 4 h.
The reaction was cooled to 0°C and quenched with water (20 mL), then extracted with Et_2O (3 x 15 mL). The pooled organic phases were dried over Na_2SO_4, filtered and the solvent was removed in *vacuo*. The crude material was purified by flash chromatography (CyHex → CyHex/AcOEt 95:05) to give 1.277 g of pure product (48% yield).

74: yellow oil.

***R*$_f$:** 0.25 (CyHex/AcOEt 9:1); UV, PMA.

^{1}H-NMR ($CDCl_3$): δ 1.46 (s, 9H), 1.96 (m, 2H), 3.33 (m, 2H), 3.51 (m, 2H), 3.89 (s, 3H), 4.47 (m, 2H), 7.39 (m, 2H); 7.93 (m, 2H).

^{13}C-NMR ($CDCl_3$): δ 23.57, 28.60, 31.42, 42.66, 52.36, 65.47, 80.48, 128.77, 128.90, 130.67, 131.96, 132.37, 139.10, 156.30, 167.12.

MS (ESI): *m/z* 342.0 $[M+H]^+$, calc. for $C_{17}H_{24}ClNO_4$ 341.83.

tert-Butyl 3-chloropropyl(3-(hydroxymethyl)benzyl)carbamate [75]

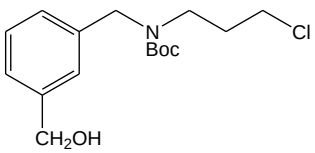

To a solution of methyl 3-((*tert*-butoxycarbonyl(3-chloropropyl)amino) methyl)benzoate **74** (1.277 g, 3.74 mmol) in dry THF (25 mL), $LiBH_4$ (406 mg, 18.64 mmol) was added, and the mixture stirred under reflux for 30 h.
The reaction was quenched with MeOH (3 mL), then concentrated in *vacuo*. The residue was taken with water (50 mL) and extracted with DCM (3 x 35 mL). The organic layers were dried over Na_2SO_4, filtered and the solvent removed in *vacuo*. The crude material was purified by flash chromatography (CyHex/AcOEt 85:15) to afford 1.05 g of pure alcohol (90% yield).

74: yellow oil.

***R*$_f$:** 0.08 (CyHex/AcOEt 8:2); UV, PMA.

^{1}H-NMR ($CDCl_3$): δ 1.47 (s, 9H), 1.97 (m, 2H), 3.31 (m, 2H), 3.50 (m, 2H), 4.44 (m, 2H), 4.67 (s, 2H), 7.15 (m, 1H), 7.27 (m, 3H).

^{13}C-NMR ($CDCl_3$): δ 28.63, 31.37, 42.67, 44.37, 50.39, 65.14, 80.37, 126.07, 128.81, 128.93, 138.66, 141.54, 141.69, 156.18.

MS (ESI): *m/z* 336.1 $[M+Na]^+$, calc. for $C_{16}H_{24}ClNO_3$ 313.82.

tert-Butyl 3-((_tert_-butyldimethylsilyloxy)methyl)benzyl(3-chloropropyl)carbamate [76]

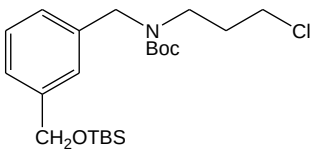

To a solution of *tert*-butyl 3-chloropropyl(3-(hydroxymethyl)benzyl)carbamate **75** (798 mg, 2.54 mmol) in DMF (1.6 mL), TBSCl (613 mg, 4.07 mmol) and imidazole (432 mg, 6.35 mmol) were added, and the mixture stirred at 35°C for 8 h.

The reaction was quenched with water (20 mL), then extracted with Et_2O (3 x 10 mL). The organic layers were washed with brine, dried over Na_2SO_4, filtered and concentrated in *vacuo*. The crude material was purified by flash chromatography (CyHex/AcOEt 98:02 $\rightarrow$ 95:05) to provide 785 mg of protected alcohol (76% yield).

76: yellow oil.

***R*$_f$:** 0.6 (CyHex/AcOEt 9:1); UV, PMA.

^{1}H-NMR ($CDCl_3$): δ 0.10 (s, 6H), 0.95 (s, 9H), 1.47 (bs, 9H), 1.98 (m, 2H), 3.32 (m, 2H), 3.51 (m, 2H), 4.45 (m, 2H), 4.73 (s, 2H), 7.12 (m, 1H), 7.26 (m, 3H).

^{13}C-NMR ($CDCl_3$): δ -5,00, 18.65, 26.20, 28.67, 31.41, 42.70, 44.80, 65.12, 74.96, 80.17, 125.24, 125.51, 126.51, 128.66, 138.32, 142.03, 156.09.

MS (ESI): *m/z* 450.1 $[M+Na]^+$, calc. for $C_{22}H_{38}ClNO_3Si$ 428.08.

(*S*)-(–)-*tert*-Butyl 2-(3-((*tert*-butyldimethylsilyloxy)methyl)phenyl)pyrrolidine-1-carboxylate [77]

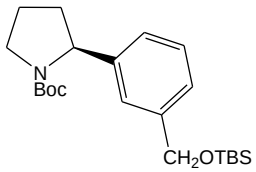

To a solution of (–)-sparteine (679 mg, 2.90 mmol) in dry toluene (4.2 mL) in an argon atmosphere at −78°C, a solution of 1.4 M *sec*-butyllithium in cyclohexane (2.72 mL, 3.01 mmol) was added dropwise. A solution of *tert*-butyl 3-((*tert*-butyldimethylsilyloxy)methyl)benzyl(3-chloropropyl)carbamate **76** (785 mg, 1.93 mmol) in dry toluene (13 mL) was added and the mixture was stirred at −78°C for 4 h.

The reaction was warmed to ambient and quenched with water (20 mL), then extracted with Et_2O (3 x 10 mL). The combined organic layers were washed once with 5% H_3PO_4 and water, then dried over Na_2SO_4, filtered and then concentrated in *vacuo*. The crude material was purified by flash chromatography (CyHex/AcOEt 95:05 → CyHex/AcOEt 90:10) to obtain 362 mg of clean product (48% yield).

77: yellow oil.

***R*$_f$:** 0.30 (CyHex/AcOEt 9:1); UV, PMA, $KMnO_4$.

^{1}H-NMR ($CDCl_3$): δ 0.09 (s, 6H), 0.92 (s, 9H), 1.18-1.45 (m, 9H), 1.86 (m, 3H), 2.30 (m, 1H), 3.62 (m, 2H), 4.72 (s, 2H), 4.76 (m, 1H), 7.04 (m, 1H), 7.15 (m, 2H), 7.26 (m, 1H).

^{13}C-NMR ($CDCl_3$): δ -5,00, 18.61, 23.38, 26.18, 28.40, 36.17, 47.28, 61.53, 65.19, 79.29, 123.40, 124.35, 124.43, 128.24, 141.55, 145.32, 154.75.

MS (ESI): *m/z* 414.2 $[M+Na]^+$, calc. for $C_{22}H_{37}NO_3Si$ 391.62.

$[\alpha]^{20}_{D}$: – 50.55 (c 1, $CHCl_3$)

E.e.: 70%; Kromasil 5-Amycoat column, eluted with 5% 2-propanol in hexane, 1.0 mL/min flow.

Rt minor peak = 3.2 min (15%)

Rt major peak = 3.8 min (85%)

(*S*)-(–)-*tert*-Butyl 2-(3-(hydroxymethyl)phenyl)pyrrolidine-1-carboxylate [78]

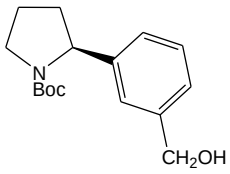

To a solution of (*S*)-(–)-*tert*-butyl 2-(3-((*tert*-butyldimethylsilyloxy)methyl) phenyl)pyrrolidine-1-carboxylate **77** (313 mg, 0.80 mmol) in dry THF (3.3 mL) and in an argon atmosphere at 0°C, TBAF (0.46 mL, 1.6 mmol) was added dropwise, and the mixture stirred at 0°C for 5 min and then for 45 min at room temperature.

The reaction was quenched with water (20 mL), then extracted with AcOEt (3 x 10 mL). The pooled organic layers were dried over Na_2SO_4, filtered and the concentrated in *vacuo*. The crude material was purified by flash chromatography (DCM $\rightarrow$ DCM/MeOH 95:05) to give 171 mg of pure alcohol (73% yield).

78: yellow oil.

***R*$_f$:** 0.40 (DCM/MeOH 95:5); UV, PMA, $KMnO_4$.

^{1}H-NMR ($CDCl_3$): δ 1.2-1.55 (m, 9H), 1.87 (m, 3H), 2.32 (m, 1H), 3.63 (m, 2H), 4.67 (s, 2H), 4.77-4.94 (m, 1H), 7.10 (m, 1H), 7.20 (m, 2H), 7.28 (m, 1H).

^{13}C-NMR ($CDCl_3$): δ 23.41, 28.38, 36.16, 47.32, 61.50, 65.20, 79.60, 124.28, 124.85, 125.29, 128.50, 141.34, 145.51, 154.90.

MS (ESI): *m/z* 314.1 $[M+Cl]^+$, calc. for $C_{16}H_{23}NO_3$ 277.36.

(*S*)-(–)-(3-(Pyrrolidin-2-yl)phenyl)methanol [79]

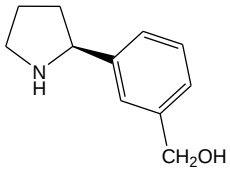

To a solution of (*S*)-(–)-*tert*-butyl-2-(3-(hydroxymethyl)phenyl)pyrrolidine-1-carboxylate **78** (166 mg, 0.57 mmol) in Et_2O (3 mL) at 0°C, 4.0 M HCl in 1,4-dioxane (1.5 mL) was added dropwise and the mixture stirred at room temperature for 3 h.

The solvent was removed in *vacuo* and the crude material was purified by acid/base extraction. The aqueous phase was concentrated by rotary evaporation and the crude material was taken with DCM and filtered through a celite-septum. The organic layers were dried over Na_2SO_4, filtered, then concentrated in *vacuo* to afford 62 mg of clean secondary amine (61% yield).

79: yellow oil.

***R*$_f$:** 0.1 (DCM); UV, Dragendorff reagent, $KMnO_4$.

^{1}H-NMR ($CDCl_3$): δ 1.68 (m, 1H), 1.84 (m, 2H), 2.14 (m, 1H), 2.94 (m, 1H), 3.12 (m, 1H), 3.87 (s, 2H), 4.03 (t, *J* = 7.70; 7.98 Hz, 1H), 4.56 (s, 2H), 7.17-7.29 (m, 4H).

^{13}C-NMR ($CDCl_3$): δ 25.63, 33.95, 46.77, 62.80, 64.73, 125.41, 125.79, 125.98, 128.72, 142.17, 143.34.

MS (ESI): *m/z* 178.1 $[M+H]^+$, calc. for $C_{11}H_{15}NO$ 177.24.

(*S*)-(–)-(3-(1-Methylpyrrolidin-2-yl)phenyl)methanol [33]

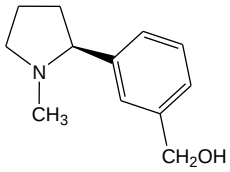

To a solution of (*S*)-(–)-(3-(pyrrolidin-2-yl)phenyl)methanol **79** (60 mg, 0.34 mmol) in MeOH (3.8 mL), 37% formaldehyde in water (0.16 mL, 2.01 mmol) was added, and the solution was stirred at room temperature for 30 min. Once cooled to 0°C, $NaBH_4$ (28 mg, 0.71 mmol) was added and the mixture stirred at room temperature for 1 h.

The reaction was quenched with water (10 mL) and extracted with AcOEt (3 x 8 mL). The organic layers were dried over Na_2SO_4, filtered and then concentrated in *vacuo*. The crude material was purified by acid/base extraction to obtain 44 mg of pure tertiary amine (68% yield).

33: yellow oil.

***R*$_f$:** 0.2 (DCM/MeOH 9:1); UV, Dragendorff reagent, $KMnO_4$.

^{1}H-NMR ($CDCl_3$): δ 1.79 (m, 2H), 1.94 (m, 1H), 2.13 (m, 4H), 2.27 (m, 1H), 3.04 (m, 1H), 3.21 (m, 1H), 4.66 (s, 2H), 7.28 (m, 4H).

^{13}C-NMR ($CDCl_3$): δ 22.64, 35.18, 40.72, 57.27, 65.36, 71.95, 126.05, 126.16, 127.15, 128.77, 141.62, 143.41.

MS (ESI): *m/z* 192.1 $[M+H]^+$, calc. for $C_{12}H_{17}NO$ 191.27.

$[\alpha]^{20}_D$: – 89.64 (c 1.1, $CHCl_3$)

E.e.: 98%; Kromasil 5-Amycoat column, eluted with 10% 2-propanol in hexane, 1.0 mL/min flow.

R_t minor peak = 8.1 min (1%)

R_t major peak = 10.1 min (99%)

(3-(4,5-Dihydro-3*H*-pyrrol-2-yl)phenyl)methanol [34]

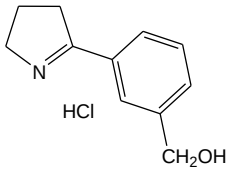

Pirrolydin-2-thione **80** (168 mg; 1.66 mmol), 3-(hydroxymethyl)phenylboronic acid (302.5 mg, 1.99 mmol), Cu(I) thiophen-2-carboxylate (950 mg, 4.98 mmol) and $Pd(Ph_3P)_4$ (78 mg, 0.066 mmol) were dissolved in dry THF (6 mL) and sealed in a MW tube in a dry atmosphere. The mixture was heated at 100°C for 2 h under MW irradiation.

The solvent was removed in *vacuo* and the residue taken with DCM (10 mL). The organic layer was then filtered through a celite-septum, washed with 25% ammonia (3 x 10 mL), dried over Na_2SO_4, filtered and then concentrated in *vacuo*. The crude material was purified by flash chromatography (DCM/MeOH 95:05) to obtain 184 mg of the title compound (63% yield).

The free imine was treated with 2.0 N HCl in Et_2O for 1 hour. The solvent was removed in *vacuo* and the residue crystallized with 2-propanol to give 64 mg of the desired derivative (29% yield).

34: colourless solid.

m.p.: 190 °C dec.

.

^{1}H-NMR (CD_3OD): δ 2.45 (m, 2H), 3.68 (m, 2H), 4.25 (m, 2H), 4.73 (m, 2H), 7.66 (m, 1H), 7.83 (m, 1H), 7.97 (m, 1H), 8.05 (m, 1H).

^{13}C-NMR (CD_3OD): δ 19.76, 35.11, 53.77, 62.78, 126.20, 128.14, 129.02, 129.73, 134.61, 144.17, 186.49.

Trimethyl(tosylethynyl)silane [82]

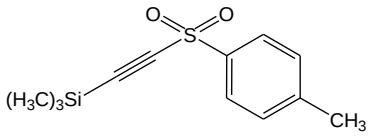

To a suspension of $AlCl_3$ (1.722 g, 12.911 mmol) in dry DCM (10 mL) under an argon atmosphere, tosyl chloride (2.461 g, 12.911 mmol) was added and the mixture stirred at room temperature until complete formation of the complex (clear solution, 30 min).

The solution was added dropwise to an ice-cooled solution of bis(trimethylsilyl)acetylene **81** (2 g, 11.737 mmol) in dry DCM (12 mL), and the mixture was stirred for 30 min at 0°C and for additional 6h at room temperature.

The reaction was poured in a mixture of 20% HCl (11 mL) and ice (11 g), the organic layer was separated and the aqueous layer extracted with DCM (5 mL). The combined organic phases were washed with water (2 x 7 mL), dried over Na_2SO_4, filtered and concentrated in *vacuo*. Crystallization from cyclohexane afforded 1.749 g of clean product (56% yield).

82: colourless solid.

***R*$_f$:** 0.20 (CyHex/AcOEt 9:1); UV, $KMnO_4$.

^{1}H-NMR ($CDCl_3$): δ 0.22 (s, 9H), 2.48 (s, 3H), 7.40 (d, J = 9.00 Hz, 2H), 7.91 (d, J = 9.00 Hz, 2H).

1-(Ethynylsulfonyl)-4-methylbenzene [83]

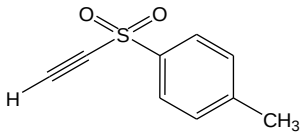

To a solution of trimethyl(tosylethynyl)silane **82** (1.749 g, 6.565 mmol) in MeOH (19 mL) under an argon atmosphere, an aqueous solution of 6.2 x 10^{-3} M K_2CO_3 and 6.2 x 10^{-3} M $NaHCO_3$ was added to reach pH 9, while maintaining the temperature below 30°C with a cold water bath. The mixture was stirred overnight at room temperature.

The reaction was diluted with water (15 mL) and extracted with DCM (3 x 40 mL). The organic layers were washed twice with water and twice with brine, dried over Na_2SO_4, filtered, and the solvent was removed in *vacuo*. The crude material was purified by flash chromatography (CyHex/AcOEt 90:10) to give 1.035 g of the title compound (88% yield).

83: colourless solid.

***R*$_f$:** 0.2 (CyHex/AcOEt 9:1); UV, $KMnO_4$.

^{1}H-NMR ($CDCl_3$): δ 2.47 (s, 3H), 3.52 (s, 1H), 7.38 (d, *J* = 8.50 Hz, 2H), 7.88 (d, *J* = 8.50 Hz, 2H).

***tert*-Butyl 2-tosyl-7-azabicyclo[2.2.1]hepta-2,5-diene-7-carboxylate [85]**

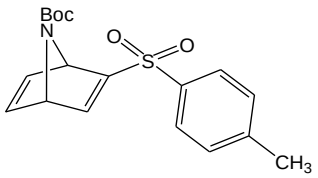

In an argon atmosphere, *N*-Boc-pyrrole **84** (1.70 mL, 10.22 mmol) and 1-(ethynylsulfonyl)-4-methylbenzene **83** (1.035 g, 5.742 mmol) were mixed and stirred at 80°C for 3 days. The crude reaction mixture was directly purified by flash chromatography (CyHex/AcOEt 80:20) to produce 794 mg of clean product (40% yield).

85: yellow oil.

***R*$_f$:** 0.6 (CyHex/AcOEt 7:3); UV, $KMnO_4$.

^{1}H-NMR ($CDCl_3$): δ 1.27 (s, 9H), 2.45 (s, 3H), 5.18 (m, 1H), 5.39 (m, 1H), 6.88 (m, 2H), 7.34 (d, *J* = 8.2 Hz, 2H), 7.58 (s, 1H), 7.76 (d, *J* = 8.2 Hz, 2H).

tert-Butyl 2-tosyl-7-azabicyclo[2.2.1]hept-2-ene-7-carboxylate [86]

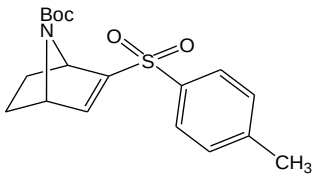

To a solution of $NiCl_2$ (1.481 g, 6.565 mmol) in dry EtOH (12 mL) under an argon atmosphere, a suspension of $NaBH_4$ in dry EtOH (12 mL) was slowly added. The mixture was stirred at room temperature for 10 min. Then a solution of t*ert*-butyl 2-tosyl-7-azabicyclo[2.2.1]hepta-2,5-diene-7-carboxylate **85** (794 mg, 2.287 mmol) in dry THF (12 mL) and conc. HCl (2.25 mL, 22.87 mmol) were added, and the mixture was stirred at room temperature for 1 h.
The reaction was filtered through a celite-septum and concentrated in *vacuo* and the residue was taken with saturated $NaHCO_3$ (30 mL) and extracted with DCM (3 x 10 mL). The organic layers were washed twice with water and twice with brine, then dried over Na_2SO_4, filtered and concentrated in *vacuo* to afford 723 mg of the title compound (91% yield).

86: yellow oil.

***R*$_f$:** 0.32 (CyHex/AcOEt 8:2); UV, $KMnO_4$.

^{1}H-NMR ($CDCl_3$): δ 1.21 (s, 9H), 1.27-1.47 (m, 2H), 2.01 (m, 1H), 2.45 (s, 3H), 4.76 (m, 1H), 4.83 (m, 1H), 7.06 (m, 1H), 7.35 (m, 2H), 7.81 (m, 2H).

tert-Butyl 2-tosyl-3-(tributylstannyl)-7-azabicyclo[2.2.1]heptane-7-carboxylate [87]

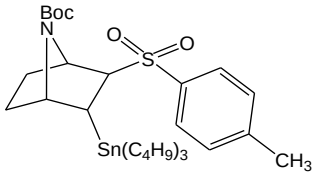

To a solution of tert-butyl 2-tosyl-7-azabicyclo[2.2.1]hept-2-ene-7-carboxylate **86** (723 mg, 2.071 mmol) in dry degassed toluene (8 mL) under an argon atmosphere, AIBN (18 mg, 0.104 mmol) was added and the mixture stirred at room temperature for 5 min. Tributyltin hydride (1.148 mL, 4.267 mmol) was then added dropwise and the mixture was heated at reflux for 6 h.
The reaction was quenched with saturated $NaHCO_3$ (15 mL) and extracted with AcOEt (3 x 10 mL). The combined organic layers were dried over Na_2SO_4, filtered and concentrated in *vacuo*. The crude material was purified by flash chromatography (CyHex → CyHex/AcOEt 97:03) to give 555 mg of pure product (33% yield).

87: yellow oil.

***R*$_f$:** 0.49 (CyHex/AcOEt 9:1); UV, $KMnO_4$.

^{1}H-NMR ($CDCl_3$): δ 0.79 (m, 4H), 0.85-0.94 (m, 9H), 1.25-1.90 (m, 27H), 2.44 (s, 3H), 2.57-2.63 (m, 1H), 3.67-3.70 (m, 1H), 4.20-4.26 (m, 2H), 7.34 (m, 2H), 7.73 (m, 2H).

tert-Butyl 7-azabicyclo[2.2.1]hept-2-ene-7-carboxylate [88]

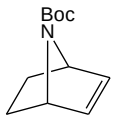

To a solution of *tert*-butyl 2-tosyl-3-(tributylstannyl)-7-azabicyclo[2.2.1] heptane-7-carboxylate **87** (555 mg, 0.882 mmol) in dry THF (5 mL) in an argon atmosphere, TBAF (1.77 mL, 1.764 mmol) was added and the mixture stirred under reflux for 16 h.

The reaction was quenched with saturated $NaHCO_3$ (15 mL) and extracted with AcOEt (3 x 10 mL). The organic layers were dried over Na_2SO_4, filtered and concentrated in *vacuo*. The crude material was purified by flash chromatography (CyHex/AcOEt 95:05) to give 157 mg of clean alkene (91% yield).

88: yellow oil.

***R*$_f$:** 0.56 (CyHex/AcOEt 9:1); $KMnO_4$.

^{1}H-NMR ($CDCl_3$): δ 1.10 (m, 2H), 1.41 (s, 9H), 1.85 (m, 2H), 4.65 (m, 2H), 6.21 (m, 2H).

tert-Butyl 2-_exo_-(3-methoxyphenyl)-7-azabicyclo[2.2.1]heptane-7-carboxylate [89]

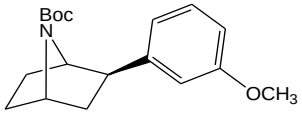

To a solution of *tert*-butyl 7-azabicyclo[2.2.1]hept-2-ene-7-carboxylate **88** (157 mg, 0.804 mmol) in dry DMF (3.5 mL) in an argon atmosphere, 3(methoxy(phenyl)bromide (0.255 mL, 2.01 mmol), $Pd(OAc)_2$ (9 mg, 0.04 mmol), TBAC (56 mg, 0.201 mmol) and potassium formate (170 mg, 2.01 mmol) were added, and the mixture stirred at 81°C for 5 h.
The reaction was cooled to ambient and poured in a mixture of conc. ammonia and water 1:1 (10 mL), then extracted with DCM (3 x 10 mL). The pooled organic phases were washed with brine (3 times), dried over Na_2SO_4, filtered and concentrated in *vacuo*. The crude material was purified by flash chromatography (CyHex/AcOEt 98:02) to give 118 mg of pure compound (49% yield).

89: yellow oil.

***R*$_f$:** 0.19 (CyHex/AcOEt 9:1); UV; $KMnO_4$.

^{1}H-NMR ($CDCl_3$): δ 1.43 (s, 9H), 1.53 (m, 2H), 1.92 (m, 4H), 2.84 (dd, *J* = 5.5; 8.8 Hz, 1H), 3.80 (s, 3H), 4.25-4.35 (m, 2H), 6.73 (m, 1H), 6.86 (m, 2H), 7.17 (m, 1H).

^{13}C-NMR ($CDCl_3$): δ 28.56, 29.02, 30.22, 40.77, 48.34, 55.30, 55.83, 62.25, 79.57, 111.83, 112.82, 119.71, 129.51, 147.68, 155.29, 159.89.

MS (ESI): *m/z* 304.2 $[M+H]^+$, calc. for $C_{18}H_{25}NO_3$ 303.40.

3-(7-Azabicyclo[2.2.1]heptan-2-*exo*-yl)phenol hydrochloride [35]

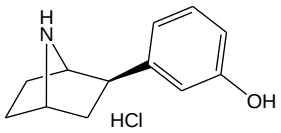

To a solution of *tert*-butyl 2-*exo*-(3-methoxyphenyl)-7-azabicyclo[2.2.1] heptane-7-carboxylate **89** (118 mg, 0.389 mmol) in dry DCM (4.6 mL) in a nitrogen atmosphere at −78°C, 1.0 M BBr_3 in hexane (0.875 mL, 0.875 mmol) was added, and the mixture stirred at −78°C for 1 h and at 0°C for further 2 h.
The solvent was removed in *vacuo* and the residue was taken with DCM (4 mL), then TEA was added until pH reached 9, followed by Boc_2O (170 mg, 0.778 mmol). The mixture was then stirred at room temperature for 2 h.
The reaction was diluted with saturated $NaHCO_3$ (5 mL), then extracted with DCM (3 x 3 mL). The organic layers were washed with 5% H_3PO_4 (5 mL), dried over Na_2SO_4, filtered and concentrated in *vacuo*. The crude material was purified by flash chromatography (CyHex/AcOEt 90:10) to give 95 mg of pure *N*-Boc protected alcohol (85% yield).
To a solution of this intermediate (82 mg, 0.284 mmol) in Et_2O (0.4 mL) at 0°C, 4.0 M HCl in 1,4-dioxane (0.660 mL, 2.64 mmol) was added and the mixture stirred at room temperature for 4 h.
The solvent was removed in *vacuo* and the residue digested with Et_2O to afford 61 mg of the title compound (99% yield).

35: colourless solid.

m.p.: very hygroscopic substance.

^{1}H-NMR (CD_3OD): δ 1.83-2.12 (m, 5H), 2.37 (m, 1H), 3.31 (m, 1H), 4.28 (m, 1H), 4.44 (m, 1H), 6.70-6.77 (m, 2H), 7.18 (m, 1H).

^{13}C-NMR (CD_3OD): δ 25.73, 27.52, 36.46, 44.74, 59.20, 63.28, 113.59, 113.77, 117.23, 129.88, 142.98, 157.92.

MS (ESI): *m/z* 190.1 $[M+H]^+$, calc. for $C_{12}H_{15}NO$ 189.25.

tert-Butyl 2-_exo_-(3-(hydroxymethyl)phenyl)-7-azabicyclo[2.2.1]heptane-7-carboxylate [90]

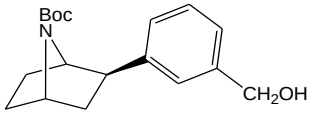

To a solution of *tert*-butyl 7-azabicyclo[2.2.1]hept-2-ene-7-carboxylate **88** (78 mg, 0.4 mmol) in dry DMF (1.8 mL) in an argon atmosphere, (3-bromophenyl)methanol (0.120 mL, 1 mmol), $Pd(OAc)_2$ (5 mg, 0.02 mmol), TBAC (28 mg, 0.1 mmol) and potassium formate (84 mg, 1 mmol) were added, and the mixture stirred at 81°C for 7 h.

The reaction was cooled to ambient and poured into a mixture of conc. ammonia and water 1:1 (10 mL), then extracted with DCM (3 x 10 mL). The organic layers were washed with brine (3 times), dried over Na_2SO_4, filtered and concentrated in *vacuo*. The crude material was purified by flash chromatography (CyHex/AcOEt 90:10 → 60:40) to obtain 35 mg of pure compound (30% yield).

90: yellow oil.

Rf: 0.32 (CyHex/AcOEt 1:1); UV; $KMnO_4$; Ninhydrin.

^{1}H-NMR ($CDCl_3$): δ 1.43 (s, 9H), 1.50-1-59 (m, 2H), 1.81-1.95 (m, 4H), 2.85 (dd, *J* = 5.5; 8.5 Hz, 1H), 4.22 (m, 1H), 4.35 (m, 1H), 4.64 (bs, 2H), 7.20 (m, 2H), 7.27 (m, 2H).

^{13}C-NMR ($CDCl_3$): δ 28.58, 29.93, 30.54, 40.75, 48.22, 54.60, 65.56, 79.74, 125.08, 125.99, 126.50, 128.85, 141.26, 146.30.

MS (ESI): *m/z* 304.2 $[M+H]^+$, calc. for $C_{18}H_{25}NO_3$ 303.40.

3-(7-Azabicyclo[2.2.1]heptan-2-*exo*-yl)phenyl)methanol hydrochloride [36]

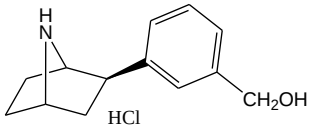

To a solution of *tert*-butyl 2-*exo*-(3-(hydroxymethyl)phenyl)-7-azabicyclo[2.2.1] heptane-7-carboxylate **90** (30 mg, 0.1 mmol) in Et_2O (0.2 mL) at 0°C, 4.0 M HCl in 1,4-dioxane (0.5 mL, 2 mmol) was added and the mixture stirred at room temperature for 6 h.
The solvent was removed in *vacuo* and the residue digested with Et_2O to afford 19 mg of the title compound (80% yield).

36: colourless solid.

m.p.: very hygroscopic substance.

^{1}H-NMR (CD_3OD): δ 1.88-2.15 (m, 5H), 2-37-2.44 (m, 1H), 3.40 (dd, *J* = 6.05; 9.45 Hz, 1H), 4.30 (m, 1H), 4.47 (m, 1H), 4.88 (s, 2H), 7.21-7.38 (m, 4H).

^{13}C-NMR (CD_3OD): δ 25.76, 27.53, 36.44, 44.82, 59.25, 63.35, 63.83, 125.05, 125.38, 125.56, 128.88, 141.50, 142.28.

MS (ESI): *m/z* 190.1 $[M+H]^+$, calc. for $C_{13}H_{17}NO$ 203.28.

tert-Butyl 5-(3-methoxyphenyl)-5-oxopentylcarbamate [92]

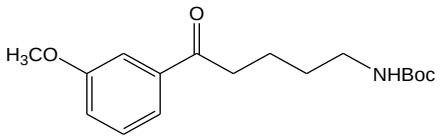

To a solution of δ-valerolactame **91** (1 g, 10.088 mmol) in dry THF (27 mL) in an argon atmosphere at −78°C, 2.5 M butyllithium in hexane (4.04 mL, 10.088 mmol) was added dropwise and the mixture stirred at −78°C for 30 min. Subsequently, a solution of Boc_2O (2.201 g, 10.088 mmol) in dry THF (3.5 mL) was added and the reaction stirred at −78°C for 3 h. Then, a solution of (3-methoxyphenyl)magnesium bromide (prepared from 2.453 g of 3-methoxy-bromobenzene and 368 mg of magnesium) in dry THF (13.5 mL) was finally added and the mixture stirred at −78°C for additional 3 h.
The reaction was warmed to ambient and quenched with 2.0 N HCl in water (10 mL), then extracted with Et_2O (3 x 15 mL). The organic layers were washed with 5% $NaHCO_3$ and brine, dried over Na_2SO_4, filtered and concentrated in *vacuo* to obtain 2.84 g of pure compound (91% yield).

92: yellow oil.

***R*$_f$:** 0.2 (CyHex/AcOEt 9:1); UV; PMA.

^{1}H-NMR ($CDCl_3$): δ 1.43 (s, 9H), 1.55 (m, 2H), 1.74 (m, 2H), 2.97 (t, *J* = 7.15; 7.42 Hz, 2H), 3.14 (m, 2H), 3.84 (s, 3H), 4.63 (bs, 1H), 7.09 (m, 1H), 7.35 (m, 1H), 7.46 (m, 1H), 7.52 (m, 1H).

6-(3-Methoxyphenyl)-2,3,4,5-tetrahydropyridine [93]

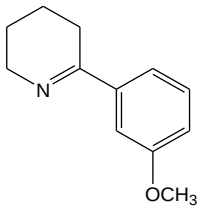

To *tert*-butyl 5-(3-methoxyphenyl)-5-oxopentylcarbamate **92** (2.74 g, 8.9 mmol) at 0°C, trifluoroacetic acid (18 mL) was added dropwise and the mixture stirred at room temperature for 4 h.

The reaction was cooled to 0°C and quenched with 30% NaOH dropwise until pH reached 10-11. The mixture was extracted with Et_2O (5 x 20 mL). The organic layers were washed with brine, dried over Na_2SO_4, filtered and concentrated in *vacuo*. The crude material was purified by flash chromatography (CyHex →CyHex/AcOEt 90:10) to afford 1.098 g of pure compound (65% yield).

93: dark yellow oil.

***R*$_f$:** 0.2 (CyHex/AcOEt 9:1); UV; PMA.

^{1}H-NMR ($CDCl_3$): δ 1.68 (m, 2H), 1.83 (m, 2H), 2.62 (m, 2H), 3.84 (m, 5H), 6.94 (m, 1H), 7.27 (m, 2H), 7.37 (m, 1H).

^{13}C-NMR ($CDCl_3$): δ 19.93, 22.03, 27.54, 50.00, 55.59, 110.99, 116.24, 118.74, 129.39, 141.67, 159.85, 166.07.

MS (ESI): *m/z* 191.1 $[M+H]^+$, calc. for $C_{12}H_{15}NO$ 189.25.

3-(3,4,5,6-Tetrahydropyridin-2-yl)phenol hydrochloride [37]

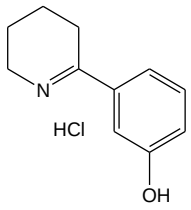

A solution of 6-(3-methoxyphenyl)-2,3,4,5-tetrahydropyridine **93** (201 mg, 1.062 mmol) in 48% HBr (3 mL) was stirred under reflux for 6 h.
The solvent was removed in *vacuo*, the residue taken with saturated $NaHCO_3$ (pH=8) and extracted with AcOEt (5 x 20 mL). The organic layers were washed with brine, dried over Na_2SO_4, filtered and concentrated. The yellow oil was treated with 1.25 M HCl in methanol for 30 min. Concentration in *vacuo* and crystallization from 2-propanol provided 142 mg of the title compound (63% yield).

37: yellow solid.

m.p.: 192-193 °C.

^{1}H-NMR (CD_3OD): δ 2.01 (m, 4H), 3.27 (m, 2H), 3.82 (m, 2H), 7.18 (dd, *J* = 2.21; 7.98 Hz, 1H), 7.26 (m, 1H), 7.33 (m, 1H), 7.45 (m, 1H).

^{13}C-NMR (CD_3OD): δ 16.99, 17.09, 19.16, 45.24, 114.21, 118.62, 121.91, 130.75, 133.13, 158.55, 183.77.

MS (ESI): *m/z* 177..1 $[M+H]^+$, calc. for $C_{11}H_{13}NO$ 175.23.

tert-Butyl 5-(3-iodophenyl)-5-oxopentylcarbamate [94]

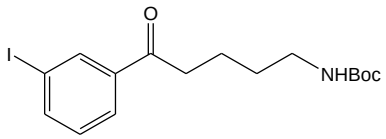

To a solution of δ-valerolactame (1 g, 10.088 mmol) in dry THF (27 mL) in an argon atmosphere at -78°C, 2.5 M butyllithium in hexane (4.04 mL, 10.088 mmol) was added dropwise and the mixture stirred at −78°C for 30 min. Subsequently, a solution of Boc_2O (2.201 g, 10.088 mmol) in dry THF (3.5 mL) was added and the reaction stirred at −78°C for 3 h. A solution of (3-iodophenyl)magnesium bromide (prepared from 1.67 mL of 3-iodo-bromobenzene and 368 mg of magnesium) in dry THF (13.5 mL) was finally added and the mixture stirred at −78°C for additional 3 h.

The reaction was warmed to ambient and quenched with 2.0 N HCl in water (10 mL), then extracted with Et_2O (3 x 15 mL). The organic layers were washed with 5% $NaHCO_3$ and brine, dried over Na_2SO_4, filtered and concentrated in *vacuo*. The crude material was purified by flash chromatography (CyHex/AcOEt 95:05→ 90:10) to give 1.75 g of pure compound (41% yield).

94: yellow oil.

***R*$_f$:** 0.2 (CyHex/AcOEt 9:1); UV; PMA.

^{1}H-NMR ($CDCl_3$): δ 1.44 (s, 9H), 1.55 (m, 2H), 1.77 (m, 2H), 2.98 (m, 2H), 3.17 (m, 2H), 4.58 (bs, 1H), 7.37 (m, 1H), 7.53 (m, 1H), 7.75 (m, 1H), 7.81 (m, 1H).

6-(3-Iodophenyl)-2,3,4,5-tetrahydropyridine [95]

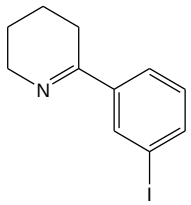

To *tert*-butyl 5-(3-iodophenyl)-5-oxopentylcarbamate **94** (5.27 g, 13.07 mmol) at 0°C, trifluoroacetic acid (16.3 mL) was added dropwise and the mixture stirred at room temperature for 3 h.

The reaction was cooled to 0°C and quenched with 30% NaOH dropwise until pH reached 10-11. The mixture was then extracted with Et_2O (5 x 30 mL). The organic layers were washed with brine, dried over Na_2SO_4, filtered and concentrated in *vacuo*. The crude material was purified by flash chromatography (CyHex/AcOEt 95:05) to afford 1.683 g of pure compound (45% yield).

95: yellow oil.

***R*$_f$:** 0.40 (CyHex/AcOEt 8:2); UV; PMA.

^{1}H-NMR ($CDCl_3$): δ 1.68 (m, 2H), 1.84 (m, 2H), 2.59 (m, 2H), 3.84 (m, 2H), 7.10 (m, 1H), 7.24 (m, 1H), 7.50 (m, 1H), 7.68 (m, 1H).

^{13}C-NMR ($CDCl_3$): δ 19.84, 21.97, 27.22, 50.19, 122.99, 124.68, 129.36, 132.63, 138.60, 142.38, 164.20.

MS (ESI): *m/z* 286.0 $[M+H]^+$, calc. for $C_{11}H_{12}IN$ 285.12.

Methyl 3-(3,4,5,6-tetrahydropyridin-2-yl)benzoate [96]

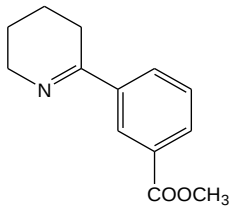

To a solution of 6-(3-iodophenyl)-2,3,4,5-tetrahydropyridine **95** (1.2 g, 4.208 mmol) in 1,4-dioxane (4.5 mL), molybdenum hexacarbonyl (1.664 g, 6.312 mmol), palladium on activated charcoal 10% (200 mg), DMAP (1.032 g, 8.416 mmol), DIPEA (1.088 g, 8.416 mmol) and MeOH (1.712 mL, 42.08 mmol) were added; the mixture was sealed in a MW tube and heated under MW irradiation (250 W) at 130°C for 1 h.

The reaction was filtered through a celite-septum and concentrated. The residue was taken with saturated $NaHCO_3$ (15 mL) and extracted with AcOEt (3 x 8 mL). The organic layers were washed with water, dried over Na_2SO_4, filtered and the solvent removed in *vacuo*. The crude material was purified by flash chromatography (CyHex/AcOEt 90:10 → 80:20) to provide 400 mg of pure compound (44% yield).

96: yellow oil.

***R*$_f$:** 0.30 (CyHex/AcOEt 7:3); UV; PMA.

^{1}H-NMR ($CDCl_3$): δ 1.68 (m, 2H), 1.83 (m, 2H), 2.65 (m, 2H), 3.84 (m, 2H), 3.91 (s, 3H), 7.44 (m, 1H), 8.02 (m, 2H), 8.38 (m, 1H).

^{13}C-NMR ($CDCl_3$): δ 19.85, 21.99, 27.29, 50.16, 52.36, 126.19, 127.28, 128.58, 130.38, 130.60, 130.78, 140.66, 165.17.

MS (ESI): *m/z* 218.1 $[M+H]^+$, calc. for $C_{13}H_{15}NO_2$ 217.26.

(3-(3,4,5,6-Tetrahydropyridin-2-yl)phenyl)methanol hydrochloride [38]

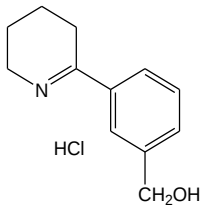

To a solution of methyl 3-(3,4,5,6-tetrahydropyridin-2-yl)benzoate **96** (400 mg, 1.841 mmol) in dry THF (37 mL) in an argon atmosphere, 65% Red-Al in toluene (2.4 mL, 7.733mmol) was added and the mixture stirred at room temperature for 1 h.

The reaction was quenched with saturated $NaHCO_3$ (10 mL) and extracted with AcOEt (3 x 8 mL). The organic layers were dried over Na_2SO_4, filtered and concentrated in *vacuo*. The crude material was purified by flash chromatography (AcOEt). The yellow oil was treated with 1.25 M HCl in methanol for 30 minutes. Concentration and crystallization with 2-propanol provided 106 mg of the title compound (26% yield).

38: yellow solid.

m.p.: 141-142 °C.

^{1}H-NMR (CD_3OD): δ 2.03 (m, 4H), 3.31 (m, 2H), 3.84 (m, 2H), 4.72 (s, 2H), 7.62 (m, 1H), 7.77 (m, 2H), 7.87 (m, 1H).

^{13}C-NMR (CD_3OD): δ 16.99, 17.10, 19.15, 45.30, 62.94, 125.79, 126.51, 129.54, 132.03, 133.15, 143.86, 183.98.

MS (ESI): *m/z* 190.10 $[M+H]^+$, calc. for $C_{12}H_{15}NO$ 189.25.

2-(3-Bromo-5-fluorophenyl)-3,4,5,6-tetrahydropyridine hydrochloride [43]

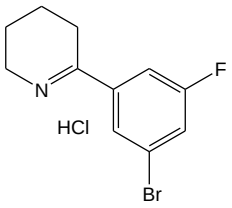

To a solution of 1,3-dibromo-5-fluorobenzene **98** (1.47 g, 5.782 mmol) in dry Et_2O (6 mL) at –78°C, a solution of 1.6 M *n*-BuLi in hexane (3.48 mL; 5.568 mmol) was added dropwise and the mixture stirred at −78°C for 1 h. The mixture was added dropwise to a solution of 5-bromovaleronitrile **97** (694 mg, 4.283 mmol) in dry THF (5 mL) and the reaction was stirred at room temperature for 2 h.

The reaction was quenched with a saturated solution of $NaHCO_3$ (20 mL) and extracted with DCM (3 x 15 mL). The organic layers were dried over Na_2SO_4, filtered and concentrated in *vacuo*. The crude material was purified by flash chromatography (DCM/MeOH 100:0 → 96:4). to provide 691 mg of the desired compound (63% yield).

The yellow oil obtained was treated with 4.0 M HCl in 1,4-dioxane for 30 minutes. Concentration and digestion with Et_2O provided 205 mg of the title compound (26% yield).

43: dark yellow solid.

^{1}H-NMR (CD_3OD): δ 2.03 (m, 4H), 3.30 (m, 2H), 3.86 (m, 2H), 7.70 (m, 1H), 7.82 (m, 1H), 7.92 (m, 1H).

^{13}C-NMR (CD_3OD): δ 16.85, 18.91, 45.70, 100.25, 114.20, 123.74, 124.53, 127.09, 135.34, 161.14, 164.49.

MS (ESI): *m/z* 256.26 $[M+H^+]^+$, calc. for $C_{11}H_{12}BrFN^+$ 256.01.

Methyl 3-fluoro-5-(3,4,5,6-tetrahydropyridin-2-yl)benzoate [99]

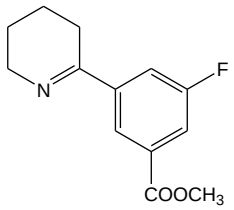

To a solution of 2-(3-bromo-5-fluorophenyl)-3,4,5,6-tetrahydropyridine **23** (122 mg, 0.476 mmol) in 1,4-dioxane (4.5 mL), molybdenum hexacarbonyl (377 mg, 1.328 mmol), palladium on activated charcoal 10% (30 mg), DMAP (117 mg, 0.952 mmol), DIPEA (123 mg, 0.952 mmol) and methanol (153 mg, 4.76 mmol) were added; the mixture was sealed in a MW tube and heated under MW irradiation (250 W) at 130°C for 2 h.

The reaction was filtered through a celite-septum and concentrated. The residue was taken with saturated $NaHCO_3$ (20 mL) and extracted with AcOEt (4 x 10 mL). The organic layers were washed with water, dried over Na_2SO_4, filtered and the solvent removed in *vacuo*. The crude material was purified by flash chromatography (CyHex/AcOEt 90:10) to provide 64 mg of pure compound (57% yield).

99: yellow oil.

***R*$_f$:** 0.38 (CyHex/AcOEt 7:3); UV; $KMnO_4$, Dragendorff reagent.

^{1}H-NMR ($CDCl_3$): δ 1.66 (m, 2H), 1.83 (m, 2H), 2.61 (m, 2H), 3.85 (m, 2H), 3.93 (s, 3H), 7.74 (m, 2H), 8.18 (m, 1H).

^{13}C-NMR ($CDCl_3$): δ 19.01, 21.90, 22.30, 48.70, 52.33, 116.82, 117.98, 125.36, 131.77, 142.11, 164.22, 165.78, 166.21.

3-Fluoro-5-(3,4,5,6-tetrahydropyridin-2-yl)phenyl)methanol hydrochloride [39]

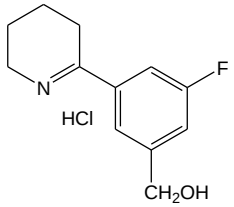

To a solution of methyl 3-fluoro-5-(3,4,5,6-tetrahydropyridin-2-yl)benzoate **99** (35 mg 0.149 mmol) in dry THF (3 mL) in an argon atmosphere, 65% Red-Al in toluene (195 mg, 0.626 mmol) was added and the mixture stirred at room temperature for 24 h.

The reaction was quenched with saturated $NaHCO_3$ (20 mL) and extracted with AcOEt (4 x 15 mL). The organic layers were dried over Na_2SO_4, filtered and concentrated in *vacuo*. The crude material was then purified by preparative TLC (AcOEt). The yellow oil obtained was treated with 4.0 N HCl in 1,4-dioxane for 30 min. Concentration and crystallization from 2-propanol provided 6 mg of the title compound (33% yield).

38: dark yellow oil.

^{1}H-NMR (CD_3OD): δ 2.03 (m, 4H), 3.31 (m, 2H), 3.85 (m, 2H), 4.72 (s, 2H), 7.55 (m, 2H), 7.69 (sa, 1H).

^{13}C-NMR (CD_3OD): δ 21.00, 21.42, 32.85, 43.71, 64.76, 111.99, 114.53, 122.51, 132.51, 143.17, 162.97, 168.12.

MS (ESI): *m/z* 207.98 $[M+H^+]^+$, calc. for $C_{12}H_{15}FNO^+$ 208.11.

2,3,4,5-Tetrahydro-6-phenylpyridine hydrochloride [40]

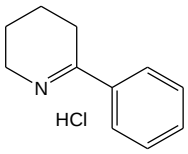

To a solution of 5-bromovaleronitrile **97** (236 mg, 1.457 mmol) in dry THF (2.5 mL), a solution of 1.8 M phenyllithium in cyclohexane/Et_2O 70:30 **100** (914 µL, 1.646 mmol) was added dropwise and the resulting mixture was stirred under reflux for 3 h.

The reaction was quenched with 1.0 N HCl in water (20 mL) and extracted with DCM (3 x 15 mL). The aqueous layer was basified with a saturated solution of $NaHCO_3$ (pH = 8/9) and extracted again with DCM (3 x 15 mL) The organic layers were dried over Na_2SO_4, filtered and concentrated in *vacuo* to provide 151 mg of the desired compound (65% yield).

The yellow oil obtained was treated with 2.0 M HCl in Et_2O for 30 min. Concentration and crystallization from EtOH/Et_2O provided 46 mg of the title compound (25% yield).

43: dark yellow solid.

m.p. = 88-89 °C.

^{1}H-NMR (CD_3OD): δ 2.03 (m, 4H), 3.31 (m, 2H), 3.85 (m, 2H), 7.63 (m, 2H), 7.76 (m, 1H), 7.91 (m, 2H).

^{13}C-NMR (CD_3OD): δ 17.12, 17.23, 17.33, 19.26, 28.84, 45.50, 128.02, 129.57, 131.98, 134.98, 183.84.

MS (ESI): *m/z* 160.92 $[M+H^+]^+$, calc. for $C_{11}H_{14}N^+$ 160.11.

2,3,4,5-Tetrahydro-6-*m*-tolylpyridine hydrochloride [41]

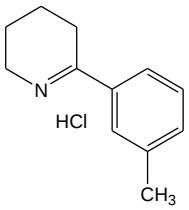

A solution of 3-bromotoluene **101** (586 mg, 3.427 mmol) in dry THF (3 mL) was added dropwise in a flame-dried flask containing magnesium powder (82 mg 3.427 mmol) and the resulting mixture was stirred at room temperature for 20 min. The resulting solution was added dropwise to a solution of 5-bromovaleronitrile **97** (555 mg, 3.427 mmol) in dry THF (3 mL) and the mixture was stirred at room temperature for 1 h.

The reaction was quenched with a saturated solution of $NaHCO_3$ (20 mL) and extracted with DCM (3 x 15 mL). The organic layers were dried over Na_2SO_4, filtered and concentrated in *vacuo*. The crude material was purified by flash chromatography (DCM → DCM/MeOH 90:10) to provide 332 mg of pure compound (56% yield).

The yellow oil obtained was treated with 4.0 M HCl in 1,4-dioxane for 30 minutes. Concentration and digestion with Et_2O provided 92 mg of the title compound (23% yield).

43: dark yellow oil.

^{1}H-NMR (CD_3OD): δ 2.03 (m, 4H), 2.47 (m, 3H), 3.32 (m, 2H), 3.85 (m, 2H), 7.52 (m, 1H), 7.60 (m, 1H), 7.73 (m, 2H).

^{13}C-NMR (CD_3OD): δ 17.15, 17.25, 19.21, 20.15, 45.29, 125.11, 128.25, 129.44, 131.96, 135.68, 139.93.

MS (ESI): *m/z* 173.88 $[M+H^+]^+$, calc. for $C_{12}H_{16}N^+$ 174.13.

2-(3-Fluorophenyl)-3,4,5,6-tetrahydropyridine hydrochloride [42]

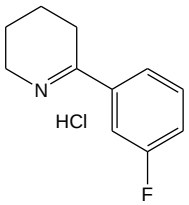

To a solution of 1-bromo-3-fluorobenzene **102** (405 mg, 2.317 mmol) in dry Et_2O (2.5 mL) at −70°C, a solution of 1.6 M *n*-BuLi in hexane (1.40 mL, 2.231 mmol) was added dropwise and the resulting mixture was stirred at −70°C for 1 h. The solution was added dropwise to a solution of 5-bromovaleronitrile **97** (278 mg, 1.716 mmol) in dry THF (2.5 mL) and the mixture stirred overnight at room temperature.

The reaction was quenched with a saturated solution of $NaHCO_3$ (20 mL) and extracted with DCM (3 x 15 mL). The organic layers were dried over Na_2SO_4, filtered and concentrated in *vacuo*. The crude material was purified by flash chromatography (DCM → DCM/MeOH 90:10) to provide 207 mg of pure compound (68% yield).

The yellow oil obtained was treated with 4.0 M HCl in 1,4-dioxane for 30 minutes. Concentration and digestion with Et_2O provided 60 mg of the title compound (26% yield).

43: dark yellow solid.

m.p.: 155 °C dec.

^{1}H-NMR (CD_3OD): δ 2.04 (m, 4H), 3.31 (m, 2H), 3.87 (m, 2H), 4.87 (m, 2H), 7.54 (m, 1H), 7.70 (m, 3H).

^{13}C-NMR (CD_3OD): δ 17.02 (2C), 19.12, 45.65, 114.87, 121.48, 124.14, 131.69, 133.98, 161.35, 164.64.

MS (ESI): *m/z* 178.01 $[M+H^+]^+$, calc. for $C_{11}H_{13}FN^+$ 178.10.

6. References

[1] C. Gotti, M. Zoli, F. Clementi, *Trends in Pharmacological Sciences* **2006**, *27*, 482.
[2] A. A. Jensen, B. Frølund, T. Liljefors, P. Krogsgaard-Larsen, *Journal of Medicinal Chemistry* **2005**, *48*, 4705.
[3] S. Wonnacott, F. Dajas-Bailador, *Trends in Pharmacological Sciences* **2004**, *25*, 317.
[4] R. Exley, S. J. Cragg, *British Journal of Pharmacology* **2007**, 1.
[5] J. A. Dani, D. Bertrand, *Annu. Rev. Pharmacol. Toxicol.* **2007**, *47*, 699.
[6] R. J. Lukas, J. P. Changeux, N. Le Novère, E. X. Albuquerque, D. J. Balfour, D. K. Berg, D. Betrand, V. A. Chiappinelli, P. B. Clarke, A. C. Collins, J. A. Dani, S. R. Grady, K. J. Kellar, J. M. Lindstrom, M. J. Marks, M. Quik, P. W. Taylor, S. Wonnacott, *Pharmacol. Rev.* **1999**, *51*, 397.
[7[P. van Nierop, S. Bertrand, D. W. Munno, Y. Gouwenberg, J. van Minnen, J. D. Spafford, N. I. Syed, D. Betrand, A. B. Smit, *J. Biol. Chem.* **2006**, *281*, 1680.
[8] N. Bocquet, L. Prado de Carvalho, J. Cartaud, J. Neyton, C. Le Poupon, A. Taly, T. Grutter, J. P. Changeux, P. J. Corringer, *Nature*, **2007**, *445*, 116.
[9] R. J. Hilf, R. Dutzler, *Curr. Opin. Struct. Biol.* **2009**, *19*, 418.
[10] M. N. Romanelli, F. Gualtieri, *Medicinal Research Reviews* **2003**, *23*, 393.
[11] U. Gorne-Tschelnokow, A. Strecker, C. Kaduk, D. Naumann, F. Hucho, *EMBO Journal* **1994**, *13*, 338.
[12] J. Monod, J. Wyman, J.-P. Changeux, *J. Mol. Biol.* **1965**, *12*, 88.
[13] J.-P. Changeux, S. J. Edelstein, *Neuron* **1998**, *21*, 959.
[14] R. Lape, D. Colquhoun, L. G. Sivilotti, *Nature* **2008**, *454*, 722.
[15] J. del Castillo, B. Katz, *Proc. R. Soc. Lond. B* **1957**, *146*, 369.
[16] V. Burzomato, M. Beato, P. J. Groot-Kormelink, D. Colquhoun, L. G. Sivilotti, *J. Neurosci.* **2004**, *24*, 10924.
[17] K. Brejc, W. J. van Dijk, R. V. Klaassen, M. Schuurmans, J. van Der Oost, A. B. Smit, T. K. Sixma, *Nature* **2001**, *411*, 269.
[18] P. H. Celie, I. E. Kasheverov, D. Y. Mordvintsev, R. C. Hogg, P. van Nierop, R. van Elk, S. E. van Rossum-Fikkert, M. N. Zhmak, D. Bertrand, V. Tsetlin, T. K. Sixma, A. B. Smit, *Nat. Struct. Mol. Biol.* **2005**, *12*, 582.
[19] C. Ulens, A. Akdemir, A. Jongejan, R. van Elk, S. Bertrand, A. Perrakis, R. Leurs, A. B. Smit, T. K. Sixma, D. Bertrand, I. J. de Esch, *J. Med. Chem.* **2009**, *52*, 2372.
[20] A. Nemecz, P. W. Taylor, *J. Biol. Chem.* **2011**, *286*, 42555.
[21] M. Brams, E. A. Gay, J. Colòn Sàez, A. Guskov, R. C. van der Schors, S. Peigneur, J. Tytgat, S. V. Strelkov, A. B. Smit, J. L. Yakel, C. Ulens, *J. Biol. Chem.* **2011**, *286*, 4420.
[22] R. E. Hibbs, E. Gouaux, *Nature* **2011**, *474*, 54.
[23] N. A. Horenstein, T. J. McCormack, C. Stokes, K. Ren, R. L. Papke, *J. Biol. Chem.* **2007**, *282*, 5899.
[24] M. W. Quick, R. A. Lester, *J. Neurobiol.* **2002**, *53*, 457.
[25] M. J. Marks, J. B. Burch, A. C. Collins, *J. Pharmacol. Exp. Ther.* **1983**, *226*, 817.
[26] R. D. Schwartz, K. J. Kellar, *Science* **1983**, *220*, 214.
[27] D. C. Perry, D. Mao, A. B. Gold, J. M. McIntosh, J. C. Pezzullo, K. J. Kellar, *J. Pharmacol. Exp. Ther.* **2007**, *322*, 306.
[28] D. Mao, D. C. Perry, R. P. Yasuda, B. B. Wolfe, K. J. Kellar, *J. Neurochem.* **2008**, *104*, 446.
[29] S. Fucile, *Cell Calcium* **2004**, *35*, 1.
[30] J. M. Lindstrom, F. Esch, P. J. Whiting, M. J. Gore, K. T. Keyser, S. Shimasaki, W. G. Conroy, R. Schoepfer, *Mol. Brain Res.* **1991**, *10*, 61.
[31] P. J. Whiting, R. Schoepfer, W. G. Conroy, M. J. Gore, K. T. Keyser, S. Shimasaki, F. Esch, J. M. Lindstrom, *Brain Res Mol Brain Res* **1991**, *10*, 61.
[32] P. Aridon, C. Marini, C. Di Resta, E. Brilli, M. De Fusco, F. Politi, E. Parrini, I. Manfredi, T. Pisano, D. Pruna, G. Curia, C. Cianchetti, M. Pasqualetti, A. Becchetti, R. Guerrini, G. Casari, *Am. J. Hum. Genet.* **2006**, *79*, 342.
[33] J. C. Hoda, M. Wanischeck, D. Bertrand, O. K. Steinlein, *FEBS Lett.* **2009**, *583*, 1599.

[34] N. L. Saccone, J. C. Wang, N. Breslau, E. O. Johnson, D. Hatsukami, S. F. Saccone, R. A. Grucza, L. Sun, W. Duan, J. Budde, R. C. Culverhouse, L. Fox, A. L. Hinrichs, J. H. Steinbach, M. Wu, J. P. Rice, A. M. Goate, L. J. Beirut, *Cancer Res.* **2009**, *69*, 6848.
[35] D. C. Perry, Y. Xiao, H. N. Nguyen, J. I. Musachio, M. I. Dàvila-Garcìa, K. J. Kellar, *J. Neurochem.* **2002**, *82*, 468.
[36] A. A. Grishin, C. I. Wang, M. Muttenthaler, P. F. Alewood, R. J. Lewis, D. J. Adams, *J. Biol. Chem.* **2010**, *285*, 22254.
[37] S. Vailati, M. Moretti, R. Longhi, G. E. Rovati, F. Clementi, C. Gotti, *Mol. Pharmacol.* **2003**, *63*, 1329.
[38] C. D. Fowler, Q. Lu, P. M. Johnson, M. J. Marks, P. J. Kenny, *Nature* **2011**, *471*, 597.
[39] S. E. McCallum, A. M. Cowe, S. W. Lewis, S. D. Glick, *Neuropharmacology* **2012**, *63*, 434.
[40] L. Tapia, J. Lindstrom, *Mol. Pharmacol.* **2007**, *71*, 769.
[41] M. Quik, J. M. McIntosh, *J. Pharmacol. Exp. Ther.* **2006**, *316*, 481.
[42] S. Valera, S. Bertrand, H. Rollema, R. Hurst, D. Bertrand, *Society for Neuroscience Meeting, San Diego CA:Poster# 476.12/NN6* **2010**.
[43] A. M. de Lucas-Cerrillo, M. C. Maldifassi, F. Arnalich, J. Renart, G. Atienza, R. Serantes, J. Cruces, A. Sanchez-Pacheco, E. Andrés-Mateos, C. Montiel, *J. Biol. Chem.* **2011**, *286*, 594.
[44] Q. Liu, Y. Huang, F. Xue, A. Simard, J. DeChon, G. Li, J. Zhang, L. Lucero, M. Wang, M. Sierks, G. Hu, Y. Chang, R. J. Lukas, J. Wu, *J. Neurosci.* **2009**, *29*, 918.
[45] J. M. McIntosh, N. Absalom, M. Chebib, A. B. Elgoyhen, M. Vincler, *Biochem. Pharmacol.* **2009**, *78*, 693.
[46] R. H. Parri, T. K. Dineley, *Curr. Alzheimer Res.* **2010**, *7*, 27.
[47] R. Srinivasan, R. Pantoja, F. J. Moss, E. D. Mackey, C. D. Son, J. Miwa, H. A. Lester, *J. Gen. Physiol.* **2011**, *137*, 59.
[48] N. Ripoll, M. Bronnec, M. Bourin, *Current Medical Research and Opinion* **2004**, *20*, 1057.
[49] S. Leonard, e. al., *Arch. Gen. Psychiatry* **2002**, *59*, 1085.
[50] G. Fumagalli, C. Chiamulera, *Central Nervous System Agents in Medicinal Chemistry* **2007**, *7*, 269.
[51] P. G. Jones, J. Dunlop, *Neuropharmacology* **2007**, *53*, 197.
[52] M. Vincler, S. Wittenauer, R. Parker, M. Ellison, B. M. Olivera, J. M. McIntosh, *Proceedings of the National Academy of Sciences of the United States of America* **2006**, *103*, 17880.
[53] E. Hamurtekin, S. M. Gurun, *Brain Research* **2006**, *1117*, 92.
[54] S. T. Nevin, R. J. Clark, H. Klimis, M. J. Christie, D. J. Craik, D. J. Adams, *Mol. Pharmacol.* **2007**, *72*, 1406.
[55] B. Gao, M. Hierl, K. Clarkin, T. Juan, H. Nguyen, M. Valk, H. Deng, W. Guo, S. G. Lehto, D. Matson, J. S. McDermott, J. Knop, K. Gaida, L. Cao, D. Waldon, B. K. Albrecht, A. A. Boezio, K. W. Copeland, J. C. Harmange, S. K. Springer, A. B. Malmberg, S. I. McDonough, *Pain* **2010**, *149*, 33.
[56] H. Rollema, J. W. Coe, L. K. Chambers, R. S. Hurst, S. M. Stahl, K. E. Williams, *Trends in Pharmacological Sciences* **2007**, *28*, 316.
[57] C. G. V. Sharples, G. Karig, G. L. Simpson, J. A. Spencer, E. Wright, N. S. Millar, S. Wonnacott, T. Gallagher, *Journal of Medicinal Chemistry* **2002**, *45*, 3235.
[58] J. E. Tonder, P. H. Olesen, *Current Medicinal Chemistry* **2001**, *8*, 651.
[59] R. A. Glennon, M. Dukat, *Bioorg. Med. Chem. Lett.* **2004**, *14*, 1841.
[60] W. H. Bunnelle, K. R. Tietje, J. M. Frost, D. Peters, J. Ji, T. Li, M. J. C. Scanio, L. Shi, D. J. Anderson, T. Dyhring, J. H. Grønlien, H. Ween, K. Thorin-Hagene, M. D. Meyer, *J. Med. Chem.* **2009**, *52*, 4126.
[61] K. R. Tietje, D. J. Anderson, R. S. Bitner, E. A. Blomme, P. J. Brackemeyer, C. A. Briggs, K. E. Browman, D. Bury, P. Curzon, K. U. Drescher, J. M. Frost, R. M. Fryer, G. B. Fox, J. H. Gronlien, M. Håkerud, E. J. Gubbins, S. Halm, R. Harris, R. J. Helfrich, K. L. Kohlhaas, D. Law, J. Malysz, K. C. Marsh, R. L. Martin, M. D. Meyer, A. L. Molesky, A. L. Nikkel, S. Otte, L. Pan, P. S. Puttfarcken, R. J. Radek, H. M. Robb,

E. Spies, K. Thorin-Hagene, J. F. Waring, H. Ween, H. Xu, M. Gopalakrishnan, W. H. Bunnelle, *CNS Neuroscience & Therapeutics* **2008**, *14*, 65.
[62] G. Mullen, J. Napier, M. Balestra, T. DeCory, G. Hale, J. Macor, R. Mack, J. Loch, 3rd, E. Wu, A. Kover, P. Verhoest, A. Sampognaro, E. Phillips, Y. Zhu, R. Murray, R. Griffith, J. Blosser, D. Gurley, A. Machulskis, J. Zongrone, A. Rosen, J. Gordon, *Journal of Medicinal Chemistry* **2000**, *43*, 4045.
[63] J. Malysz, D. J. Anderson, J. H. Grønlien, J. Ji, W. H. Bunnelle, M. Håkerud, K. Thorin-Hagene, H. Ween, R. Helfrich, M. Hu, E. Gubbins, S. Gopalakrishnan, P. S. Puttfarcken, C. A. Briggs, J. Li, M. D. Meyer, T. Dyhring, P. K. Ahring, E. Ø. Nielsen, D. Peters, D. B. Timmermann, M. Gopalakrishnan, *J. Pharmacol. Exp. Ther.* **2010**, *334*, 863.
[64] A. A. Othman, R. A. Lenz, J. Zhang, J. Li, W. M. Awni, S. Dutta, *J. Clin. Pharmacol.* **2011**, *51*, 512.
[65] T. A. Hauser, A. Kucinski, K. G. Jordan, G. J. Gatto, S. R. Wersinger, R. A. Hesse, E. K. Stachowiak, M. K. Stachowiak, R. L. Papke, P. M. Lipiello, M. Bencheriff, *Biochem. Pharmacol.* **2009**, *78*, 803.
[66] M. Hendrix, F. G. Böß, C. Erb, T. Fleßner, M. van Kampen, J. Luithle, C. Methfessel, W. B. Wiese, *PTC WO 03/055878 A1* **2003**.
[67] A. Mazurov, J. Klucik, L. Miao, T. Y. Phillips, A. Seamans, J. D. Schmitt, T. A. Hauser, R. T. Johnson Jr., C. Miller, *Bioorg. Med. Chem. Lett.* **2005**, *15*, 2073.
[68] P. H. Celie, S. E. van Rossum-Fikkert, J. W. van Dijk, K. Brejc, A. B. Smit, *Neuron.* **2004**, *41*, 907.
[69] S. B. Hansen, G. Sulzenbachre, T. Huxford, P. Marchot, P. Taylor, Y. Bourne, *EMBO J.* **2005**, *24*, 3635.
[70] R. E. Hibbs, G. Sulzenbacher, J. Shi, T. T. Talley, S. Conrod, W. R. Kem, P. Taylor, P. Marchot, Y. Bourne, *EMBO J.* **2009**, *28*, 3040.
[71] W. R. Kem, V. M. Mahnir, L. B. Bloom, B. J. Gabrielson, *Toxicon* **1995**, *33*, 306.
[72] G. Grazioso, A. Cavalli, M. De Amici, M. Recantini, C. De Micheli, *J. Comput. Chem.* **2008**, *29*, 2593.
[73] J. Sgrignani, C. Bonaccini, G. Grazioso, M. Chiccioli, A. Cavalli, P. Gratteri, *J. Comput. Chem.* **2009**, *30*, 2443.
[74] W. H. Bunnelle, J. F. Daanen, K. B. Ryther, M. R. Schrimpf, M. J. Dart, A. Gelain, M. D. Meyer, J. M. Frost, D. J. Anderson, M. Buckley, P. Curzon, Y. J. Cao, P. Puttfarcken, X. Searle, J. Ji, C. B. Putman, C. Surowy, L. Toma, D. Barlocco, *J. Med. Chem.* **2007**, *50*, 3627.
[75] A. Cantoni, *Undergraduate Thesis in "Chimica e Tecnologia Farmaceutiche" at the University of Milan* **2010**.
[76] M. N. Nalam, A. Peeters, T. H. Jonckers, I. Dierynck, C. A. Schiffer, *J. Virol.* **2007**, *81*, 9512.
[77] H. Newman, *J. Heterocycl. Chem.* **1974**, *11*, 449.
[78] P. A. Sturm, D. W. Henry, *J. Med. Chem.* **1974**, *17*, 481.
[79] J. B. Ducep, B. Heintzelmann, K. Jund, B. Lesur, M. Schleimer, P. R. Zimmermann, *Tetrahedron: Asymmetry* **1997**, *8*, 327.
[80] J. E. Leffler, R. D. Temple, *J. Am. Chem. Soc.* **1967**, *89*, 5235.
[81] W. Xie, B. Herbert, J. Ma, T. M. Nguyen, R. A. Schumacher, C. M. Gauss, A. Tehim, *PCT WO 2005/063767 A2* **2005**.
[82] T. K. Morgan, R. Lis, A. J. Marisca, T. M. Argentieri, M. E. Sullivan, S. S. Wong, *J. Med. Chem.* **1987**, *30*, 2259.
[83] H. Meerwein, R. Schmidt, *Justus Liebigs Annalen der Chemie* **1925**, *444*, 221.
[84] E. J. Corey, M. Chaykovsky, *J. Am. Chem. Soc.* **1965**, *87*, 1353.
[85] A. Davis, A. F. Kluge, M. L. Maddox, M. L.; Sparacino, *J. Org. Chem.* **1983**, *48,* 255.
[86] S. Yong, D. Hong, T. Weidong, L. Liguang, H. Lihong, *Bioorg. Med. Chem.* **2007**, *15*, 5061.
[87] S. R. Breining, M. Bencherif, S. R. Grady, P. Whiteaker, M. J. Marks, C. R. Wageman, H. A. Lester, D. Yohannes, *Bioorg. Med. Chem. Lett.* **2009**, *19*, 4359.
[88] A. A. Mazurov, D. C. Kombo, T. A. Hauser, L. Miao, G. Dull, J. F. Genus, N. B. Fedorov, L. Benson, S. Sidach, Y. Xiao, P. S. Hammond, J. W. James, C. H. Miller, D. Yohannes, *J. Med. Chem.* **2012**, *55*, 9793.

[89] S. Wu, S. Lee, P. Beak, *J. Am. Chem. Soc.* **1996**, *118*, 715.
[90] H. Prokopvová, C. O. Kappe, *Adv. Synth. Catal.* **2007**, *349*, 448.
[91] F. I. Carroll, G. F. Liang, H, A. Navarro, L. E. Brieaddy, P. Abraham, J. Damaj, B. R. Martin, *J. Med. Chem.* **2001**, *44*, 2229.
[92] F. I. Carroll, W. Ma, Y. Yokota, J. R. Lee, L. E. Brieaddy, H, A. Navarro, J. Damaj, B. R. Martin, *J. Med. Chem.* **2005**, *48*, 1221.
[93] R. Gandolfi, G. Tonoletti, A. Rastelli, M. Bagatti, *J. Org. Chem.* **1993**, *58*, 6038.
[94] A. Kasyan, C. Wagner, M. E. Maier, *Tetrahedron* **1998**, *54*, 8047.
[95] A. Giovannini, D. Savoia, A. Umani-Ronchi, *J. Org. Chem.* **1989**, *54*, 228.
[96] C. Mustazza, A. Borioni, M. R. Del Giudice, F. Gatta, R. Ferretti, A. Menequz, M. T. Volpe, P. Lorenzini, *Eur. J. Med. Chem* **2002**, *37*, 91.
[97] J. Georgsson, A. Hallberg, M. Larhed, *J. Comb. Chem.* **2003**, *5*, 350.
[98] Y. Wada, N. Nishida, N. Kurono, T. Ohkuma, K. Orito, *Eur. J. Org. Chem.* **2007**, *26*, 4320.
[99] S. Guizzetti, M. Benaglia, F. Cozzi, R. Annunziata, *Tetrahedron* **2009**, *65*, 6354.
[100] C. Dallanoce, P. Magrone, C. Matera, F. Frigerio, G. Grazioso, M. De Amici, S. Fucile, V. Piccari, K. Frydenvang, L. Pucci, C. Gotti, F. Clementi, C. De Micheli, *ChemMedChem* **2011**, *6*, 889.